Emerging Contaminants 10 (2024) 100303

Contents lists available at ScienceDirect

Emerging Contaminants

journal homepage: www.keaipublishing.com/en/journals/emerging-contaminants

Non-conventional sorption materials for the removal of legacy and emerging PFAS from water: A review

Francesco Calore [a], Elena Badetti [a], Alessandro Bonetto [a], Anna Pozzobon [a], Antonio Marcomini [a, *]

[a] Department of Environmental Sciences, Informatics and Statistics, University Ca' Foscari of Venice, Via Torino 155, Venezia-Mestre, 30172, Italy

ARTICLE INFO

Article history:
Received 2 November 2023
Received in revised form
3 January 2024
Accepted 27 January 2024
Available online 8 February 2024

Keywords:
Per- and polyfluoroalkyl substances (PFAS)
adsorption
Ion-exchange
activated carbon
Short-chain
GenX

ABSTRACT

Per- and polyfluoroalkyl substances (PFAS) are a class of ubiquitous, persistent, and hazardous pollutants that raise concerns for human health and the environment. Typically, PFAS removal from water relies on adsorption techniques using conventional sorption materials like activated carbons (ACs) and ion exchange resins (IERs). However, there is a continuous search for more efficient and performing adsorbent materials to better address the wide range of chemical structures of PFAS in the environment, to increase their selectivity, and to achieve an overall high adsorption capacity and faster uptake kinetics. In this context, results from the application of non-conventional sorption materials (i.e., readily available biological-based materials like proteins and advanced materials like nanocomposites and cyclodextrins) are reported and discussed in consideration of the following criteria: i) removal efficiency and kinetics of legacy PFAS (e.g., PFOA, PFBA) as well as newly-introduced and emerging PFAS (e.g., GenX), ii) representativity of environmental conditions in the experimental setup (e.g., use of environmentally relevant experimental concentrations), iii) regenerability, reusability and applicability of the materials, and iv) role of the material modifications on PFAS adsorption. From this review, it emerged that organic frameworks, nano(ligno)cellulosic-based materials, and layered double hydroxides are among the most promising materials herein investigated for PFAS adsorption, and it was also observed that the presence of fluorine- and amine-moieties in the material structure improve both the selectivity and PFAS uptake. However, the lack of data on their applicability in real environments and the costs involved means that this research is still in its infancy and need further investigation.

* Corresponding author.
E-mail address: marcom@unive.it (A. Marcomini).
Peer review under responsibility of KeAi Communications Co., Ltd.

https://doi.org/10.1016/j.emcon.2024.100303

Acronyms

Material type	Acronym	Full name/general description	Ref.
Bio-based materials			
Proteins and protein-rich materials	Hemp protein	Cannabis Sativa L. (hemp) protein powder	[1]
	_	Proteins	[2]
	_	Moringa oleifera seed powder encapsulated in alginate beads	[3]
	CA-SPI	Electrospun cellulose acetate-based nanofibrous membranes with soy protein coating (CA-SPI)	[4]
	CE-SPI	Electrospun cellulose-based nanofibrous membranes with soy protein coating (CE-SPI)	
	Alginate- encapsulated albumin	Alginate- encapsulated albumin	[5]
Polysaccharide-based materials	Crosslinked chitosan beads	Epichlorohydrin-crosslinked chitosan beads	[6]
	Quaternized cotton	Quaternized cotton obtained by quaternization of [poly(2-dimethylamino) ethyl methacrylate]-grafted cotton	[7]
	_	Aminated rice husk	[8]
	PEI-f-CMC	Poly(ethylenimine)-functionalized cellulose micro-crystals	[9]
	RAPIMER	Multifunctional lignocellulosic nano-framework	[10]
	PEI-BA, PEI-LF, PEI-PP	Polyethilenimine (PEI)-grafted balsa wood (BA), loofah (LF), and pomelo peel (PP)	[11]
	PDA-CGF, PAN-CGF, pMPD-CGF	Polydopamine (PDA), polyaniline (PAN), and poly(*m*-phenylenediamine) (pMPD) − modified Calotropis gigantea fibers (CGF)	[12]
	QNC or QNC 12:1	Positively charged quaternized ammonium functionalized nanocellulose or quaternized nanocellulose (QNC) adsorbent prepared by the addition of GTMAC (glycidyltrimethylammonium chloride) at the ratio of 12:1 mol/mol of AGU (anhydroglucose unit)	[13]
	QWP1.5	Quaternized wood pulp with a charge density of 1.5 mmol $-NR_3^+$/g	[14]
Polyanilines and polyacrylonitrile	ASFPAN10	Amidoxime surface-functionalized PAN nanofibrous material (PAN = polyacrylonitrile), collected after a 10-min. Immersion in a 1 M NH_2OH solution at 70 °C	[15]
	ES(PAN/Algae)	Electrospun PAN/Algae bicomponent nanofibrous membrane	[16]
	PANI	Polyaniline	[17]
	POT	Poly-o-toluidine	
	POA	Poly-*o*-anisidine	
	PASNT	Polyaniline emeraldine salt nanotubes	[18]
	PANI_PFA	Paraformaldehyde-crosslinked polyaniline	[19]
Advanced materials			
Covalent organic frameworks (COFs)	28%[NH_2]- COFs	28% amine-loaded covalent organic framework	[20]
	Chitosan/F−COF	Chitosan-coated fluoro-functionalized covalent organic framework	[21]
	FSQ-1	Fluorinated squaramide-based COF	[22]
	Cys-COF	2D- hollow Cys-COF nanospheres	[23]
	COF1 and COF2	BT-BDB-COF (COF2), where BT = 1,2,4,5-Benzenetetramine tetrahydrochloride; BDB = 4,7-bis(4-formylphenyl)-1,3-dimethyl-1H- benzo[*d*]imidazole-3-ium bromide	[24]
	β-CD-COFs	β-Cyclodextrin covalent organic framework COF1, i.e. β-CD-TPA-COF, where TPA = terephtalaldeyde	[25]
	CTF COF	Covalent triazine-based framework	[26]
	COF−F1N5	COF with a given ratio of fluorinated vs quaternary ammonium monomers obtained by reaction of 0.2 mmol of TFB + 0.05 mmol BFT + 0.25 mmol BAB, where: TFB = 1,3,5-tris(*p*-formylphenyl)benzene; BFT = 2,5-bis ((3,3,4,4,5,5,6,6,6-nonafluorohexyl) oxy) terephthalohydrazide; BAB = 1,1′-bis(4-amino- phenyl)-[4,4′-bipyridine]-1,1′-diium chloride	[27]
Metal-organic frameworks (MOFs)	NU-1000	Zirconium-based metal−organic framework (MOF)	[28]
	MIL-101 (Cr)	Cr-based MOF with terephthalic acid as a ligand	[29]
	MIL-101 (Cr)−NH_2	Cr-based MOF with 2-aminoterephtalic acid as a ligand	
	MOF-808	Zr-based MOF	[30]
	PCN-222	Zirconium-metalloporphyrin based MOF (PCN = porous coordination network)	[31]
	DUT-5-2	Al-based MOF	[32]
Other organic frameworks	SCU-8	Mesoporous cationic thorium-organic framework	[33]
	PAF-45	Porous aromatic framework	[34]
Cyclodextrin polymers	CDP-1	Aminated (CDP-1) and amidated (CDP-2) cyclodextrin Polymers with tris(2-aminoethyl)amine (TREN)-based tripodal crosslinkers	[35]
	CDP-2		
	DFB-CDP	Decafluorobiphenyl- β-Cyclodextrin Polymer	[36]
	TFN-CDP	β-Cyclodextrin Polymer Network linked with tetrafluoroterephthalonitrile	[37]
	β-CD 6	β-CD polymer copolymerized with a methacrylate bearing a cationic functional group	[38]
Hydrogels	Functionalized PEGDA	Fluoridated and aminated hydrogel sorbent (poly(ethylene glycol)) diacrylate)	[39]
	IF-20+	Ionic fluorogels with 20% (weight) ammonium groups	[40]
	DMAPAA-Q	Hydrogel (poly (N-[3-(dimethylamino)propyl]acrylamide, methyl chloride quaternary)	[41]
	CD_{66}-0.2E/P	Carbon dots (CD)- modified polyethylene glycol diglycidyl ether (PEG)/polypropylene glycol diglycidyl ether (PPG)-based hydrogels (0.66 = % weight of CD; 0.2 = weight ratio of PEG vs PPG)	[42]
	PNIPAm	Poly-N-isopropylacrylamide	[43]
	FCH2	Fluorous-core nanoparticle-embedded hydrogel	[44]
Magnetic NPs-based materials	2-MNPs @ FG	Magnetic nanoparticles (MNPs) attached to a fluorographene (FG) framework with a 3:5 ratio of MNP:FG	[45]
	1/19-MF-VT	Fluorinated vermiculite-based adsorbent (F-VT) loaded with Fe_3O_4 nanoparticles (NPs) with a 1:19 ratio of F-VT: NPs	[46]
	$Fe3O_4$@SiO_2−NH_2&F_{13}	Silica membrane functionalized with an amino group and octyl-perfluorinated chain on the periphery of Fe_3O_4 nanoparticle	[47]
	Fe_3O_4-CDI-IL MNPs	Multifunctional magnetic sorbent (Fe_3O_4 nanoparticles modified with β-cyclodextrin ionic liquid (β-CD-IL) polyurethanes)	[48]
	P2-9+@IONPs	Fe_3O_4 NPs grafted with perfluoropolyether-containing polymers with a 2:9 degree of polymerization of the two monomers (2-dimethylaminoethyl acrylate and oligo(ethylene glycol)methyl ether acrylate)	[49]

(*continued*)

Material type	Acronym	Full name/general description	Ref.
Zeolites	–	Zeolite-sodium silicate composite materials	[50]
	–	All-silica Zeolite β	[51]
	CP811C unmodified	β-Zeolite with a 300:1 SiO_2:Al_2O_3 ratio	[52]
	CP811C CTAB-coated	cetyltrimethylammonium bromide-coated CP118C	
	CP814E unmodified	β-Zeolite with a 25:1 SiO_2:Al_2O_3 ratio	
	CP814E PDADMAC-coated	poly(diallyldimethylammonium chloride)-coated CP814E	
	–	All-silica Zeolite β	[53]
Layered double hydroxides	CF-LDH	Polyfluoroalkyl-modified layered double hydroxide	[54]
	HT-NO_3	Nitrate-intercalated hydrotalcite as such (HT-NO_3) and chemically treated with acetone (AHT-NO_3)	[55]
	AHT-NO_3		
	Zn−Al LDH	Zn−Al and Mg−Al layered double hydroxides	[56]
	Mg−Al LDH		
	YOHCl	Ultrathin $Y_2(OH)_{4.86}Cl_{1.44} \times 1.07H_2O$ nanosheets	[57]
	CHT	Calcinated hydrotalcite	[58]
Modified activated carbons	PAMTAg and CAMTAg	Physically activated maize tassel silver (PAMTAg) and chemically activated maize tassel silver (CAMTAg)	[59]
	PolyDADMAC-GAC	Poly(diallyldimethylammonium chloride) − functionalized GAC	[60]
	MIL-101(Cr)@AC	AC coated with a metal organic framework (MIL-101 (Cr))	[29]
	Fe_3O_4@GAC	Fe_3O_4 nanoparticles loaded on a commercial granular activated carbon with a Fe^{2+}: Fe^{3+} ratio of 2:1	[61]
	DeCACF	Defunctionalised activated carbon felt	[62]

1. Introduction

PFAS are a class of highly fluorinated substances that emerged as global contaminants in the last two decades and have been used in many commercial and industrial products and applications, owing to their oil and water repellence and thermal/chemical stability [63,64]. These highly persistent, bioaccumulable, mobile, and toxic [65−67] substances are ubiquitous in the environmental media [68]. PFAS have been associated with relevant negative health effects on the biota, including humans, among which carcinogenicity, hepatotoxicity, nephrotoxicity, neurotoxicity, and developmental effects [69−72]. PFAS can be classified according to their physicochemical characteristics, including the length of the alkyl chain, functional group(s), fluorination level, and the presence of other halogens or hydrogen atoms in the structure. The most widely investigated PFAS are carboxylic (PFCA) and sulfonic (PFSA) acids (characterized by a fully fluorinated alkyl chain), which are considered long-chain when exhibiting a number of perfluorinated carbons $\geq$7 and $\geq$ 6, respectively [73]. Regulatory restrictions and established thresholds mostly focus on this subset of PFAS, especially the more bioaccumulable long-chain PFAS [70]. Therefore, short-chain PFCA and PFSA production has increased, and new PFAS, like perfluoroether substances, have been introduced in the market over time [74]. Other long-time used PFAS, including zwitterionic, cationic, and non-ionic PFAS [75], were detected in the environment only recently. Thus, novel and emerging PFAS are present in the environment at increasing concentrations. Their simultaneous removal has become an increasingly urgent need, as exemplified by GenX. This increasingly detected [76,77] perfluorooctanoic acid (PFOA) substitute has been recently linked to non-negligible toxic effects on the biota [78−80], and it has been estimated that 4 times higher treatment costs are needed for its removal (by means of traditional sorption materials) with respect to PFOA [81].

The wide range of physical-chemical properties of environmentally relevant PFAS makes a class-wise removal of PFAS from solid and aqueous environmental matrices challenging. Many well-established and newly developed removal/destructive technologies and materials (e.g., catalysts, adsorbents) have been employed to remove PFAS in the last 10−15 years [82]. Such physical-, chemical-, and biological-based treatments can be categorized as non-destructive or destructive (or a combination of these) and come with different pros and cons in terms of removal effectiveness and efficiency, field-applicability, costs, maturity (i.e., field-scale implementation), environmental impacts [83−85]. In this context, this review focuses on materials for PFAS sorption, a feasible, widely used approach for their removal from water. In fact, ingestion of contaminated food and water represents a major pathway for human exposure to PFAS. Natural, drinking, and wastewaters worldwide are widely contaminated by PFAS in concentrations typically ranging from some ng/L to a few μg/L [76]. Despite the impressive performance of other separation-based membrane technologies like reverse osmosis (see SI part 1), sorption is widely applied in water treatment operations owing to fundamental advantages like straightforward design and operational procedures, as well as lower costs [86]. Activated carbons (ACs) and ion exchange resins (IER) are by far the most used sorption materials for wastewater and drinking water treatment and in the remediation of contaminated sites because of their accessibility, maturity, and capability to simultaneously remove multiple organic and inorganic contaminants at ppm to ppt level. They can efficiently remove long-chain legacy PFAS but proved less adequate for the adsorption of the increasingly detected, more hydrophilic short-chain PFAS [87−90]. To bypass this limitation, other adsorbents were investigated to achieve a more effective removal of the overall set of PFAS occurring in natural, drinking, and wastewater [83,91,92], including both highly engineered and tailorable materials - such as covalent organic frameworks or cyclodextrins- as well as natural, readily available biomaterials - like crosslinked chitosan beads and polysaccharide-based materials. The former include materials with high abundance of active sites, extreme adjustability of pore dimensions and pore structure, or that show potential for alternative ways of separation and regeneration. The latter can be broadly grouped as materials that can be prepared from low-cost, abundant, renewable, recyclable biological sources. Therefore, their advantages as alternative bio-based sorbents generally relies on economic and environmental sustainability. Some of these materials have been modified at the surface and/or structural level to provide more adsorbing sites and, ultimately, enhance the adsorption performance [93,94]. The additional sorption sites provide specific adsorbent-adsorbate interactions, such as electrostatic attraction, fluorine-fluorine interaction, and ion-exchange, while adjusting pore size also has an influence on the pollutant diffusion, kinetic, uptake, and affinity. In addition, multi-component materials have been produced to exploit the advantages of the combination of different materials (e.g. high surface

area, diamagnetic properties) [29,61].

However, evaluating the efficacy of sorption materials under environmentally realistic conditions is important. Environmental waters are multi-component systems containing a wide variety of dissolved and suspended organic and inorganic components typically present in concentrations up to 8 orders of magnitude higher than PFAS [84] that can diversely interact with both adsorbent and adsorbate. The interaction between PFAS and an adsorbent material can be affected not only by the chemical-physical properties of the adsorbate (e.g., functional group, chain length) and the material (e.g., surface charge, hydrophobicity, pore shape/granule dimension) but also by the solution chemistry (e.g., occurrence of ions, pH) [88,89,95–101]. For example, organic matter (OM, which encompasses both natural and artificial carbon-based substances) in suspended and dissolved form can hinder the adsorption of PFAS by competing for sorption and blocking the canals of porous materials [102,103]. Nevertheless, OM as humic acid (HA) has also been found to improve the adsorption of PFAS in gel-type resins due to the induced expansion of the polymeric structure that allowed PFOA and PFOS to reach previously inaccessible sorption sites [26]. A low pH (i.e., higher protonation of certain functional groups on the adsorbent surface) can enhance the adsorption process of negatively charged PFAS via electrostatic interaction. Divalent cations in solution can cause cation bridging between PFAS and the sorbent. However, the subsequent possible decrease of the zeta potential of a charged material can lead to the agglomeration and precipitation of the material or reduce available ion-exchange sites.

Regenerability (i.e., re-use) and management of the spent sorption materials represent another relevant aspect from both environmental and economic standpoints [104,105], and it is pivotal to evaluate the pilot- or full-scale applicability of a sorbent and its competitivity with respect to commercial materials. The use of solvents or other means of regeneration can nevertheless affect the sorption process [86,106]: for example, solvent washing can modify the adsorbent structure and, therefore, its adsorption capacity.

2. Scope of the review, data collection, and relevant sorption parameters

The purpose of this work is to critically review the performance of sorption materials recently proposed for PFAS removal with respect to 1) the capability to remove PFAS (including short-chain and novel PFAS), 2) the adsorption performance under environmentally relevant conditions, 3) regenerability and reusability of the adsorbing materials, 4) materials functionalities relevant to improve the selectivity towards PFAS (vs. other organic molecules) and/or towards short-chain PFAS over the long-chain ones. To this end, a literature review on non-conventional materials used for PFAS removal in batch experiments was carried out on the Scopus database by opportunely combining the following keywords: PFAS, perfluoroalkyl, short-chain, novel PFAS, sorption, adsorption, removal, ion-exchange, polymeric materials, MOFs. As a result, 62 peer-reviewed papers, published between 2011 and 2023 were selected. Among alternative carbon-based materials, biochars, carbon nanotubes, and graphene oxides were not included in the review as they have been exhaustively covered by other works [86,107]. Only layered double hydroxides (hydrotalcites) were considered as representative of clays-based adsorbents due to their outstanding PFAS removal capacity compared to other unmodified and modified materials of the same kind [108,109]. The sorption performance of PFAS by hydrogel-based sorbents is also reviewed for the first time.

Information collected for the evaluation of the adsorption performance of ACs and IER (Tables S1–S2) and non-conventional materials (Tables 1–10) includes: i) type of PFAS tested, ii) sorption efficiency, iii) tested initial concentrations (C_0) of PFAS and of the adsorbents, and iv) time required to reach adsorption equilibrium (eq. time). Sorption efficiency is commonly evaluated by applying adsorption isotherm models and kinetic laws. The former are used to describe the interaction between adsorbent and adsorbate at equilibrium and at constant temperature [110,111]. The Langmuir and Freundlich isotherms are the most widely applied models used to describe the adsorption of organic pollutants on solid materials. Kinetic models to describe sorption kinetics are usually modelled by means of pseudo-first and pseudo-second order (PFO and PSO) rate laws [112]. Collectively, kinetic models and isotherm models can be used to derive the amount of adsorbed substance at equilibrium (q_e) and the maximum amount of adsorbable substance (Q_m). Additional information on kinetics, isotherms, and derived parameters of the most used models are available in the SI-part 1. Additional variables were considered for the critical review of non-conventional materials, namely evaluation of the influence of OM on adsorption, use of environmentally

Table 1
Modified ACs used for PFAS sorption and relevant parameters investigated.

Material	Mat. Conc. (mg/L)	PFAS	C_0 PFAS (mg/L)	Adsorption capacity (μmol/g)	% removal	Eq. time (hours)	Recyclability	Ref.
PAMTAg	2000	PFOS	0.01–0.1[a]	57[c]	79-81[e]	–	–	[59]
		PFOA		46[c]				
CAMTAg		PFOS		588[c]	81-83[e]		–	
		PFOA		690[c]				
polyDADMAC-GAC	6660	PFOA	–	758[c]	–	<96	Ultrasound sonication (900 kHz, 15.8 W), 3 cycles, 2–4%[f]	[60]
		PFBA	–	774[c]	–			
MIL-101 (Cr)@AC	100	PFOS	0.5–2[a]	51[c]	80.4	2	50:50 EtOH:H_2O (vol/vol), 4 cycles, 50%[f]	[29]
Fe_3O_4@ GAC	500	PFOA	200–450[a]	1431[c]	80	29	NaOH solution and MeOH, 5 cycles, 12%[f]	[61]
				880[d]			Pure MeOH, 5 cycles, maintained 80%	
DeCACF		PFOA		193[c]				
	–	PFBA	–	24[c]	–	–	Desorption of PFOA and PFBA maintained >90% over 5 cycles	[62]
		PFOS		206[c]				

b = Kinetic model.
[a] Isotherm experiments.
[c] Q_m (Langmuir).
[d] Q_e (pseudo-second-order).
[e] Removal of 10 PFAS (C4–C10 PFCA, PFBS, PFHxS, PFOS).
[f] Decrease in adsorption capacity.

Table 2
Proteins and protein-rich materials used for PFAS sorption and relevant parameters investigated.

Material	Mat. Conc. (mg/L)	PFAS	C_0 PFAS (mg/L)	Adsorption capacity (μmol/g)	% removal	Eq. time (hours)	Recyclability	Ref.
Hemp (*Cannabis sativa*) protein	Not disclosed	C4–C8 PFCA, C4–C8 PFSA	~0.2 (∑PFAS)		PFBS: ~80% PFPeS: ~76% PFHxS: ~85% PFHpS: ~96% PFOS: ~96% PFPeA: ~92% PFOA: ~86%	<3	–	[1]
Proteins (BSA, casein, egg white albumin, lysozyme, and RNase A)	3.5–350 μM	PFOA	0.001		BSA: 83–92% Lysozime: 93% (UPW) RNase A: 75% (UPW), 25–28% (TW- CW) Albumin: 37–47% (in saltier/buffered solutions)	–	–	[2]
		GenX	0.001		BSA (350 μM): 91% (UPW), 99% (TW), and 94% (CW) Lysozime: 96% (UPW) RNase A: 69% (UPW), 53% (TW)	–	–	
		PFBA	0.001		Lysozime: 78% (UPW), 64% (TW)	–	–	
		PFBS	0.001		BSA: 70% (UPW), 93% (at pH = 8 and high salinity), 75% (TW), 81% (CW) Lysozime: 82% (UPW), 41–60% (CW, salt-free buffer, OW), 78–80% in saline buffer.	–	–	
Alginate beads-encapsulated *Moringa oleifera* seed powder	1500	PFOS	0.1[a] 0.1–1[b]	0.09[c] 2[d]	–	30 min.	60%[f]	[3]
		PFBS					10%[f]	
Alginate- encapsulated albumin	500–1500	PFOS	0.1	6[d]	87% (after 72 h)	<3	–	[5]
CA-SPI	240[g]	GenX	100	1000[e]	25% (pH = 4), 90% (pH = 6)	–	–	[4]
CE-SPI				–	15% (pH = 4), 69% (pH = 6)	–	–	

[a] Kinetic experiments.
[b] Isotherm experiments.
[c] Q_e (pseudo-second order).
[d] Q_m (Langmuir).
[e] Experimental Qe; CW = creek water; TW = tap water; OW = ocean water; UPW = ultrapure water.
[f] After 24 h contact time.
[g] The material was used as a filter/adsorbent and 100 mL of a 100 mg/L GenX solution was passed through 24 mg of the material.

relevant conditions, use of real environmental aqueous samples, and recyclability of the adsorbent materials tested. Additional information on PFAS adsorption, experimental conditions, and results of non-conventional materials are reported in SI-part 2. For a more consistent comparison of the adsorption efficiency of different PFAS among different materials, adsorption capacity is reported on a mol/weight base.

3. Adsorbent materials

3.1. ACs and ion-exchange resins

The adsorption of PFAS employing ACs and IERs has been extensively discussed in the literature [105,113]. Here, the most relevant information is reported, and useful supplemental details are available in section S1, Tables S1.1 and S1.2.

ACs are highly micro-/mesoporous materials available in both granular (GAC) and powdered (PAC) form. According to the dimensions and porosity of the grains, they show different surface areas and intraparticle diffusion kinetics. In detail, Q_m reported for PFOA, PFOS, PFBS, PFBA, and GenX adsorbed on ACs (Table S1) are 35–1050, 32–1428, 790, and 330 μmol/g respectively, where the higher values refer to PAC. The latter usually show higher PFAS removal [114–117] and faster equilibrium kinetics (indicatively ≤24 h vs > 100 h) than GAC due to the smaller granule size, the higher surface area, and faster intraparticle diffusion kinetics. Because of the small granulometry, PAC is less frequently employed in water treatment plants as i) it is more easily fouled by natural organic matter (NOM, i.e., the fraction of OM found in natural environments primarily arising from the decomposition of animals and plants) [37]. And ii) it implies a greater flow resistance in a packed column to an equivalent volume of GAC. PFAS removal by AC is reported to be mainly driven by hydrophobic interactions [60]. In general, pore dimensions significantly affect the adsorption process of PFAS on AC [118–120] and highly microporous AC can be more easily blocked by NOM [120–122]. Nevertheless, the chemistry and dimensions of OM also plays an important role: low molecular weight DOC seems to selectively adsorb on the microporous fraction of ACs, competing with anionic PFAS. Differently, adsorption of PFOA and PFOS on activated carbon felts (ACFs) did not noticeably decrease in co-presence of 5 mg/L of Suwannee River NOM (which shows a relatively high molar weight of 24 kDa). This result was attributed to a size exclusion effect by the microporous materials [123].

Some recent works also underlined that the surface chemistry of activated carbons (and, by extension, of carbon-based materials

Table 3
Polysaccharide-based materials used for PFAS sorption and relevant parameters investigated.

Material	Mat. Conc. (mg/L)	PFAS	C_0 PFAS (mg/L)	Adsorption capacity (μmol/g)	% removal	Eq. time (hours)	Recyclability	Ref.
Crosslinked chitosan beads	Not specified	PFOS	165	5500[a] 1830[b,j]	–	30–108	–	[6]
Quaternized cotton	100	PFOA	190	3100[i]	–	4	–	[7]
		PFOS	230	3300[i]		12		
Aminated rice husk	100	PFBA	10	1700[a] 300[c]	–	3	–	[8]
		PFOA	10	2488[a] 1260[c]		5		
		PFOS	10	2649[a] 1660[c]		9		
PEI-f-CMC	20[d] 10[e]	PFOA	0.001[d] 0.002–0.05[e]	6[a]	~87%[d]	~15–20 min	The performance of PEI-f-CMC was maintained over eight consecutive adsorption/desorption cycles to remove PFOA.	[9]
	25	22 additional PFAS	0.001 (each PFAS, tested separately)	–	C4–C6 PFCA/PFSA, 4:2 FTS, ADONA: <50% C6–C7 PFSA, 6:2 FTS: ~60% C8–C13 PFCA, C8–C10 PFSA, F–53B, 8:2 FTS, C9–C10 FOSAs: >90%[l]	2		
RAPIMER	25[d] 20[e]	PFOA	100[d] 25–400[e]	7735[a] 8522[c]	99%[g] 98.4%[h]	30	(Designed as self-degrading material)	[10]
		PFOS	0.001[f]	5998[a] 8299[c]	100%[g] 99.2%[h]	45		
PEI-BA	250[d],[e]	PFOA	50[d] 25–500[e]	675[a] 275[c]	–	4	50%/50% (v/v) H_2O/EtOH PFOA only partially desorbed, and the removal efficiency of PFOA decreased by ~ 50% in 5 cycles	[11]
PEI-LF				609[a] 285[c]				
PEI-PP				663[a] 180[c]				
PDA-CGF	500[d],[e]	PFOA	50[d] 25–250[e]	501[a] 111[c]	–	3	5 cycles, MeOH Re-sorption of PFOA on the adsorbents maintained at ≥80% over 5 cycles	[12]
PAN-CGF				562[a] 152[c]				
pMPD-CGF				552[a] 104[c]				
		PFBA		125[b]		–		
QNC	32[d],[e]	PFOA	5[d] 1-50 (PFOA, PFOS);	978[a] 140	–	~2	[k]	[13]
		PFOS	1–100 (PFBA); 1–250 (PFBS)[e]	1118[a] 375[c]	–	1 min		
	320[d],[e]	PFBA	60 (for each PFAS, in multi-PFAS experiments)	565[a] 91[c]	–	~15 min		
		PFBS		1063[a] 74[c]	–	~15 min		
QWP1.5	10[d],[e],[m]	PFOS	375–4000[e]	1526	>95% (after 30 s), >95% (after 60 min)[m]	8	[k]	[14]
		PFOA	380–3437[e]	1461	>80% (after 30 s), >80% (after 60 min)[m]	24		
		PFBA	–	–	~13% (after 30 s), ~20% (after 60 min)[m]	–		
		PFBS	–	–	~30% (after 30 s), ~40% (after 60 min)[m]	–		
		GenX	–	–	~25% (after 30 s), ~30% (after 60 min)[m]	–		
		6:2 FTS	–	–	~85% (after 30 s), ~90% (after 60 min)[m]	–		

[a] Q_m (Langmuir).
[b] Experimental Q_e.
[c] Q_e (pseudo-second order).
[d] In kinetics experiments.
[e] In isotherm experiments.
[f] In continuous flow experiments.
[g] In PFOS + PFOA flowing solution.
[h] In mixed pollutants solution.
[i] Experimental Q_m.
[j] According to the double exponential model.
[k] Not designed to be reused.
[l] % removal of 21 additional PFAS from lake water.
[m] In adsorption experiments with a mixed PFAS (PFOS + PFOA + PFBS + PFBA+6:2 FTS + GenX) solution (concentration of each PFAS = ~2.5 μg/L).

Table 4
Polyaniline -based and polyacrylonitriles materials used for PFAS sorption and relevant parameters investigated.

Material	Mat. Conc. (mg/L)	PFAS	C_0 PFAS (mg/L)	Adsorption capacity (μmol/g)	% removal	Eq. time (hours)	Recyclability	Ref.
ASFPAN10	240	GenX	100	600[b]	35	not applicable	–	[15]
ES(PAN/ Algae)	240	GenX	100	~900[b]	65–75	not applicable	–	[16]
PANI	10[d,e,h]	PFHpA	0.05[d] (PFOA)	–	~80[h]	–		[17]
		PFOA	0.001–1[e] (PFOA)	**99**[a]	~99[h]			
			0.005[f]	**11**[c]				
		PFNA		–	~99[h]			
		PFBS		–	~75[h]			
		PFHxS		–	~99[h]			
		PFOS		–	~99[h]			
		6:2 FTS		–	~75[h]			
POT		PFHpA		–	~99[h]		MeOH + 10 g/kg NaCl	
		PFOA		**120.75** [a]	~99[h]		>90% PFOA removed over 5 cycles	
				12[c]				
		PFNA		–	~99[h]		>93% of PFAS in the PFAS mix. Desorbed except for PFBS	
		PFBS		–	~99[h]			
		PFHxS		–	~99[h]			
		PFOS		–	~99[h]			
		6:2 FTS		–	~99[h]			
PASNT	200[d,e]	PFOA	250[d]	3301[a]	–	40	–	[18]
		PFOS		2657[a]		40		
PANI	10[d,e]	PFOA[i]	0.05[d] (PFOA)	99[a]		5	MeOH with 1% NaCl, room temperature, 6 h	[19]
			0.001–1[e] (PFOA)	11[c]				
		PFHpA	0.2×10^{-3} - 0.3[e] (multi-PFAS solution)	4	91.2		At least 63% recovery of each PFAS in desorption tests (multi-PFAS solution)	
		PFOA		5	97.8			
		PFNA	0.001[g] (multi-PFAS solution)	9	99.9			
		PFBS		6	92.0			
		PFHxS		13	99.5			
		PFOS		15	100.0			
		6:2 FTS		17	93.9			
PANI_PFA_2.4		PFOA[i]		197[a]		5		
				12[c]				
		PFHpA		3	74.6			
		PFOA		8	90.0			
		PFNA		12	97.8			
		PFBS		–	54.2			
		PFHxS		10	53.7			
		PFOS		13	98.9			
		6:2 FTS		8	89.2			

[a] Q_m (Langmuir).
[b] Experimental Q_m.
[c] Q_e (pseudo-second order).
[d] In kinetics experiments.
[e] In isotherm experiments.
[f] Concentration of each PFAS in a multi-PFAS solution.
[g] In batch removal efficiency experiments.
[h] In multi-PFAS removal experiments.
[i] Only PFOA tested in both single-PFAS solution and as part of the multi-PFAS solution.

obtained by chemical-thermal treatment) is of great importance for the uptake of anionic PFAS [123].

As far as IERs are concerned, they show better overall results than ACs [124,125], with yet great variability in sorption equilibrium time and efficiency depending on experimental conditions [105] or the resins constituent material [126,127].

Compared to ACs, resins can be more easily regenerated and reach equilibrium earlier [99]. However, IERs are less frequently applied in full-scale plants than ACs, being more expensive by weight and often having to be pre-treated [84,92]. Moreover, resins and sorbents that mostly rely on ion-exchange as the main removal mechanism are particularly affected by naturally occurring ions and ionic substances that can both compete with PFAS for exchange sites and/or promote salting-out effects [128–130], as opposed to adsorbents that rely on hydrophobic interactions/hydrogen bonding [98].

Breakthrough of the more hydrophilic, short-chain compounds is reached sooner in continuous-flow systems [88,100,119,131]. This necessitates the early replacement of the material and significantly increases treatment costs [92,132]. However, the removal performance of PFAS other than the legacy long-chain PFAA still needs to be studied (Tables S1–S2). Moreover, ACs and IERs are hardly assessed at environmentally relevant concentrations in batch experiments (ng/L-μg/L range).

3.2. Alternative adsorption materials

3.2.1. Modified ACs

Owing to their limitations, ACs have been physically and chemically modified to enhance PFAS uptake, with different but relevant results (Table 1). Physically- and chemically-modified nanocomposite ACs (PAMTAg and CAMTAg) showed relevant adsorption capacity of PFOA and PFOS, especially as regards CAMTAg (690 μmol/g and 588 μmol/g, respectively) and impressive

Table 5
COFs and MOFs used for PFAS sorption and relevant parameters investigated.

Material	Mat. Conc. (mg/L)	PFAS	C_0 PFAS (mg/L)	Adsorption capacity (μmol/g)	% removal	Eq. time (hours)	Recyclability	Ref.
28% [NH_2]- COF	0.2–100[a] 10[c,f]	GenX	10[a] 0.2–100[c]	605.95[d] 636.25[g]	~90% (GenX) >90% (12 PFAS) and 63% (PFBA)[f]	1–30 min.	–	[20]
Covalent triazine-based COF	250[a,c]	PFOA PFOS PFHxA PFHxS PFBA PFBS	4- 259[a] and 0.006–0.015[a] 60-415[a] and 0.006–0.015[a] 7–217[a] 19–180[a] 7–204[a] 6–247	650[d] 1330[d] 1200[d] 560[d] 430[d] 470[d]	–	–	Desorption medium = 50:50 (v/v) EtOH/H_2O 4 cycles Adsorption of PFOA and PFOS remained quite constant (~70%), as for desorption (~95% for PFOS, ~90% for PFOA)	[26]
Chitosan/F–COF	1–100[a] 0.2[c] 100[h,j]	PFOS	100[a] 1–1000[c]	198.35[g] 16610[d]	~100% UPW ~97% LW ~95% SW	4	–	[21]
		PFOA		209.63[g] 14918[d]	~100% UPW ~90% LW ~88 SW			
		GenX		237.12[g] 13263[d]	~100% UPW ~90% LW ~92% SW			
FSQ-1	1000[a] 100[f]	PFOS	1–250[a] 0.001[f]	709.82[e] 749.81[d]	85% (in >15 min)[f]	15 min.	–	[22]
		PFOA		876.66[e] 893.57[d]				
		GenX		999.82[e] 1033.15[d]				
		F–53B		590.53[e] 597.54[d]				
		6:2 FTAB		573.31[e] 592.60[d]				
Hollow Cys-COF nanospheres	100[a] 1000[c] 10[j] 50[f]	PFOS	1–350[a] 1000[c]	1159.70[d] 197.31[e]	>95% (PFOS, PFOA, PFOPA) 95–100% for 20 PFAS, and 80–90% for PFBS and PFBA[f]	5 min.	3 cycles, ~5% decrease in the uptake of 22 PFAS	[23]
		PFOA		1393.48[d] 232.59[e]				
		PFOPA		1065.12[d] 205.32[e]				
		PFBS		1182.94[d]				
		PFBA		1149.32[d]				
β-CD-TPA-COF (COF1)	250	PFBS	0.1 mmol/L[c]	330[d]	~40%	2 min.	MeOH, 4 cycles, 4% uptake reduction of PFOS	[25]
		PFHxS	0.05–0.65 mmol/L[a]	550[d]	~60%			
		PFOS		1510[d]	>95%			
		F–53B		1900[d]	~95%			
BT-BDB-COF (COF2)	50[a,c]	GenX	24.95[c] 16.50–198.03[a]	1260[e] 2060[d]	80% (in 6 h)[c]	<12	70% MeOH and 1% NaCl, 4 cycles, 8% and 14% lower uptake of GenX and HFPO-TA, respectively	[24]
		HFPO-TA	37.51[c] 24.81–297.66[a]	1550[e] 2160[d]	92% (in 6h), 100% (within 12 h)[c]	<12		
COF–F1N5	250[a,c]	PFOS	50[c] 50[j] 10–40[a]	879.8[d] 298.3[e]	78%[j]	6 h	Spent COFs were regenerated via 70% MeOH- 1% NaCl	[27]
		PFHxS	40[c] 40[j] 8–32[a]	300.2[d] 228.8[e]	60%[j]	6 h	Over 4 cycles, PFOS and PFHxS adsorption decreased by ~10% and ~16%, respectively, and desorption of both compounds was maintained at ~90%	
		PFHxA	31.4[j]	–	50%[j]	–		
		PFBS	30[j]	–	55%[j]	–		
		GenX	33[j]	–	45%[j]	–		
		F–53B	53[j]	–	80%[j]	–		
NU-1000	200[g,f]	TFA	100	1760[g]	–	1 min	30:70 (v/v) of a 0.1 M HCl:MeOH solution, 5 cycles, no appreciable decrease in PFBS removal	[28]
		PFBA		1280[g] 2125[d]	85%[f]	10 min		
		PFPeA		1300[g]	97%[f]	1 min		
		PFHpA		1160[g]	99%[f]	1 min		
		PFOA		1220[g]	99%[f]	1 min		
		PFDA		1170[g]	99%[f]	1 min		
		PFBS		1350[g]	99%[f]	1 min		
		PFHxS		1370[g]	99%[f]	1 min		
		PFOS		1240[g]	99%[f]	1 min		
SCU-8	5000[c]	PFOS		89.56[d]	>95%[c]	10 min	Desorb. Medium = mixed salts solution. 43% PFOS desorbed (1st cycle),	[33]

Table 5 (*continued*)

Material	Mat. Conc. (mg/L)	PFAS	C_0 PFAS (mg/L)	Adsorption capacity (μmol/g)	% removal	Eq. time (hours)	Recyclability	Ref.
							sorption rate ~44% (2nd to 4th cycle)	
PCN-222	75[a,c]	PFOS	50–500[a] 500[c]	4058.94[d] 4512.83[e]		30 min.	–	[31]
MOF-808	75[a,c]	PFOS	50–500[a] 500[c]	1878[d] 1666[e]		30 min.	–	[30]
MIL-101 (Cr)	100[a]	PFOS	0.5–2[a]	20.30[d]	71.19%[a]	15 min	1:1 (v/v) EtOH:H_2O, 4 cycles, 60% reduction of PFOS uptake	[29]
MIL-101 (Cr) $-NH_2$		PFOS	0.5–2[a]	5.66[d]	20.52%[a]	30 min	–	
DUT-5-2	200[a,c,i]	PFOS	30 mg/L[c] 10–140 mg/L[a]	2029.47[d] 294.92[e]	96.6 (pH = 3) <60% (pH = 7)	~10 h	30 mL MeOH (once) and ultrapure water (3 times), 4 cycles	[32]
		PFOA		1144.01[d] 218.32[e]	60 (pH = 3) <30% (pH = 7)		After 4 cycles, the ads. The efficiency of PFOS and PFOA was ~10% lower, and the regeneration efficiency ~92%	
PAF-45	12.5[a,c,i]	PFOS	100[c] 50–200[a]	10190[e] 11692[d]	~60%[i]	30 min	NaOH (0.5 M) + acetone (90/10 v:v), 6 cycles, no loss in adsorption capacity	[34]

b = Equilibrium concentration.
[a] In isotherm experiments.
[c] In kinetics experiments.
[d] Q_m (Langmuir model).
[e] Q_e (pseudo-second-order).
[f] Adsorption experiments carried out with a multi-PFAS solution.
[g] Experimental Q_e.
[h] In experiments with LW, SW.
[i] Equilibrium sorption experiments.
[j] In single-PFAS adsorption experiments, UPW = ultrapure water; LW = lake water; SW = sewage water.

Table 6
β-Cyclodextrins polymers used for PFAS sorption and relevant parameters investigated.

Material	Mat. Conc. (mg/L)	PFAS	C_0 PFAS (mg/L)	Adsorption capacity (μmol/g)	% removal	Eq. time (hours)	Recyclability	Ref.
DFB-CDP	400[c] 100[d]	PFOA	0.001	82.11[a]	96%[c]	13	4 cycles, MeOH, 10 min.	[36]
TFN-CDP	10	C4– C10 PFCA, PFBS, PFHXS, PFOS, GenX	0.001	–	C6–C10 PFCA, C4–C8 MPFSA: >95%[f] PFBA >80%[f] GenX: ~90%[f]	9[g]	–	[37]
CDP-1	400 (GenX)[c] 100 (GenX, PFOA)[d]	PFOA GenX	10–200[d] 0.2 1–200[d]	1316.69[b] 672.60[b]	 98%[c]	10 min (GenX)	–	[35]
	10[e]	PFBA GenX Other PFAA	0.001[e]		40%[e] 65%[e] >95%[e]			
CDP-2		GenX GenX, PFBA PFHxA, PFHpA, PFOA Other PFAA	0.2 0.001		98% <5%[e] 15–43%[e] 53–75%[e]	24 (GenX)		
β-CD "6	10	C4–C10 PFCA	0.001		>99% for all PFAS in NP >90% for PFHpA, PFOA, PFNA, PFDA; ~85% for PFHxA; 70% for PFHxA; 20% for PFBA	<4h for all PFAS	–	[38]

[a] Experimental Q_e.
[b] Q_m (Langmuir model).
[c] In kinetics experiments.
[d] In isotherm experiments.
[e] In multi-PFAS removal experiments.
[f] After 10 min.
[g] (for a PFOS + PFOA mixture at 1 μg/L for each PFAS); f = in nanopure water: g = in a 1 mM Na_2SO_4 solution.

Table 7
Hydrogels used for PFAS sorption and relevant parameters investigated.

Material	Mat. Conc. (mg/L)	PFAS	C_0 PFAS (mg/L)	Adsorption capacity (μmol/g)	% removal	Eq. time (hours)	Recyclability	Ref.
Bifunct. PEGDA	500	PFOA	103.6	110.6[a]	100	–	70% MeOH with 1% NaCl desorption of PFOA, PFOS, PFBA, and PFBS from both sorbents: >90%; ~84 and 70% GenX released from monofunct. And bifunct. Sorbent, respectively)	[39]
		PFOS	33.3	30.4[a]	91			
		PFBA	106.3	158[a]	60			
		PFBS	111.5	168.9[a]	96			
		GenX	63.8	98.7[a]	95			
Monofunct. PEGDA		PFOA	103.6	109.9[a]	100			
		PFOS	33.3	30.4[a]	91			
		PFBA	106.3	199.5[a]	78			
		PFBS	111.5	190.6[a]	100			
		GenX	63.8	86.7[a]	95			
DMAPAA-Q	70	C4–C8 PFCA, C4–C8 PFSA, GenX, ADONA, F–53B	0.001[d]	–	C4–C8 PFSA: 85–100%; C4–C8 PFCA: ~ BTWN 75–85%; GenX, ADONA, F–53B: ~75–100%; X:2 FTS (X = 4,6,8): ~85–95% ▫▫	<2	Conditions: 0.5 g/L material, 10 mg/L of PFAS (GenX + PFBA + PFOA) solution, 6 h. Desorb. Solution: 50 mL of NaCl/MeOH >95% desorption of GenX, PFBA, and PFOA over 6 cycles	[41]
IF-20+	100	PFOA, PFHxA, GenX[c]	0.05[g] 0.001 and 0.2 mg/L[d]	801[b] (GenX)	PFHxA, GenX: ~80%; PFOA: ~100% (in NOM-spiked and ∑3PFAS-spiked simulated natural water)[c]	~100%, 30 s (GenX)[l]	Washing solution: 400 mM MeOH/$NH_4CH_3CO_2$, 2 min	[40]
		GenX[d,e]	0.2–50 mg/L[e]		C5–C10 PFCA, C4–C6–C8 PFSA, GenX: >95%; PFBA ~50% (2 h)[p]	94%, ≤30 min (GenX)[o]	Removal efficiency of GenX (>90%) and regen. Of IF-20+ were maintained for at least 5 cycles ▫	
		Real matrix tests: 21 legacy and emerging PFAS	0.001 mg/L[f]					
carbon-dot (CD) hydrogelCD66-0.2E/P	25[f] (PFOS) 50[e] 100[d]	PFOS	50[d]	7134.15[b] 939.76[n]		~20 h[d]	Removal of PFOS (>90%) was maintained over 5 cycles (desorption solvent: MeOH).	[42]
			6–460[e]			30 min[m]		
			20[h]					
			0.52×10^{-3}[i]					
		PFBS		2000[b]				
		PFHxS		>3800[b]				
FCH2 (fluorous-core nanoparticle-embedded hydrogel)	1.8	PFOA	10	5.97 (pH = 3.5)	>99% ◊◊	~2 h	acetone/H_2O/2-methyl-tetrahydrofuran; initial ads. Capacity of PFOA maintained over 5 cycles	[44]
			0.001–1	8.60 (pH = 10.5)				
				~6.6 ◊				
	1.8	PFNA, PFOA, PFOS-NH_4, PFOSAmS, PFOSNO[o]	0.001	–	>98.9 % (each PFAS)	–	–	
PNIPA and PNIPAm-functionalized PVDF membranes	4000[d]	PFOA	1000 mg/L[d]	–		15	Desorption of PFOA via temperature swing 5 cycles ~60% of PFOA desorbed after the 1st cycle, then constant desorption over other 4 cycles	[43]

▫ = In near-saturation conditions IF-20+ was suitable for at least a second cycle; ▫ = % removal of PFAS from DI and lake water. % removal from treated WW was 10–20% lower than that of surface waters.
◊ = in the presence of decanoic acid (20 mg/L) or of inorganic salts (100 mg/L).
◊◊ = both in solutions with varying conc. Of PFOA and in solutions with PFOA (1 μg/L) + decanoic acid (20 mg/L) + inorganic salts (100 mg/L).
[a] Experimental Q_e.
[b] Q_m (Langmuir).
[c] Initial PFAS removal efficiency experiments.
[d] In kinetic experiments.
[e] In isotherm experiments.
[f] Batch adsorption tests in environmental water sample.
[g] PFAS removal efficiency experiments.
[h] Experiments on the competition with other hydrocarbons (binary aqueous solutions).
[i] PFOS adsorption in wastewater.
[m] In simulated environmental water.
[n] Q_e pseudo-second order.
[l] Kinetics experiments, high PFAS concentration.
[o] Kinetics experiments, low PFAS concentration.
[p] Removal of 21 PFAS including PFHxA, GenX, PFBS, in real matrix tests.

Table 8
Magnetic NPs-based materials used for PFAS sorption and relevant parameters investigated.

Material	Mat. Conc. (mg/L)	PFAS	C_0 PFAS (mg/L)	Adsorption capacity (μmol/g)	% removal	Eq. time (hours)	Regeneration	Ref.
Fe_3O_4@SiO_2 $-NH_2$&F_{13}	2500[c,d,j]	PFHxS	10-1000[c,i] 200 and 9000[d,j]	32.87[a] 7.3[b]	63-72[h,j]	5 min	5 cycles, separation by external magnetic field, washed thrice with NH_3:MeOH and H_2O:EtOH The removal efficiency of each PFAS and of ∑9PFAS was reduced by 5% over 5 cycles	[47]
		PFOS	$5 \times 10^{-7} - 5 \times 10^{-5}$[k]	139[a] 19.63[b]	86-101[h,j]			
		PFHpA		64.91[a] 10.63[b]	64-75[h,j]			
		PFOA		330.98[a] 15.38[b]	84-91[h,j]			
		PFNA		829.58[a] 19.91[b]	83-99[h,j]			
		PFDA		1453.72[a] 21.16[b]	79-87[h,j]			
1/19-MF-VT		PFOS	25[d] 22.5[e]	2253.41[a] 676.82[b]	98%[l]	~4	MeOH Adsorption efficiency maintained over 5 cycles	[46]
	20–250	PFBS		873.04[a]				
		PFBA		775.56[a]				
		PFOA		1644.65[a]				
Fe_3O_4-CDI-IL MNPs	25-800[c,g]	PFOS	0.05[d]	16.17[a]	93–96[g]	4	10 cycles, no loss of removal efficiency Conditions: [PFOA] = [PFOS] = 200 μg/L, [Cr(VI)] = 1000 μg/L, [Fe_3O_4-CDI-IL MNPs] = 3 g/L, desorption medium = 0.2 M NaOH + 0.5 M NaCl solution	[48]
	200[d]	PFOA	0.04–1[c]	7.5[a]	99[g]	6		
2-MNPs @ FG	250[c] 400[d]	PFOA	0.18[h2] 0.5–40[h1]	121.72[a]	92–95[d]	2 min	5 cycles, sonication, MeOH, 30 min, negligible effects on the adsorption of PFOA and PFOS	[45]
		PFOS	0.18[h2] 0.5–40[h1]	34.39[a]	94–97[d]	2 min		
P2-9+@IONPs	100[c,d] 500[j]	PFBA	0.1[j]	–	84%[j] 40% ◊◊	–	Conditions: conc. GenX = 10 mg/L, conc. P2-9+@IONPs = 1 g/L, 10 min Duration. Desorbing medium: 400 mM methanolic ammonium acetate >99% (>9.9 mg/g) adsorption of GenX, as well as its complete desorption was maintained over 4 cycles	[49]
		PFPeA	0.1[j]	–	97.3%[j] >75%◊◊	–		
		PFHxA	0.1[j]	–	>99.5%[j] >95%◊◊	–		
		PFHpA	0.1[j]	–	>99.5%[j] >95%◊◊	–		
		PFOA	0.1[j]	–	>99.5%[j] >98%◊◊	–		
		PFNA	0.1[j]	–	>99.5%[j] >98%◊◊	–		
		PFDA	0.1[j]	–	>99.5%[j] >98%◊◊	–		
		PFBS	0.1[j]	–	>99.5%[j] >95%◊◊	–		
		PFHxS	0.1[j]	–	>99.5%[j] >98%◊◊	–		
		PFOS	0.1[j]	–	>99.5%[j] >98%◊◊	–		
		GenX	0.1[j]	663.52[a] 605.95[f]	>99.5%[j] >95%◊◊	3 min		
			100[d]					
			0.1–50[c]					

[a] Q_m (Langmuir).
[b] Q_e (pseudo-second-order).
[c] Isotherm experiments.
[d] Kinetics experiments.
[e] Removal of PFOS from AFFF wastewater.
[f] Experimental Q_e.
[g] In batch sorption experiments.
[h] The removal range is based on results of PFAS removal at three different concentrations (0.5, 5, and 50 ng/L).
[i] Single PFAS conc.
[j] In multi- PFAS solution.
[k] Experiments in river water spiked with multi-PFAS solution.
[l] In AFFF WW (aqueous film-forming foam wastewater).

removal kinetics (1min-2 hours) in comparison with commercial ACs (up to approx. ~160 h) owing to the small dimensions of particles [59]. However, aggregation of the nanocomposites (C_0 = 2 g/L) was probably the cause of the limited uptake of CAMTAg. The surface chemistry of ACs was also modified by introducing amine and quaternary ammonium functionalities that greatly increased electrostatic interactions and ion-exchange sites, respectively [60,133,134]. Both functionalities significantly increased the adsorption uptake of selected PFAS, as highlighted for other types of materials [40,93]. Coating the sorbents with molecularly imprinted polymers significantly improved carbonaceous adsorbents' selectivity and uptake kinetics towards PFOS [135]. The adsorption

Table 9
Zeolites used for PFAS sorption and relevant parameters investigated.

Material	Mat. Conc. (mg/L)	PFAS	C_0 PFAS (mg/L)	Ads. Capacity (μmol/g)	% removal	Eq. time (hours)	Recyclability	Ref.
All-silica zeolite β	1000	PFOA PFOS	0.1–500[a] 0.1–250[a,g]	~850[d] ~450[d]	–	~24 ~24	Thermal regeneration (PFOA): 360 °C, 1 cycle, complete removal	[51]
β-zeolite CP811C	1000[a]	PFOA PFBA	5–500[a] 100[c]	222[c] 439[b] 36[c] 130[b]	–	<1	–	[52]
CTAB-coated CP811C		PFOA PFBA		166[c] 41[c]				
β-zeolite CP814E		PFOA PFBA		140[c] 28[c]				
PDADMAC-coated CP814E		PFOA PFBA		128[c] 50[c]				
zeolite– sodium silicate composite	1000	PFBA PFBS PFPeA PFHxS PFDA PFOSA PFPeS 4:2 FTS	1 mg/L for each PFAS in mixture solutions		<20%[f] 30%[f] ~70%[f] 40%[f] 30%[f] 100%[f] 100%[f] 100%[f]	Not applicable[h]	–	[50]
All-silica zeolite β	1000[a]	PFBA PFHxA PFOA PFDA	0.1–500[a]	120[e] 650[e] 870[e] 750[e]			Thermal reg. (PFOS): (550 °C), 3 cycles. Solvent reg. (PFOS): 1 cycle, complete regeneration[i]	[53]

[a] Isotherm experiments.
[b] Q_m (Langmuir model).
[c] Q_e (pseudo-second-order).
[d] Experimental Q_m.
[e] Freundlich model.
[f] In adsorption experiments carried out in WWTP effluent with 53 PPCPs (pharmaceuticals and personal care products) and 8 PFAS (simultaneous occurrence).
[g] a different concentration range was used in isotherm experiments with PFOS to avoid micellation
[h] Continuous flow setup.
[i] Through octane, MeOH + octane, trifluoroethanol + octane.

Table 10
Clay-based materials used for PFAS sorption and relevant parameters investigated.

Material	Mat. Conc. (mg/L)	PFAS	C_0 PFAS (mg/L)	Ads. Capacity (μmol/g)	% removal	Eq. time (hours)	Recyclability	Ref.
Zn–Al LDH	250 [c, d]	PFOA [f] PFBA, PFHpA,	10 [d] 10	1510 [a] 90 [b]	98% at equil.	1–2 h	3 cycles Conditions: pH = 6, [PFOA] = 10 mg/L, [Zn–Al LDH] = 250 mg/L, 24 h,	[56]
Mg–Al LDH		PFOA, PFNA, PFDoA [g]	–300 [c]	1420 [a] 60 [b]	66% at equil.	8 h	solvent washing (MeOH) >98% PFOA removal in all 3 cycles	
CHT	150 [c, d]	PFOS	50 –500 [c] 200 [d]			30 min.	Calcination (450 °C) allowed full regeneration of the material	[58]
YOHCl	250 [c, d]	PFOA	20 [d] 10 –600 [c] 0.5 [e]	2311 [a] 185 [b]	97.1% [h] >91% at lower PFOA conc. (0.5 mg/L) [h]	8h	Conditions: pH = 7, [PFOA] = 20 mg/L, [YOHCl] = 250 mg/L, 24 h solvent washing (MeOH + 1 M NaCl, vol:vol = 1:1) 4 cycles Removal efficiency >80.2% after 4 (down from ~98% in the 1st cycle)	[57]
LDH-CF	250 [c]	PFOA	0.5	3220 [a]	100% [f]	5 min	3 cycles	[54]
LDH-CH	1000 [d]		–350 [c]	2420 [a]	100% [f]	30 min	Conditions: pH = 6, adsorbent conc. = 1 g/L, PFOA conc. = 500 μg/L, 48 h,	
unmodified Zn–Al LDH			0.5 [d]	1150 [a]	approx. 95% [f]	2h	regeneration solvent = 50%:50% H_2O:MeOH added with 1% wt. NaCl LDH-CH and LDH-CF removed ~100% PFOA, while removal by unmodified LDH decreased from approx. 96% (1st cycle) to approx. 86% (3rd cycle)	
HT-NO_3	250 [c, d]	PFOA PFOS		2100 [a] 3219 [a]	96.4% [d] 100% [d]	40 min 5 min	–	[55]
AHT-NO_3		PFOA PFOS		2195 [a] 3215 [a]	45.5% [d] 85.8% [d]	80 min 20 min		

[a] Q_m Langmuir.
[b] Q_e pseudo-second-order.
[c] Isotherm experiments.
[d] Kinetics experiments.
[e] Separate set of low-concentration experiments.
[f] Isotherm and kinetic experiments.
[g] Batch removal experiments of single-solute solutions.
[h] After 8h

capacity towards PFBA and PFBS in a mixed PFAS system increased because of the introduction of quaternary ammonium groups on the GAC via surface modification with poly diallydimethylammonium chloride (polyDADMAC). However, it decreased with an excessive polymer addition because of inner pore blockage induced by the functionalities [60]. A Fe_3O_4 nanoparticles-GAC composite material showed faster equilibrium kinetics (29 h vs > 75 h), equilibrium uptake (880 μmol/g vs 778 μmol/g), and maximum adsorption capacity (1431 μmol/g vs 1110 μmol/g) of PFOA with respect to unmodified GAC. This was attributed to the shifting of the majority of active sites involved in the adsorption from the inner pores of the material to its surface after the functionalization [61]. A MOF-functionalized GAC (MIL-101 (Cr)@AC) also showed faster uptake kinetics (2 vs 3 h) and similar but lower maximum PFOS removal (85% vs 92%) with respect to the non-functionalized AC [29]. The authors proposed that either or both the i) reduction of AC pore size following surface modification and the ii) increased hydrophilicity of the MIL-functionalized GAC (hence the hindrance of hydrophobic interactions between PFOS and GAC) caused the lower removal of PFOS by the functionalized GAC.

Other works highlighted that the defunctionalisation of a carbonaceous surface is another promising path to tailor it for PFAS sorption. Some authors found that the best among different activated carbon felts (ACFs) that were used to sorb PFOS and PFOA showed high anion exchange capacity (AEC) and low oxygen content [123]. Building on those findings, a commercial ACF (CACF) was thermally treated with H_2 (900 °C) to i) reduce the density of repulsive anionic sites and ii) enhance the number of charge-balancing cationic surface sites, facilitating the adsorption of perfluoroalkyl acids (PFAA) anions while preserving the predominantly non-polar nature of the carbon surface [62]. The treatment allowed for removing acidic oxygen-containing groups and increasing the p-electron-based basicity, obtaining defunctionalized CACF (DeCACF). CACF was also functionalized with ethylenediamine (aminofunctionalization) for comparison ($CACFNH_2$). DeCACF turned out as the best of the three adsorbents, showing a 40-fold, 23-fold, and 20-fold higher Q_m for PFOA, PFOS and PFBA, respectively, with respect to CACF. This trend was reflected in a 1 to 3 order of magnitude higher adsorption affinity for the analytes. Not only did $CACFNH_2$ not match DeCACF in terms of increased sorption affinity and efficiency, but because of the sole increase of net positive surface charge (higher AEC than CACF), a significant competition between NOM and PFAS occurred. Carbonaceous sorbents obtained via thermal methods usually show heterogeneous surficial chemistry, and the work by Saeidi et al. highlights the importance of taking this aspect into account when developing a tailoring strategy for the sorption of PFAS. The high affinity of DeCACF for PFOS and PFOA (K_L in the range of 10^7 L/kg) is the result of the combination of surface modifications leading to i) low surface polarity due to decreased oxygen content, ii) a low density of acidic sites (corresponding to a diminished electrostatic repulsion), while maintaining at the same time iii) a sufficient density of charge-balancing cationic sites for organic anions.

3.2.2. Bio-based polymeric and non-polymeric materials

Bio-based adsorbents (bioadsorbents) include natural materials (such as plant-derived parts) that have been used as such or that have been modified by biological, physical, or chemical processes (or a combination thereof). These sustainable materials are widely available and generally low-cost, and they are often obtained from recycled agricultural or industrial waste.

3.2.2.1. Proteins and protein-rich materials.

Due to inherent surface functionality, rigidity, and high specific surface area, proteins are increasingly studied for water remediation [136]. Proteins could be produced in relevant quantities and at very low price starting from highly proteinic biowaste deriving from sectors like agriculture and food industry [2,137]. Proteins and protein-rich materials have been recently tested for removing PFAS from deionized water (DI water) and natural waters (Table 2). Proteins are known to bind PFAS thanks to the presence of differently charged and uncharged terminal groups that allow both physi- and chemisorption [1]. It was found that protein content in extracellular polymeric substance (EPS) in sludge samples is positively correlated to the adsorption capacity of PFOA and that the latter simultaneously interact through the aromatic groups (hydrophobic interactions) and the positively charged amide groups (electrostatic interactions) of EPS with the fluoroalkyl chain and the deprotonated functional group, respectively [138].

Five proteins (in the concentration range of 3.5–350 μM) were used to test the individual removal of 4 PFAS (1 μg/L) in DI, tap, creek, ocean water, and high-ionic strength aqueous media (60 g/L NaCl) in 24 h [2]. Bovine serum albumin (BSA) was able to remove 83–99% of PFOA and GenX from all aqueous media tested, similarly to lysozyme (93% and 96%, respectively, in ultrapure water). Tenfold higher BSA concentration was needed to achieve a similar removal efficiency for PFBA, which was adsorbed by lysozyme by approx. 64–78% in ultrapure water. Additionally, around 75% of PFBS was removed by both proteins in ultrapure water. BSA was affected the least by pH and ionic strength changes, representing the best candidate for removing PFAS from water. BSA is a widely available, low-cost protein easily extractable from by-products of the cattle industry [136]. Nevertheless, increasing ionic strength/salinity via the addition of NaCl (i.e., competition of Cl^- for the binding sites) clearly hindered the uptake of PFAS, as observed for hemp proteins (i.e., a 1:4 albumin:edestin mixture) [1], underlining the role of electrostatic interactions for PFAS removal by proteins. In fact, the highly hydrophilic short-chain PFBA was the most difficult to adsorb and showed the lowest removal at high ionic strength. This is consistent with recent findings suggesting that more hydrophobic PFAS like GenX or PFOS interact with human serum albumin (HSA) mainly via hydrophobic interactions [139,140].

Hemp protein removed >95% $\sum$12 PFAA (C_0 = approx. 160–190 μg/L) from contaminated groundwater, similar to a commercial GAC that is three times more expensive by weight [1], and achieved equilibrium concentration of the same PFAS within 3 h.

With an overall protein composition of globulin (53%) and albumin (44%), powdered *Moringa oleifera* seeds resulted in poor removal of PFOS (Q_m = 1.88 μmol/g) and especially PFBS (10% after 24 h). Globulin has a higher content of aromatic and hydrophobic functional groups with respect to albumin [141]; hence, electrostatic interactions, which are pivotal for short-chain PFAA adsorption, are less likely to occur. However, the encapsulation in nanoporous alginate beads granted the size-exclusion of the high molecular weight (~400 Da) HA (5 mg/L as dissolved organic carbon, DOC) from the pores, as for alginate-encapsulated albumin [5].

Soy protein was used to coat cellulose-based and cellulose acetate-based nanofibrous membranes (CE-SPI and CA-SPI, respectively), increasing GenX uptake (C_0 = 100 mg/L) by approx. three times at pH = 6. In particular, CA-SPI removed up to 90% of GenX (~1100 μmol/g) in a few min. [4].

Proteins can widely differ in aminoacidic composition and can therefore accommodate different types of PFAS in the adsorption process. Although showing exploitable features, the use of the sole proteins as adsorbents is unlikely due to their dimension and

dissolved state, for which recovery methods are not easily implementable. For example, Hernandez et al. (2022) separated the proteins utilizing a molecular weight cutoff-based device. Other than surficial grafting on materials (e.g., CA-SPI), other strategies for the technical implementation of proteins have been carried out. Recently, proteins (albumin) have been used to prepare alginate beads, which adsorbed 87% and ~10% PFBS (beads conc. = 1.5 g/L, C_0 PFAS = 100 μg/L each) after 72 h [5]. Protein nanofibrils (PNFs, also known as amyloid fibrils) are supramolecular structures that can be obtained by the self-assembling of peptides derived from the unfolding of globular proteins [136]. They are emerging as water decontamination agents because of their stiffness, toughness, and flexibility. They can be synthesized by different protein precursors and assembled into filtration membranes that can both adsorb and size-exclude organic and inorganic pollutants [137]. For example, BSA-based PNFs have been used to remove heavy metals, showing high flexibility and durability. Other than full-proteins and hybrid membranes, they can be formed into aerogels and hydrogels by leveraging changes in pH and ionic strength [137]. This indicates the possibility to modulate their composition, physical-chemical, and mechanical properties variedly, and to composite them into hybrid materials. In addition to their chemical and surface area tunability, PNFs are considerably more resistant to enzymatic degradation than other protein-based materials [136,137].

Other strategies, like the coating of nanoparticles with proteins-amino acids (already applied for the removal of other contaminants), could also be explored for PFAS [142,143].

Being environmentally and economically more sustainable than conventional adsorbents, protein-enriched materials are worthy of being further investigated as candidates for PFAS removal from waters. To this end, adsorption kinetics and adsorption capacity should be developed by applying sorption models to the experimental results to compare them to AC and IER properly.

3.2.2.2. Polysaccharide-based materials. A wide range of natural polymers have shown potential applicability for water treatment [113]. Some the low-cost and renewable polysaccharide-based materials such as crosslinked chitosan beads, quaternized cotton, aminated rice husk, poly(ethylenimine)-functionalized cellulose microcrystals (PEI-f-CMC) have been tested for the removal of PFAS, showing high maximum adsorption capacities (2650−5500, 2490−3100, and 1700 μmol/g for PFOS, PFOA and PFBA, respectively) and relatively fast adsorption kinetics (eq. time ranging between a few min. to 12 h) (Table 3) except for materials where intraparticle diffusion played a relevant role for the adsorbent-adsorbate interaction, showing kinetics comparable to those of GAC [6].

Poly(ethylenimine)-functionalized cellulose micro-crystals (PEI-f-CMC) maintained the selective removal capability of 22 PFAS (1 μg/L each) in NOM-spiked solutions (2 mg C/L, correspondent to <5 mg/L NOM) and in lake water, with respect to DI water [9]. However, the competitive removal of the 22 PFAS in DI and lake water was highly dependent on the PFAS chain length. The low adsorption capacity of PFOA (Q_m = 5.6 μmol/g) is possibly related to its low surface area (7.8 m^2/g). The NOM used for the study encompassed two types of organic molecules, with low (and high) specific ultraviolet absorbance (SUVA) and small (and high) molecular weight (<1 kDa and >30 kDa, respectively). The smaller and more hydrophilic molecules hindered the adsorption slightly more, and their presence only slightly affected adsorption, as opposed to conventional adsorbents. This result was ascribed to the mainly mesoporous nature of the functionalized microcrystals, i.e. the increased pore accessibility for the smaller molecules.

Other authors have grafted aminated polymers onto agricultural or industrial residues like balsa wood and plant fibers to adsorb PFOA ($C_0 \geq$ 25 mg/L) [11,12]. The obtained aminated biosorbents showed relatively high adsorption capacities at the low pH = 3 (between 500 and 670 μmol/g) but decreased by roughly 40−50% at pH = 7, indicating the dominant role of electrostatic attraction provided by the amine-rich functionalities for the removal of PFOA. Similarly, wood pulp was used to produce aminated (quaternized) nano- and micro-sized cellulose (QNC and QWP1.5) that were used to remove PFAS from contaminated groundwater ($\sum$PFAS = approx. 11.7 μg/L) and from a mixed 6-PFAS solution (C_0 of each PFAS = ~2.5 μg/L) with comparable results concerning the low uptake of short-chain PFAS (e.g. <10−20% of PFBA removal) and novel PFAS (30% removal of GenX by QWP1.5) [13,14]. Differently form PEI-f-CMC, the addition of mainly high-SUVA HA (20 mg/L) caused a dramatic drop in the adsorption of PFAS (removal % of PFBA, PFOA, GenX, and 6:2 FTS were approx. 5, 4, 4, and 11 times lower after 60 min), probably showing the effect of the highly positive zeta potential (+43 mV). The authors indicated the hydrophobic-driven adsorption of HA to the surface of wood pulp as a barrier to the adsorption sites. The different result with respect to PEI-f-CMC could be due to the more than 10-fold higher OM concentration used for QWP 1.5, or to the different content in lignin (more hydrophobic than cellulose) in the latter, that could have facilitated hydrophobic interactions with the material. This is in contrast with what is reported for other materials like PAN and anion exchange resins for which the experimental results were explained by the inverse relationship between hydrophobicity and material interaction with NOM.

Other highly positive surface charged materials like polyDADMAC-coated GAC (zeta potential = 21.2 ± 1.7 mV) showed enhanced removal of anionic PFAS when in presence of 15 mg/L of HA, a behaviour attributed to the suppression of the surficial electrostatic repulsion between PFAS and the adsorbed HA.

In general, and not limitedly to the materials cited in this section, the relationship between the characteristics of NOM and the chemistry of the sorbents should be better examined in consideration of the NOM chemistry, charge, and dimensions.

The lignocellulosic-based nanoframework RAPIMER [10] stands out not only in terms of adsorption capacity (Q_m = 7735 μmol/g and 5998 μmol/g for PFOA and PFOS, respectively, according to the Langmuir model), but also as an agricultural residue-derived material that can simultaneously adsorb and degrade PFAS. This is due to the synergistic combination of a nano-dimensioned amphiphilic sorption framework and the in-situ enzymatic degradation of PFAS provided by a white rot fungus that is also able to biodegrade the material itself. The identification of two degradation products after two weeks ($C_7HF_{13}O$ and $C_6HF_{11}O_2$, hypothesized to be perfluoroheptanal and perfluorohexanoic acid, respectively) confirmed the potential biodegradability of the material. PFOA and PFOS were efficiently removed (>98%) both in continuous-flow experiments from a PFOS + PFOA mixed solution (1 μg/L each) and from a pre-filtered rainwater sample spiked with PFOS, PFOA, naturally occurring metal ions, and an anionic dye (1 mg/L each).

The materials presented hereby contain a mixture of cellulose, hemicellulose, and lignin. Lignocellulosic raw materials required for their production are widely available and can be cheaply obtained by waste and byproducts of many sectors. The synthesis of the materials is quite simple: in the case of microcellulosic and nanocellulosic materials, it relies on the depolymerization of the polysaccharide structure by sequential addition of NaOH, followed by acid hydrolysis (typically using HCl) and pH neutralization, and washing with water. Functionalizing agents are added in the solution at given pH [9,11,13,14]. Some polysaccharide-based materials maintained high removal efficiencies over 5 to 8 regeneration-adsorption cycles, and others were tailored to be one-shot materials given the low production costs [10,13,14]. This further

corroborates their use as alternatives to AC and resins. Although promising, polysaccharide-based materials represent a quite unexplored alternative for the removal of micropollutants. Some evident downsides from the existing literature include the high starting concentration of PFAS, and the low removal of short-chain PFAS in mixed solutions. The latter could be compensated by the simple addition of more of the low-cost adsorbents, but experimental evidence indicate that excessive dosage decreased the uptake of PFAS [14]. These trends should be verified and further investigated in future studies.

3.2.3. Polymeric materials

3.2.3.1. Polyanilines and polyacrylonitriles. Bearing both amine- and imine-groups and benzene rings in the backbone, polyanilines show potential for PFAS sorption mostly by means of hydrophobic and electrostatic interactions (other than accommodation of (hemi) micelles in the mesopores [17,18]. Such low-cost polymeric materials are characterized by a large surface area, are easily synthetized, and implemented in terms of both functionalization and increase of the SSA and are therefore appealing for water remediation.

Polyaniline (PANI) and PANI-derived polymers have been tested for the adsorption of PFAS and compared with AC and resins, showing similar adsorption equilibrium kinetics (1 h–40 h) than the conventional adsorbents but higher tolerance to NOM (2 mg/L) [17,19]. The small polymeric-specific surface area (SSA) of powdered PANI (approx. 25.4 m^2/g vs the 1–2 order of magnitude greater SSA of GAC) may limit its use [18], and strategies to increase SSA were implemented. As result, polyaniline nanotubes (PASNT) were able to adsorb up to 3300 μmol/g and 2650 μmol/g of PFOA and PFOS, and Q_m (PFOA) of paraformaldehyde-crosslinked PANI, PANI_PFA_2.4, (SSA = 490.3 m^2/g) doubled with respect to PANI. However, intraparticle diffusion of short-chain PFAA in PANI_PFA_2.4 was hindered in a multi-PFAS solution because of pore blockage by long-chain PFAA, a mechanism already documented for intraparticle diffusion-based materials like GAC. On the other hand, POT showed a better adsorption performance than PANI in multi-PFAS solutions at environmental concentrations, matching that of PAC at lower initial PFAS concentrations (>98% for all PFAS, including PFBS and 6:2 FTS) but was outclassed by PAC at higher concentrations and at higher ionic strength.

Polyacrylonitriles (PAN, a synthetic polymer with a repeating unit composed of acrylonitrile monomers) have been chemically modified to bestow PFAS adsorption properties. Electrospun nanofibrous PAN have been functionalized with hydroxylamine to yield ASFPAN, that was able to adsorb up to 600 μmol/g of GenX (100 mg/L) at pH = 4 [15]. The high content of positively charged amidoxime at low pH countered the typical overall negative charge of PAN but made ASFPAN sensibly less effective at higher pH.

Moreover, these materials have the potential to be combined with other non-conventional treatment methods to yield satisfactory results. For example, Mantripragada et al. [16] enhanced electrospun polyacrylonitrile nanofibrous membrane with microalgae (*Chlorella*) to entertain a synergistic effect and improve the removal efficiency of GenX from water, obtaining ES(PAN/Algae). They observed that at pH = 6, the maximum removal capacity of ES(PAN/Algae) was ~900 μmol/g, significantly higher than the electrospun PAN nanofibrous membrane (ESPAN). The main adsorption mechanisms could be attributed to hydrophobic interaction, dipole–dipole interaction, and hydrogen bonding, all of which were synergistically enhanced in the algae-functionalized material according to FTIR and XPS analysis.

3.2.3.2. Organic frameworks. Organic frameworks are two- or three-dimensional crystalline porous materials in which monomers are linked via strong covalent bonds with great precision so that a defined chemical composition and porosity characterize the whole structure. Covalent organic frameworks (COF) differ from metal-organic frameworks (MOF) as the latter includes metal ions in their structure, thus allowing Lewis acid-base interaction between PFAS and the metal node, in addition to hydrophobic/electrostatic interactions and hydrogen bonding. Both COFs and MOFs show exceptional porosity, surface area (in the range of thousands of m^2/g), and tunability [21,144]. MOFs are receiving significant attention among recently developed materials to be used as adsorbents for PFAS and other organic pollutants, and several reviews have already been produced on this topic [113,145,146]. This review will only cover aspects relevant to its scope.

COFs and MOFs showed exceptional removal performances for long- and short chain PFAA, as well as substitutes (Table 5). Reported Q_m (Langmuir model) of PFBS, PFBA, PFOA, PFOS, GenX, F–53B and HFPO-TA range between 330 and 1183, 1149–2125, 893–14918, 90–16600, 576–13260, 598–1900, and 2160 μmol/g, respectively. Sorption equilibrium is also typically achieved in ≤30 min, even in multi-PFAS solutions. Many authors underlined that the different interactions (electrostatic, fluorophilic, and hydrophobic interactions, as well as ion-exchange and hydrogen bonding) offered by COFs and MOFs, together with the channel size dimension, are at the base of their high adsorption capacity.

Differently modified COFs were able to achieve very high removal of PFAS in mixed solutions, in environmental samples (as such and spiked with ng/L to μg/L level of PFAS), and in presence of NOM. 28%[NH_2]-COF removed >90% of 12 PFAA and >60% of PFBA (1 μg/L each) within 30 min. Chitosan/F–COF removed 88–98% of PFOS, PFOA, and GenX (200 μg/L each) in natural surface water and sewage water. FSQ-1 and hollow Cys-COF were tested for the removal of 22 (FSQ-1) and 24 (hollow Cys-COF) PFAS (1 μg/L each), among which long- and short-chain PFAA, 2 PFECA (hollow Cys-COF), and 2 cationic and 1 zwitterionic PFAS (FSQ-1). They both removed 95–100% of 20 out of 22 PFAS (approx. 80% of PFBA and PFBS) in DI water and were only partially affected (approx. 10% or lower removal of every compound) by an equivalent concentration of co-occurring contaminants like phenol and n-nonanoic acid (hollow Cys-COF), as well as NOM-enriched waters and river water (FSQ-1) in the same conditions. In particular, FSQ-1 showed a broad-spectrum removal of zwitterionic, cationic, and anionic PFAS at environmental pH values. Only PFBA, PFBS, GenX and F–53B suffered a >10% uptake reduction by hollow Cys-COF in the presence of the tested co-occurrent organics. Similarly, the sorption of GenX and HFPO-TA by COF-2 in the presence of 70 mg/L of HA was only reduced by 20% and 2–3%, respectively. However, the environmental matrix significantly affected the adsorption efficiency on COF-2: the removal of GenX and HFPO-TA in wastewater was approx. 70% and 30% lower than in DI water. This result shows that HA is not an exhaustive proxy for NOM, and tests with sorption competitors as other micropollutants should be carried out (especially in the case of materials with a precise pore size), e.g., with structurally equivalent PFAS compounds with similar dimensions, like non-fluorinated surfactants. NOM influence on PFAS sorption depends on OM dimension [121] and chemical composition [147].

Hollow Cys-COF, FSQ-1, COF-2, and COF–F1N5 were also benchmarked against AC and resins in the same experimental conditions, showing improved performance (Fig. 1) in both multi-PFAS (Hollow Cys-COF, FSQ-1, COF–F1N5) and single-solute (COF-2) adsorption experiments, carried out in ultrapure water (Hollow Cys-COF, FSQ-1, COF-2) or electroplating wastewater (COF–F1N5). Hollow Cys-COF also showed a consistently better removal of a wide range of PFAS in as-such and NOM-enriched DI water with respect to commercial PAC.

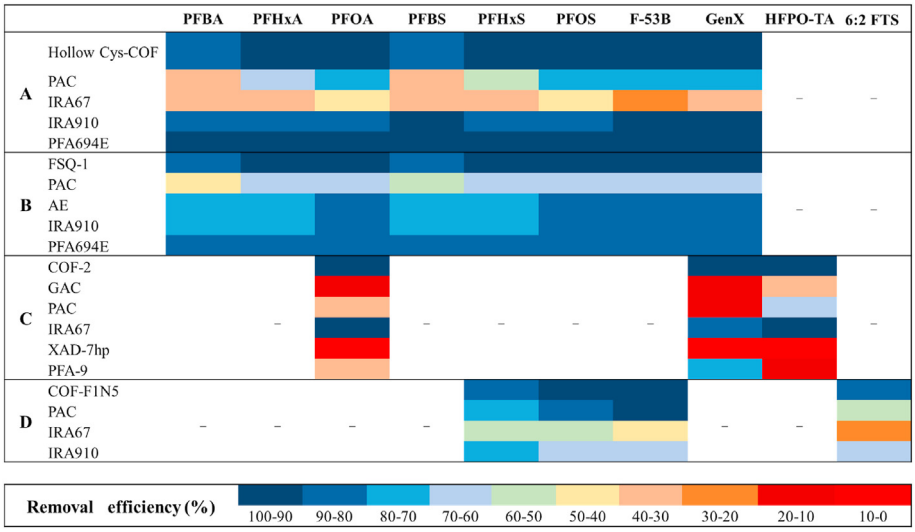

Fig. 1. Removal of selected PFAS by COFs (hollow Cys-COF, FSQ-1, COF2, COF−F1N5), activated carbons (PAC, GAC), commercial resins (IRA67, IRA910, PFA694E, XAD-7hp, PFA-9). Experimental conditions: A) C_0 of each PFAS = 1 μg/L, C mat. = 50 mg/L; B)) C_0 of each PFAS = 1 μg/L, C mat. = 100 mg/L; C)) C_0 GenX = 25 mg/L, C_0 PFOA = 31 mg/L, C_0 HFPO-TA = 38 mg/L, C mat. = 66.7 mg/L, D) C_0 PFOS = 392.1 mg/L, C_0 PFHxS = 10.9 mg/L, C_0 6:2 FTS = 93.4 mg/L, C_0 F−53B = 2.0 mg/L, C mat. = 250 mg/L "-" = not tested. Figure adapted from: [22,23].

MOFs are commercially available and have been produced on a ton scale [148]. Among MOFs, NU-1000 showed extremely fast equilibrium kinetics (1−10 min) for all tested PFAS, and the removal of PFAS in mixed solution (PFSA C4-6-8, PFCA 4-5-7-8-10, 100 μg/L each) was around 97% (90% for PFBA). In experiments with polluted groundwater samples (C4 to C8 PFSA and PFCA, and 6:2 FTS, μg/L range) long- and short-chain PFAA were still efficiently removed (approx. 80−100%), but in samples with higher conductivity (300−26000 μs/cm) the removal of short-chain PFAA like PFPeA and PFBA dropped dramatically (down to 18% and 10% respectively). This could be attributed to a high concentration of anions that act as sorption competitors since anion exchange was found to be the leading sorption mechanism in NU-1000.

According to their structure (especially to their metal node composition), three MOFs (NU-1000, UiO-66, and ZIF-8) showed consistently different selectivity towards anionic, non-ionic, and zwitterionic PFAS, as opposed to the non-selective GAC. Sorption of anionic PFAS was mainly dependent on electrostatic interactions, while acid-base interactions dominated the non-ionic/zwitterionic PFAS sorption [130].

As far as regeneration and reusability of the adsorbent materials are concerned, the sorption efficiency of PFOS by SCU-8 [33] decreased significantly after the first desorption cycle (and still adsorbing around 44% from the 2nd to the 4th cycle), possibly because of immobilization of the PFAS molecule in the organic framework occupying active sites. The strong electrostatic bonds between PFOA and the amine functionality of a polyacrylamide-modified MOF also allowed a max. Desorption rate of 77% [149]. NU-1000 on the other hand showed very good removal capacity (96−100%) and recovery rates (86−105%) of PFBS (10 mg/L) after 5 sorption-desorption cycles. COFs maintained very good removal rates of different PFAS after 3−5 cycles. In particular, the removal efficiency of 22 PFAS by Hollow-cys-COF was only 10% lower in the 3rd cycle.

In the case of MOFs, the type of metal nodes (in addition to the nature and length of the ligands used as linkers in the synthesis step and the presence of structural defects) play an important role in the adsorption process. Longer ligands were related to a larger pore size and therefore to a higher sorption capacity due to the easier diffusion of PFOS in the framework [150]. Cr^{3+} as a metal node showed a higher affinity (i.e., higher binding energy) and consequently increased sorption capacity towards PFOS compared to the equivalent Fe-based MOF [151]. Inducing structural defects in a defect-free UiO-66 MOF increased the structure's surface area, allowing a fast diffusion of PFOS in the larger pores. The maximum value of sorption efficiency obtained for this modified material was twice the AC and IER [152]. In some cases, the increased degree of electrostatic interactions offered by amine-containing functionalities played a more important role than surface area for PFOA uptake, which was lower for the non-functionalized MOF despite its higher surface area [153]. The modification of another (Cr)MIL-based MOF also negatively impacted the overall porosity, and therefore, the uptake kinetics (eq. time up to approx. 180 h) of PFOA, although higher overall PFOA removal was still observed compared to an AC with 15-fold higher surface area [149].

In general, the degree of functionalization and the nature of functionalities have to be properly evaluated and balanced, as an excess of functional groups can hinder the accessibility to the pores, obstacle the surficial hydrophobic interactions [20], or modify the pore size with different results depending on the single PFAS dimensions [24]. For example, nanosized AC proved to be a better PFOS adsorbent with respect to the hydrophilic MIL-101(Cr) and its aminated version MIL-101(Cr)−NH_2 and was only outperformed in terms of sorption equilibrium kinetics (but not adsorption capacity) by MIL-101(Cr)-functionalized AC. The lower removal of PFOS by the MOF-functionalized AC could be attributed either to the hydrophilic nature of the MOF, the reduced pore size of the composite material, or the hindrance of the PFOS-AC hydrophobic interactions induced by the MIL-101(Cr) coating. More interestingly, MIL-101(Cr)−NH_2 showed the worst adsorption performance despite having the highest pore size, possibly because of the steric hindrance induced by the amine groups in the mesopores [29].

Many fluorinated functionalities/crosslinkers could be used to improve selectivity towards and uptake of PFAS. Computational simulations can assist the researcher in the selection of the most effective ones by predicting structural and behavioural changes. Some authors used virtual modelling (e.g., density functional theory -DFT- and Monte Carlo simulations) to study the effect of post-

synthetic surficial grafting of perfluoro alkanes on selected MOFs, as well as the substitution of their linkers with trifluoromethyl groups or with fluorinated inorganic anions, on PFOA adsorption [154]. Differently from the organic linker and the organic functionality, the fluorinated inorganic anions incorporation increased the hydrophilicity of the MOFs (by acting as water-attractive sites) resulting in a lower adsorption capacity towards PFOA with respect to organofluorinated MOFs (though it could be advantageous for the removal of the more hydrophilic PFAS).

While the impact of OM on organic frameworks (SI part 2) is minimal, it has been limitedly discussed. HA in the 10–40 mg/L concentration range did not negatively affect the adsorption of PFOA on a covalent triazine framework (CTF), and that of PFOS was only reduced by 12%. The small pore size (1.2 nm) of the material with respect to those of the tested adsorbates (0.8 × 0.36 nm and 1.04 × 0.40 nm for PFOA and PFOS, respectively) was indicated as the cause [26]. Reasonably, this also applies to other COFs like chitosan F–COF, hollow cys-COF, FSQ-1, COF1 and COF2 (pore size <5 nm) and to MOFs that are reported to exhibit pore sizes <10 nm [28]. The applicability of COFs and MOFs is limited by the granule dimensions, as for all powdered materials. Column packing comes at the expense of important pressure drops, while effective dispersion in the fluid has to be granted to avoid aggregation of particles [146]. Furthermore, they can agglomerate in aqueous environments. Most MOFs are also unstable in aqueous environments and show a lifespan ranging from hours to days, after which ligand displacement and/or hydrolysis can occur [145], a topic that should be further addressed as a major downside of MOF as pollutants adsorbents in aqueous environments. Moreover, MOFs are very expensive, with a retail price of some commercialized MOFs reported between 10000 (e.g., MIL-101) and 15000 USD/Kg [155].

3.2.3.3. Cyclodextrins. Cyclodextrins (CD) include both natural (starch-derived) and artificial cyclic oligosaccharides composed by a different number (≥6) of α-1,4 -linked glucopyranose units that form a truncated cone-shaped three-dimensional structure with amphiphilic nature (hydrophobic inner and hydrophilic external surface area, respectively) that enables a host-guest interaction mechanism in which guest molecules can be encapsulated in the hydrophobic cavity.

β-Cyclodextrins (β-CD) are cheap (reportedly 1 USD/Kg, metric ton scale) and sustainably-produced materials [156,157] and have been modified in different ways to enhance the affinity towards PFAS (Table 6). Namely, β-CD-based materials for PFAS adsorption have been prepared in a cross-linked polymeric configuration, with β-CD linked via different units providing different properties to the final polymer. For example, a highly fluorophilic perfluoroarene cross-linked β-CD polymer (DFB-CDP) removed approx. 100% of PFOA (C_0 = 1 μg/L) after reaching adsorption equilibrium, as opposed to a tetrafluoroterephthalonitrile cross-linked β-CD that showed insignificant PFOA removal [36]. The DFB-CDP with the lowest degree of fluorine content (i.e. lower cross-linking degree) also showed the best removal efficiency and kinetics for PFOA adsorption in the same conditions (>95% removal in 13.5 h) as a result of the increased accessibility to the hydrophobic cavity of β-CD. The material exhibited approx. 40% higher PFOA removal than PAC in equilibrium adsorption experiments, a max. Adsorption capacity (82 μmol/g) comparable to that of GAC [158,159], and adsorption kinetics similar to that of PAC (i.e. >90% removal achieved in approx. 24 h). CDPs also showed removal of different PFAS comparable to that of AC with small particle size (10–212 μm) after 4 h [98]. The same authors noted that smaller compounds could be more easily and better adsorbed on large-sized ACs than smaller-sized ACs and CDPs because of the easier intra-particle diffusion process.

Together with the host-guest interaction, structural crosslinkers also play a major role in the interaction with PFAS and in CDs' high degree of tunability. The nitrile groups of tetrafluoroterephthalonitrile crosslinkers in a β-CD (TFN-CDP) were reduced to primary amines that switched the affinity of the polymer from cationic to anionic micropollutants due to the now available electrostatic interactions offered by the protonated amino groups [37]. A mixture of 9 short- and long-chain PFAA and GenX (C_0 = 1 μg/L) was exposed to the aminated TFN-CDP (C_0 = 10 mg/L), showing a >98% removal of the analytes after 30 min, except for GenX and PFBA (80%), and doubling the removal efficiency towards PFBA and GenX concerning AC. These results align with other experiments comparing PFAS adsorption by AC and protonated β-CD after a 4h contact time [98]. Amine-containing β-CD showed significantly higher affinity and sorption capacity for GenX with respect to amido-containing β-CD ($K_L = 8.8 \times 10^4$ M^{-1}, Q_m = 536 μmol/g and $K_L = 1.8 \times 10^6$, Q_m = 12.1 μmol/g, respectively) [35], comparable to that of some amine-functionalized COF [20] but also of GAC and PAC. The protonated groups can, therefore, assist the formation of inclusion complexes by binding with anionic PFAS.

The abovementioned works show that the removal of PFAS by the reported β-CD polymers strongly depends on i) availability of protonated groups (for anionic or zwitterionic PFAS), although pH and divalent cations (that can form weak complexes with anionic PFAS) can affect the removal efficiency of β-CD more strongly than for AC, that mostly rely on hydrophobic interactions [98]; ii) accessibility to the binding sites of the inner cavity of β-CD, as also indicated by the higher removal of short perfluoroalkane sulfonamides with respect to the longer chain but branched homologues [95]; and iii) fluorophilic interactions. Both electrostatic and fluorophilic interactions can be provided by the crosslinkers.

The removal efficiencies of this class of materials proved comparable, or superior, to that of ACs. Benchmarking experiments support their employability in water treatment operations. Sorption tests performed on groundwater contaminated by 68 differently-charged (zwitterionic, cationic, and anionic) PFAS using 3 β-CD, 1 AC, and 1 resin clearly underlined i) the significantly faster adsorption kinetics of the positively charged β-CD (30 min. adsorption time) with respect to AC due to the overall easier accessibility to the binding sites of the former, although ii) the less-selective AC shows both a better overall removal of the totality of PFAS and higher median removal compared to the best-performing β-CD after a longer contact time (48 h) [95]. The overall moderate selectivity of GAC for anionic, non-ionic, and zwitterionic PFAS has been brought out also in adsorption experiments with AFFF-contaminated groundwater where it was compared with three MOFs, showing a removal capacity range of approx. 37% (for PFBA) - 44% (for FOSA) for 21 PFAS [130]. The more selective behaviour of cyclodextrin polymers as compared to AC has also been observed for many other types of organic pollutants [157]. In another work, CDPs outperformed AC in experiments with PFAS-spiked groundwater and non-spiked PFAS-contaminated groundwater ("AA-A", "WA-A", "WA-D") for the adsorption of PFBA, PFPeA, PFBS, and PFPeS [98]. Other works involving cationic β-CD showed that uptake of short- and long-chain PFAA was significantly inhibited by monovalent and, especially, divalent salts (1 mM), presumably because of direct binding site competition and/or screening effect [38]. The uptake of PFAS by negatively charged, hydrophobic β-CDs under the same conditions was, in contrast, significantly improved (although still inferior to the cationic β-CD) for long- and short-chain PFAS, a trend that was attributed to the (inversed) screening effect of the negative ions and/or the salting out effect (i.e. lower solubility of PFAA and consequently promoted adsorbent-adsorbate hydrophobic interactions). Cations also

negatively affected the uptake of PFAS on cationic β-CDs and ACs, possibly due to the formation of complexes with anionic PFAS that weakened the extent of electrostatic interactions with positively charged surface groups [98]. According to data reported in Table 6, CDPs achieved sorption equilibrium within hours at low PFAS concentration, therefore proving superior to conventional adsorbents.

The adsorption of long- and short-chain PFAA on DFB-CDP and TFN-CDP was only slightly affected by the presence of HA (20 mg/L). In fact, HA in the same concentration had no effect on the adsorption of 83 different micropollutants (among which PFBA and PFOA) on β-CDs, as opposed to a coconut-shell-derived GAC [157]. The overall modest effects of high molecular weight NOM components like HA on CDPs has not been deeply discussed so far. Analogue results for the removal of other micropollutants were linked to the size-exclusion effect from the inner cavity of β-CDs [160]. In contrast, the smaller fulvic acids (FA) could potentially fit the cavity.

The study of the recovery and reuse of PFAS-loaded β-CDs has been little investigated so far. PFOA removal capacity was reduced by approx. 5% after 4 adsorption/desorption cycles in DFB-CDP (24 h contact time), demonstrating the good reusability of solvent-regenerated cyclodextrins, as outlined in previous works [161]. In general, solvent-based desorption of other micropollutants from β-CD adsorbents revolved around 75−90% [160].

Though AC and IER achieved comparable removal of some PFAS, β-CD can be tailored to selectively target the most problematic compounds and PFAS with opposite/different charge at environmental pH. Important advances are being made to improve their adsorption performance. For example, a new synthesis platform has been proposed to overcome the challenges associated with sorption limitations that arise from the partially random crosslinking process of β-CDs. This process involves the introduction of electron-deficient aromatic crosslinkers via nucleophilic aromatic substitution during polymerization, as the latter gives rise to irregular substitution patterns and structural modifications of some crosslinkers (i.e. less homogeneous overall structural architecture of the resulting polymer). This resulting cationic β-CD was able to remove ~100% of 8 PFAA (C_0 = 1 μg/L) at the exceptionally low adsorbent load of 1 mg/L [38]. Noticeably, >99% of PFBA and PFOA were removed, surpassing an IER tested in analogous conditions that removed 46% of PFBA and 54% of PFOA.

Overall, cyclodextrin polymers outperformed AC and resins regarding removal kinetics of PFAS and other pollutants, removal efficiency, NOM-fouling, and selectivity towards specific compounds [157]. Some authors estimated the economic competitiveness of a porous CDP (manufacturing cost estimated around 5−25 USD/Kg) vs that of some commercial ACs (9−22 USD/Kg) [161]. Before their full-scale application, however, a deeper insight into the isothermal adsorption of these composite materials towards single PFAS is needed. This has also been stated in relation to other micropollutants [160]. A more solid evaluation of the reusability of β-CD adsorbents is needed as well, with a focus on desorption mode and contact time needed for desorption.

3.2.3.4. Hydrogels. Hydrogels are highly hydrophilic crosslinked three-dimensional polymers capable of retaining a significant fraction of water molecules within their structure [162]. Recently, hydrogels with various types of comonomers and crosslinkers have been applied for PFAS sorption (Table 7). Some publications provided valuable insights on tailoring strategies to increase the selectivity towards PFAS (vs other co-contaminants), short-chain PFAA, and PFECA (vs long-chain PFAA). This includes the incorporation of moieties and functional groups that allow fluorophilic interactions and ion-exchange other than the typical combination of electrostatic and hydrophobic interactions. For example, Kumarasamy and collaborators [40] tested ionic fluorinated hydrogels with different levels of amine or ammonium co-monomers to remove PFOA, PFHxA and GenX (1 μg/L each) in water amended with 200 mg/L of NaCl and 20 mg/L of HA. The authors highlighted the better removal by fluorogels with high ammonium content (~80% of PFHxA, GenX and ~100% of PFOA) as compared with GAC, PAC and IX (~18−30%, 18−25%, and 5−80% for PFHxA, GenX and PFOA, respectively) in the same conditions, and of quaternary ammonium-containing fluorogels with respect to tertiary amine-containing fluorogels. The gels showed outstanding removal of short chain PFAS even in effluent water from a treatment plant (TOC = 1.3 mg/L) spiked with 21 among legacy and novel PFAS (>95% of PFBS, PFHxA, and GenX, and 60% removal of PFBA). Consequently, the effectiveness of fluorogels in removing PFAS molecules can be attributed to a combination of electrostatic and hydrophobic interactions, the synergistic effect of fluorophilicity and ion-exchange along with the unique structure of the fluorogels [163].

Aminated poly(ethylene glycol) diacrylate (PEGDA) showed higher removal efficiency towards PFBA and PFBS (199.5 and 190.6 μmol/g, respectively) with respect to the bifunctionalized (fluoridated and aminated) PEGDA [39], and this result was mainly attributed to the higher positive surface charge of the monofunctionalized gel that favoured the short chain compounds. Both sorbents showed lower removal of long-chain PFAA than two commercial resins, but 8- to 63-fold higher sorption efficiency towards short-chain PFAS. Moreover, up to 92−97% removal of PFOA and PFOS was achieved in 2 min. thanks to the introduction of hydrophobic regions in the structure. In fact, hydrogels show very fast equilibrium sorption kinetics: IF-20+ was able to achieve >95% removal of numerous co-occurring PFAS including PFBS and GenX at ng/L level after 2h in wastewater samples, similar to DMAPAA-Q in equilibrium kinetics experiments [41], and almost complete removal of GenX after 30 s and 30 min. at high (200 μg/L) and low (1 μg/L) GenX concentrations, respectively. Both gels also showed impressive desorption efficiency (≥95%) and degree of regenerability over 5−6 cycles, maintaining almost identical adsorption efficiency. DMAPAA-Q also maintained a high adsorption efficiency in water with high level of DOC (approx. 2.5 mg/L) although it decreased roughly by 10−20% in wastewater with respect to surface water. Noticeably, selectivity towards short-chain PFCA and PFSA was very high in multi-PFAS spiked lake water (1 μg/L of each PFAS) as indicated by the similar removal efficiency (%) with respect to their long-chain homologues. Increasing aminated comonomers loading in PNIPAAm-based hydrogels did not linearly correlate with increased swelling (i.e., hydrophilicity) of the gel, supposedly because of the interactions between the comonomers and other functionalities [164].

Due to their extremely high surface area (other than low cost and low toxicity), carbon quantum dots (CD) were used to modify hydrogels (CD_{66}-0.2E/P), resulting in very high PFAS adsorption capacities (7100, 3800, and 2000 μmol/g of PFOS, PFHxS, and PFBA, respectively) [42]. PFOS was also efficiently (86.6%, C_0 = 516 ng/L) and quickly (30 min.) removed from a simulated wastewater solution (200 mg/L NaCl, 20 mg/L HA), as well as from AFFF-simulated wastewaters after 24h (>95%, C_0 PFOS = 20 mg/L). Furthermore, the adsorbent was not significantly affected by the presence of four hydrocarbon surfactants in concentrations up to five times higher than those of PFOS. A proper balance between hydrophilic and hydrophobic functionalities of the adsorbent's backbone granted the best amphiphilic behaviour and, therefore, the best removal performance (Q_e, Q_m) among the differently CD-modified hydrogels due to the easier transport of PFOS towards CDs during the adsorption process.

A fluorous-core nanoparticle-embedded hydrogel (FCH2) was synthesized to maximize affinity towards differently ionized long-chain perfluoroalkyl and polyfluoroalkyl substances, which were almost completely removed at low concentrations (μg/L) in multi-PFAS solution, and at low to high concentration (PFOA, 0.001−10 mg/L) in the presence of decanoic acid and inorganic salts at mg/L level [44].

The removal efficiency of hydrogels is remarkable for both long- and short-chain PFASs and comparable to that of resins and AC. For example, IF-20+ was able to remove up to 800 μmol/g of GenX (Q_m, Langmuir model), as reported for PAC and GAC in other works [165].

In the case of fluorogels, it was highlighted that a balance between surface wettability and swelling capacity (increased via e.g. amination and decreased via e.g. incorporation of highly hydrophobic comonomers) and fluorination is required to maximize uptake of and selectivity towards PFAS [40]. In this regard, the moisture content of a PNIPAAm-based gel copolymerized with DMAPAQ did not significantly change with increasing pH due to the quaternary ammonium groups introduced by DMAPAQ, which allowed the polymer to remain hydrated as the H^+ concentration decreased [164]. A uniform distribution of mesh sizes within the resin structure, achieved by using either shorter or longer monomers during the gel synthesis process, also led to increased selectivity towards both shorter and longer PFAA molecules. This suggests that employing multiple structurally equivalent but varied-length monomers is advisable for effectively removing PFAS compounds across a wider hydrophilicity spectrum [163].

To avoid the loss of fluorinated portions such as perfluoropolyethers, it is also fundamental that the fluorinated sorbents have a stable structure [163]. Choudhary and Bedrov investigated the adsorption of GenX on polycationic hydrogels with differently fluorinated backbones and crosslinkers, proving that the use of non-fluorinated crosslinkers only minimally influences the adsorption of GenX [166]. Furthermore, they showed the relevance of the combined effect of electrostatic and hydrophobic interactions given by cationic and fluorophilic groups close to each other. The high selectivity towards GenX was further underlined in co-sorption experiments with Br^- and 2-propoxypropanoate (a non-fluorinated GenX equivalent) as sorption competitors.

Hydrogels are not as cost-competitive as AC and resins, but the use of natural and cheap polymers as a backbone polymer network for the synthesis of these materials is increasingly explored: among others, cellulose is expected to be a promising renewable, economically competitive starting material for practical applications [167]. Conversely and depending on their application field, ensuring a minimum mechanical strength could be required for full-scale applications of hydrogels; therefore, the starting materials (backbone polymers, crosslinkers) actually useable to synthesize the gels and the degree of polymerization could be limited [167]. Among hydrogels, stimuli-responsive hydrogels are of particular interest as they can undergo mechanical and/or structural changes in response to changes in environmental conditions (e.g., temperature, pH). As far as regeneration is concerned, thermoresponsive hydrogels can spontaneously desorb PFAS at temperatures above their LCST, offering an alternative low-cost and solvent-free regeneration. For example, a PNIPAm-functionalized PVDF-based separation membrane was able to desorb 50−60% of PFOA after the first cooling cycle (that was carried out within a 35 °C−20 °C temperature range) and >90% from the second to the fifth cooling cycle [43]. However, the use of these materials was limited to two types of PFAS (i.e., PFOA, PFOS), a fact that should be considered when comparing the efficacy of such methods for other PFAS (e.g., Gen-X, PFBS, etc.).

Notably, the efficacy of hydrogels varies depending on the specific per- and polyfluoroalkyl substances (PFAS) in question. Some hydrogels exhibit high adsorption capacities and removal percentages for certain PFAS but may not perform as effectively for others. Equilibrium time and recyclability also exhibit discrepancies across different hydrogels. Crucially, certain hydrogels, while highly effective for legacy PFAS such as perfluorooctanoic acid (PFOA), are still in the early stages of development and lack comprehensive testing for newer generation PFAS like Gen-X. This underscores the need for a discerning selection of hydrogels based on the types of PFAS present in real-life matrices. For instance, for a wastewater discharge predominantly containing PFOA, PNIPA and PNIPAm-functionalized polyvinylidene fluoride (PVDF) membranes may represent a more sustainable option. In contrast, for a mixed and complex matrix encompassing PFOS, PFOA, and PFNA, FCH2 could emerge as an economically viable choice.

Consequently, the decision on which hydrogel to employ for PFAS adsorption hinges on the specific PFAS to be eliminated, as well as considerations of equilibrium time, recyclability, and site-specific conditions. Furthermore, the role of the sole OM during the adsorption of PFAS has not been discerned so far. It is evident that hydrogels, in their current state, may not provide a comprehensive solution and necessitate further development and research.

3.2.4. Magnetic NPs-based/-grafted materials

The advantage of using magnetic nano-based materials as potential pollutant adsorbents is mainly due to their i) high specific surface area, ii) ease of being functionalized on the surface, and iii) easy separation (recovery) under external magnetic fields [168]. Despite these advantages, magnetic nanoparticles (MNPs) tend to be more expensive to produce than resins and carbons, due to the additional process steps required for nanomaterial synthesis and surface modification. Moreover, a full-scale magnetic separation process has yet to be assessed operatively and economically. There are also concerns about the environmental impact and toxicity of engineered nanomaterials [169,170] While MNPs can be removed from treated water using magnetic separation, there is a possibility of nanoparticles leaching into the environment during water treatment or improper disposal of spent adsorbents. Nevertheless, their use in functionalizing different materials brought out valuable results.

For example, a magnetic nanocomposite (Fe_3O_4@SiO_2−NH_2&F_{13}) was prepared by coating the surface of Fe_3O_4 NPs with a silica membrane functionalized with an amino group and octyl-perfluorinated chain [47] to combine electrostatic attraction and fluorophilic interaction. This system was used for the rapid and selective removal of nine perfluorinated compounds from surface water samples, and the performances were compared with powdered activated carbon (PAC). The composite showed a better efficiency (86.29%) in the simultaneous removal of 9 PFAS (at low ng/L concentration) than the PAC (58.61%). The influence of HA (5−50 mg/L) on the sorption process was also investigated, showing no significant impact on the removal performance of the magnetic-composite for a mix of PFAS (10% reduced uptake), as opposed to PAC (12−54% reduced uptake). In addition, the material could be reused several times after the sorption process, and no significant decrease in the removal efficiency was observed.

Du et al. [46], reported the synthesis and application of a magnetic fluorinated adsorbent obtained by ball milling Fe_3O_4 NPs and vermiculite loaded with a cationic fluorinated surfactant (Fe_3O_4-loaded F-VT, 1/19-MF-VT). The magnetic NPs embedded into the adsorbent surfaces increased the dispersibility of fluorinated vermiculite in water (improving the hydrophilicity of its external surface). 1/19-MF-VT showed impressive maximum adsorption capacity of C4 and C8 PFAA. The selectivity towards PFAS was better highlighted by competitive adsorption experiments involving PFOS

and its non-fluorinated equivalent 1-octanesulfonate (in the same starting concentration of 46.5 μmol/L): PFOS exhibited fast (4 h) and substantially higher removal rates due to the fluorine-fluorine interaction with the vermiculite-interlayered fluorosurfactant. Moreover, the IRA67 resin showed a higher adsorption capacity of PFOS, PFOA, PFBS, and PFBA with respect to Fe_3O_4-loaded F-VT and PAC in the same conditions but significantly slower kinetics (equilibrium time = 48 h). Additionally, the adsorbent material was able to remove PFOS from fire-fighting foam wastewater (22.5 mg/L) with a higher sorption capacity (98%) than PAC and resin (<40%) at the same adsorbent amount (150 mg/L), and it could be regenerated by methanol and reused five times without reducing the PFOS removal efficiency or the magnetic performances.

Another multifunctional magnetic sorbent was prepared by modifying magnetic Fe_3O_4 NPs with β-cyclodextrin−ionic liquid polyurethanes (Fe_3O_4-CDI-IL MNPs) [48]. The coupling of ionic liquid with the β-cyclodextrin polymer backbone could significantly enhance the removal efficiencies of both PFOS and PFOA. According to the sorption isotherms, the composite nanomaterial showed sorption capacities of 16 μmol/g for PFOS and 7.5 μmol/g for PFOA. A 10% and 25% decrease in adsorption efficiency was reported with high concentrations of HA (1 g/L) for PFOA and PFOS, respectively. The sorbent material was regenerated and reused at least 10 times without any significant loss in the sorption efficiency.

Magnetic nanoparticles-attached fluorographene-based (MNPs@FG) sorbents were synthesized by exfoliating commercial fluorographite and mixing it at different mass ratios (1:1, 3:5, and 1:3) with MNPs [45]. The 3:5 FG:Fe_3O_4 composite (2-MNPs@FG) removed 92−95% and 94−97% of PFOA and PFOS in 2 min, respectively, and significantly outmatching PAC.

In addition, 2-MNPs@FG maintained its adsorption performance in the presence of 2 mg/L of DOC and in lake, river, and tap water samples where it removed >99.2% of co-occurring PFOA and PFOS (C_0 = approx. 3−7 μg/L each). Moreover, it was possible to regenerate the used sorbent materials by methanol washing and to reuse them up to five times without observing a significative reduction in PFOA/PFOS desorption and removal, and in the magnetic separation performances.

In another work, Fe_3O_4 MNPs were modified by attaching a variety of PFPE-containing polymers, either non-ionic or cationic in nature. These PFPE-containing polymers were synthesized to have consistent levels of fluorine but varied in the amount of cationic quaternized ammonium groups by manipulating the degree of polymerization of the two constituent monomers. Among these modified sorbents, P2-9+@IONPs, which had the highest concentration of cationic groups (39% by weight), exhibited the most effective performance in eliminating 11 co-occurring PFAS (0.1 mg/L each) in 24 h, including PFBA and GenX (84% and >99.5 % removal, respectively) in environmentally relevant conditions (200 mg/L NaCl and 20 mg/L humic acid). Activated carbon and ion exchange resin in the same concentration and under the same conditions showed systematically lower adsorption of all compounds, especially short-chain PFAA and GenX. When tested in multi-PFAS spiked wastewater (30 min. adsorption), only the removal of PFBA and PFPeA decreased substantially (~40% and ~75%, respectively). P2-9+@IONPs also showed almost complete elimination of GenX alone within 30 s, a max. adsorption capacity as high as 664 μmol/g, and excellent regenerability over 4 cycles [49].

In summary, magnetic nanoparticles-modified materials are a promising alternative to conventional adsorbents for removing PFAS from water, but critical aspects regarding cost, standardization, environmental impact, and cost-benefit analysis (in comparison with traditional materials) [171] must be addressed before they can be applied widely and at large scale for water treatment.

3.2.5. Zeolites and clay-based minerals

3.2.5.1. Zeolites. Zeolites are porous aluminosilicate minerals characterized by a precise chemical structure and tunability of pores and therefore a regular crystalline framework. Some recent works helped elucidate the mechanisms of action and the effect of functionalization of these materials (Table 9).

A beta-type all-silica zeolite was tested for the adsorption of PFOA and benchmarked against other types of zeolite and AC [51]. The absence of local defects in its structure (compared to the other zeolites) and, therefore, the higher hydrophobicity, was pivotal to allow PFOA uptake, for which a Q_m of approx. 845 μmol/g was calculated from adsorption isotherm experiments. Adsorption equilibrium was reached in approx. 24 h for both PFOA and PFOS, significantly outperforming GAC but with similar kinetics to PAC. Different results were obtained with faujasites for the removal of PFOA (Q_m = 48−145 μmol/g) and PFOS (Q_m = 20−60 μmol/g) (equilibrium time = 1 h or less) [172]. Interestingly, outstanding selectivity towards PFOA and PFOS was proven in experiments with 5 occurring organic co-contaminants (3 carboxylic aliphatic acids, 1 carboxylic aromatic acid, and phenol) at different molar ratios (1:5 up to 1:15 of PFAS:co-contaminants). The uptake of both PFAS was only slightly reduced, as opposed to AC. Density Functional Theory simulations pointed out the extremely favourable enthalpy-driven process explaining the high selectivity of the zeolite towards PFAS. C8 PFCA also showed a higher affinity than C10 PFCA on the same type of zeolite, which was explained by the particularly favourable dimensions of PFOA molecules with respect to the channel dimensions [53].

An all-silica zeolite is somewhat expected to be efficient towards long-chain PFAS because of its markedly high hydrophobicity. The higher the Al/Si ratio, the more hydrophilic the behaviour of the zeolite. In a recent research, the adsorption of PFOA and PFBA using 2 β-type zeolites with different Si/Al ratios (25:1 and 300:1) and by the same materials coated with cetyltrimethylammonium bromide (CTAB) or poly(diallyldimethylammonium chloride) (PDADMAC) was carried out [52]. The adsorbed amount of PFOA on the Si-rich zeolite was almost double that of the other zeolite. The coating with organic functionalities made the surface less negative. The PDADMAC-coated zeolites showed up to 51.3% increased sorption capacity towards PFBA, but the uptake of PFOA by CTAB-coated and PDADMAC-coated zeolites was 58.7% and 15.45% lower than with uncoated zeolites. This was attributed to the reduction in specific surface area caused by the organic coating.

Licato and collaborators evaluated the simultaneous removal of several pharmaceuticals, personal care products, and PFAS in spiked clean water and wastewater samples by 4 synthetic and 1 natural zeolite [50]. Only approx. 20% of the occurring PFBS (C_0 = approx. 2−9 ng/L) and PFBA (C_0 = approx. 5−6 ng/L) was removed from the WWTP (wastewater treatment plant) effluent sample. The typically negative surface charge of zeolites was probably unfavourable for the adsorption of the short-chain PFAA. Nevertheless, the low removal capacity must be evaluated in consideration of the co-occurrence of the high number of micropollutants.

Zeolites are stable catalysts used in numerous sectors because of their structural/pore dimension tunability coupled with varying acidity and ion-exchange capacity [173]. Fe(III)-loaded BEA-type zeolite particles were shown to catalyse the degradation of PFOA and PFOS in different concentrate-and-destroy setups, representing novel scalable strategies for the removal of PFAS at low concentrations. Ferric ions-PFOS complexes ($[PFOS\text{-}Fe]^{2+}$) can be irradiated with UV light to induce ligand-to-metal electron transfer and the formation of $C_8F_{17}SO_3^{\bullet}$ radicals. After the desulfurization of the radical in aqueous solution, it can be gradually decomposed, yielding shorter and shorter perfluorinated alkyl radicals that

cyclically react with O or H radicals. In the work by Qian et al., the use of Fe^{3+}-doped BEA-35 zeolite significantly increased the rate of PFOS degradation previa adsorption on the zeolite, showing 69% defluorination along with the formation of 25% C2−C4 PFCA intermediates after 96 h irradiation (C_0 PFOS = 1 mg/L, C_0 BEA-35 = 0.5 g/L, pH = 3). The short-chain PFCA (that could less efficiently adsorb on the zeolite) decomposed (~95%) via the addition of $Na_2S_2O_8$ (i.e., the introduction of sulphate radicals, which cannot degrade PFOS directly). Such a heterogeneous system showed good results up to pH = 5.5 (56% defluorination, >95% desulfurization rate) even with real groundwater samples (C_0 PFOS = ~500 ng/L). However, around neutral pH the increase of adsorbed PFOS with respect to the Fe^{3+}-complexed PFOS drastically inhibited the formation of the latter and therefore the overall process and the decomposition of the molecule [174].

In another work, Fe^{3+}-doped BEA-35 (C_0 = 50 g/L) was used to accelerate the stepwise decomposition/defluorination of PFOA by sulphate radicals, achieving a >99% degradation and 71% defluorination of PFOA (C_0 = 100 mg/L) within 90 min at pH = 3, far exceeding the efficiency of the chemically-driven decomposition without zeolite. The catalytic activity was consistently maintained for 6 adsorption/regeneration cycles, and negligible leaching of Al^{3+} (0.09−0.12%) was detected. At pH = 7 and in the same conditions, PFOA degradation rate (speed) decreased but not efficiency with respect to pH = 3 [175]. In both studies, the solvent-free regeneration of the zeolite could be achieved i) via photochemical degradation of the adsorbate and ii) tandem closed-loop recirculation of persulfate and heating of a bed-fixed zeolite.

Because of the thermally stable structure of zeolites, both thermal and solvent-based regeneration are viable options. All-silica zeolite β showed complete desorption of PFOA (360 °C) and PFOS (550 °C) [51,53]. Re-uptake of PFOS slightly diminished over three thermal regeneration cycles, possibly because of slight initial alteration of the framework. Among the 12 solvents tested in their pure form and when combined with octane, the latter emerged as the most effective single solvent for desorbing PFOS, exhibiting a 100% desorption capacity. This superiority was attributed to the markedly high hydrophobic nature of this zeolite type.

Concerning OM, neither Suwannee River NOM nor HA and FA affected the adsorption of PFAS on all-silica zeolite β [53]. This was attributed to the combination of negative surface charge of the NOM, FA, and HA (i.e., electrostatic repulsion) and the size exclusion effect caused by the smaller diameter of the zeolite pores (0.62 nm).

So far, for the hydrophobic beta type zeolite, electrostatic interactions do not seem to be involved in PFAA uptake. Yet, the addition of divalent cations in solution, especially Ca^{2+}, hindered the uptake of PFOA. As compression of the electrical double layer could not explain the phenomenon, the complexation of the ion with two molecules of ionized PFOA in the bulk phase was hypothesized. Such dimer is sterically unfavourable to enter the zeolite pores and modifies the speciation and solubility of PFOA. The very mild reduction of PFOS uptake in the same conditions suggests that cation bridging of sulphate groups is not favourable [53].

More studies are needed on the removal of PFAS using functionalized and pristine zeolites. The effect of OM (with reference to high-SUVA/high molecular weight molecules like HA) is still overlooked. A proper evaluation in this sense is complicated by the highly variable price of zeolites [176]. Taking type A zeolites as an example, it ranges between 26 (synthetized at lab-scale)-84 USD/Kg [176,177]. Some authors obtained eco-friendly, low-cost zeolites from fly ash (3.8−6.4 USD/Kg) [177]. Natural occurring zeolites are nevertheless considered as low-cost with respect to synthetic zeolites [178]. Even though information on material and operational costs is scarcely reported in peer reviewed literature, they represent well-known materials that, based on available evidence, showed a high affinity for PFAS together with a size-exclusion effect and a low affinity for OM, particularly with respect to ACs. They are also potentially competitive cost-wise and show the advantage of thermal regeneration. In conclusion, these inorganic sorbents/catalysts are a promising option for PFAS remediation.

3.2.5.2. Layered double hydroxides and layered rare earth hydroxides. Clay minerals are naturally widespread, low-impact materials among which phyllosilicates and metal oxides have been used to remove many organic pollutants due to their high surface charge and surface area [108]. The uptake mechanisms of PFAS using clay-based materials mainly rely on hydrophobic and electrostatic interactions, together with anion exchange [108]. Layered double hydroxides (LDH) refer to a group of minerals with a layered structure, comprising positively charged brucite-like layers and exchangeable anions within the interlayers. LDH are particularly valuable for removing anionic pollutants as they maintain a high positive charge over a wide range of pH values. LDH are widely available and can be easily synthesized [179]. Some recently published insightful works shed light on the role of the metal cations occupying the octahedral centres in the hydroxide layers, of the type of interlayered exchangeable anions, and of surficial functionalization, on the uptake of PFAS (Table 10).

A Zn−Al LDH was functionalized with alkylsilane (LDH-CH) and polyfluoroalkylsilane (LDH-CF) and the three of them were compared for the sorption of PFOA [54]. Q_m (3220 μmol/g) of the LDH-CF was approx. 25% and 75% higher than that of the unmodified LDH and LDH-CH, respectively. The adsorption equilibrium time of LDH-CF also significantly decreased (5 min) compared to pristine LDH (2 h) and was comparable to that of many advanced materials like organic frameworks and nano-sized adsorbents. As indicated by K_L values, the affinity for PFAS greatly increased as well after grafting with organosilanes and was maximum for LDH-CF despite the lower LDH:functional group loading ratio with respect to LDH-CH (1:1 vs 1:0.2). The increase in adsorption affinity directly correlated with the increase in adsorption capacity and was greater than that of AC, resins, and other materials. Moreover, LDH-CF performed consistently better in the presence of naturally occurring anions and NOM and maintained its removal efficiency after 3 adsorption/desorption cycles (as did LDH-CH). The better performance of LDH-CF in the presence of NOM with respect to LDH-CH and unmodified LDH was attributed to the fluorophilic interactions between PFOA and the organofluorinated functional groups of the material, which allowed a higher adsorption affinity towards PFOA.

Interlayered anions also influenced the adsorption capacity of LDH. A NO_3^- interlayered hydrotalcite (HT-NO_3) showed higher removal of PFOA and PFOS (Q_m = 2101 μmol/g and 3219 μmol/g, respectively) than the CO_3^{2-} intercalated hydrotalcite because of the higher affinity of NO_3^- anions for the HT interlayer. The maximum adsorption capacity remained substantially similar (Q_m = 2195 μmol/g and 3215 μmol/g, respectively) after treating the material with acetone (AHT-NO_3, to increase the pore size of HT-NO_3 and HT-CO_3 [55], and exhibited superior sorption kinetics than IER and AC (eq. time = 5−20 min, C_0 PFOS=C_0 PFOA = 25 mg/L). Despite the impressive maximum adsorption capacity shown at high PFAS concentrations (50−2000 mg/L), the removal efficiency dramatically dropped with a non-fluorinated surfactant competitor, indicating low selectivity towards PFAS.

The cation composition of LDH affects the uptake of PFAS as well. In comparison to an Mg−Al -based LDH, Zn−Al LDH exhibited superior adsorption capability (1510 vs 1420 μmol/g) and faster equilibrium uptake kinetics (1−2 h vs 8h) towards PFOA. These favourable characteristics can be attributed to the higher surface

charge, expanded surface area, and possible easier accessibility of PFOA to the sorption sites because of the slightly larger basal spacing of Zn−Al LDH [56].

Suwannee River NOM in concentrations up to 1 mM had no significant effect on PFOA removal by Zn−Al LDH and CF-LDH, similar to HA (2−20 mg/L) for YOHCl (a rare-earth-based double hydroxide). A slight inhibition was observed for Mg−Al LDH. This could be attributed to the hydrophilic nature of LDHs, for which the adsorption of the NOM by means of hydrophobic interactions is supposedly negligible [57]. Even though fluorination increased the overall hydrophobicity of CF-LDH, it also enhanced its selectivity towards PFAS, which could explain both the high removal in the presence of NOM and the tolerance towards similar concentrations of sulphate anions.

On the other hand, carbonate, bicarbonate, and sulphate anions significantly suppressed the removal efficiency of PFOA in non-fluorinated LDHs-LRHs [56,57] due to the affinity of such anions to the materials and subsequent saturation of the ion exchange sites.

According to the thermogravimetric analysis (TGA) of the examined LDH and LRH, an overall ~20% weight loss up to ~200 °C is associated with the loss of adsorbed and crystalline water, and no significant weight loss is observed up to 100 °C. This suggests the thermal stability of LDHs at adsorption-operating temperatures.

LDH can be obtained by numerous methods such as co-precipitation, hydrothermal synthesis, urea hydrolysis (synthesis of LDH) or pre-existing LDH can be treated, for example via exfoliation or ion exchange, to obtain LDH with given characteristics [180]. Commercially, LDH is normally synthesized to grant a more specific composition, morphology, and properties. To this end, they can be obtained from low-cost precursors like metal nitrate salts [56] or salts of other ions. The metals they are typically interlayered with, like aluminium, zinc, or magnesium, are quite cheap. For Mg−Al LDH a commercial production cost of 2−3 USD/Kg has been reported [181]. The studies here reported show the possibility of greatly enhancing the selectivity of such materials towards PFAS in environmentally relevant conditions by increasing the fluorophilicity of the sorbent, as confirmed by the efficient removal of a 10-PFAS mixture (C_0 PFAS = 10 μg/L each) in lake water (e.g. ~85% PFBA and GenX removal) by LDH-CF [54].

In general, this type of material showed adsorption capacities comparable to those of COFs and MOFs and greatly outperformed traditional adsorbents [56]. For example, YOHCl was able to remove >97% PFOA in 8 h, while GAC and IRA resin only removed 31% and 68% of PFOA under the same experimental conditions [57]. LDH are potential commercially- and performance-competitive alternative PFAS sorbents, but Huo and collaborators recommended further research to elucidate the adsorption mechanisms of a wider set of PFAS in more environmentally relevant settings and concentrations, and to improve the design of LDH-based materials to tackle the competition with other anions [56]. In addition, there is evidence that using organic solvents to wash the saturated LDH can affect the physical, chemical, and structural properties of the LDH [166 and refs. therein] an aspect that should be deepened for a correct evaluation of the regenerability of LDH and LRH.

4. Discussion

4.1. Role of the material modification and properties on PFAS adsorption

From the information brought out in this review concerning material properties and enhancement strategies relevant to the removal of PFAS, it emerged that:

i) Fluorine contained in the monomer structure and on the material's surface introduced fluorine-fluorine interactions, increasing the selectivity towards PFAS. Indeed, different results are to be expected from structural modification and/or functionalization carried out with different fluorine-containing groups on PFAS adsorption. Selectivity achieved through the introduction of fluorophilic interactions also allows targeting a broader suite of PFAS including cationic, non-ionic, and zwitterionic PFAS other than anionic ones [44]. “Fighting PFAS with PFAS” is therefore a promising way forward if considering the challenges posed by the adsorption-based strategies, but it requires careful evaluation to avoid turning the solution into an additional problem, i.e. into a secondary PFAS source [94]. For example, fluorinated polymers were put under aggressive accelerated degradation conditions (50 °C, pH = 8.7) to test their hydrolytic stability, and some of them released fluorinated oligomers over time [163]. This drawback could be a limitation for their environmental application. As a further remark, computational simulation can assist the researchers in selecting the most appropriate fluorinated functionality/ligand/intercalant to increase affinity towards PFAS while taking into account/predicting the possible modification of the material structure and accessibility to sorption sites and, ultimately, the induced steric hindrance [154,182]. In fact, it has been shown that an excessive dose of functionality or excessive crosslinking degree can decrease sorption efficiency since they can block pore entrances and/or alter the chemical groups already present on the surface of the modified material [20,36,60]. Competitive adsorption experiments with non-fluorinated PFAS homologues such as 1-octanesulfonate can help elucidate the selectivity towards the former in pristine materials vs materials modified at the surface or structural level via the addition of fluorine.

ii) Electrostatic interactions are pivotal for the uptake of anionic PFAS (especially short-chain PFAA) and are typically achieved via the incorporation of aminated and quaternary ammonium groups. This allows to increase the hydrophilicity/wettability of the adsorbent and the electrostatic interactions between the sorbent and ionic PFAS [21] but in the case of amine-containing sorbents, it could also increase the adsorption or ion exchange of co-occurring ions [11,38,164] according to the pH values [11], upon which depends the degree of protonation of commonly used aminated functionalities like polyethyleneimine. Instead, the protonation of quaternary ammonium salts does not depend on pH [93]. Advanced materials functionalized with negatively charged or neutral groups for the removal of non-ionic and zwitterionic PFAS should be further explored [94].

iii) A change in pore dimensions and in the overall availability of the binding sites has to be taken into account when modifying the materials, especially micropore- and ultramicropore-rich materials with pores in the dimensions of a few Angstrom, i.e. in the range of dimensions of PFAS [154,183].

iv) Particle size is another crucial factor in PFAS uptake kinetics for both traditional and alternative/advanced materials [95,98] since the smaller the granule size, the less important the role of intraparticle diffusion dynamics. Therefore, when conducting benchmarking sorption studies, it is important to select resins and AC that closely match the reference material's particle size.

Overall, the development of alternative materials for PFAS sorption relies on the interplay between electrostatic forces and

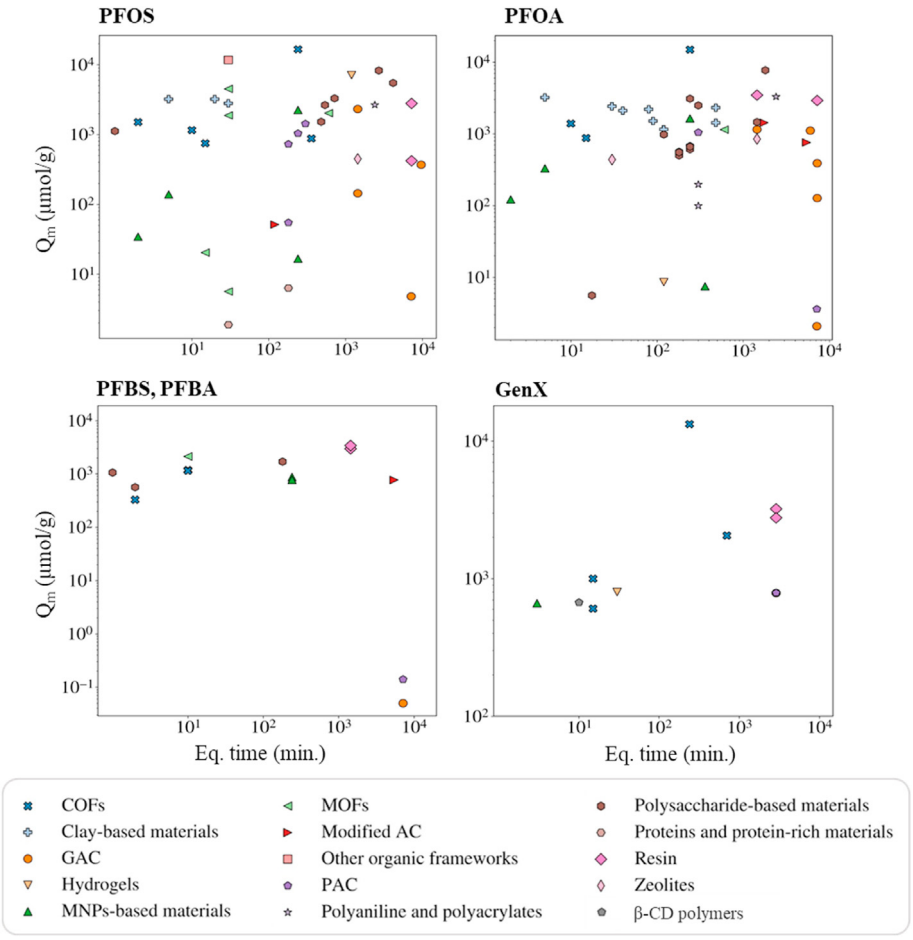

Fig. 2. Max. Sorption capacity (Q_m) vs equilibrium time of 5 representative PFAS by the reviewed adsorbents.

hydrophobic/fluorophilic interactions (to grant high affinity and selectivity towards PFAS while balancing the increased uptake of shorter and/or hydrophilic PFAS vs the increased influence of pH and ionic constituents in the medium) [27,49]. Conversely, by adjusting the ratio between the hydrophilic and hydrophobic groups a change in the specific surface area, accessibility of active sites, wettability/dispersion in water, and in the influence of pH and co-occurring ions is to be expected.

4.2. Removal efficiency and kinetics of legacy and emerging PFAS

Fig. 2 reports on the Q_m vs equilibrium time of ACs, resins, and alternative materials concerning PFOS, PFOA, PFBA, PFBS, and GenX (as representatives of legacy long- and short-chain PFAS and emerging PFAS).

All alternative adsorbents consistently exhibited higher removal rates for longer-chain PFAS compounds compared to their shorter-chain counterparts, including materials for which electrostatic interaction presumably governed the adsorption of some PFAS [56]. This is due to the lower hydrophobicity of short-chain PFAS vs longer-chain homologues. The same applies to PFSA with respect to PFCA of the same alkyl chain length, as the latter shows a lower adsorption affinity.

Even though some resins and ACs among those reported in Tables S1 and S2 showed impressive removal performances [114,118,128,129,165], they generally required <4–196 (ACs) and <4–168 (IER) hours to reach equilibrium. Among newly proposed materials, some MNPs-based sorbents (1/19-MF-VT, 2-MNPs@FG, Fe_3O_4@SiO_2–NH_2&F_{13}, P2-9+@IONPs), organic frameworks (SCU-8, NU-1000, PAF-45 and 28%[NH_2]-COF, FSQ-1, hollow Cys-COF, β-CD-COFs, PAF-45), biomaterials (PEI-f-CMC, powdered *Moringa oleifera* seeds, RAPIMER), hydrogels (DMPAA-Q, PNIPAm, CD66-0.2E/P) and clay-based materials (LDH-CF, LDH-CH, HT-NO_3, AHT-NO_3) only needed 1–30 min. This is particularly valuable when the water flow to be treated is high (i.e., low adsorbent/contaminant contact time). With respect to GenX, IRA67 and IRA400 showed the highest sorption capacity on a μmol/g basis (2780–3220 μmol/g) [165] except for Chitosan/F–COF (13260 μmol/g), and PAC and GAC showed Q_e comparable to that of 28%[NH_2]-COF, CDP-1, IF-20+, P2-9+@IONPs. However, activated carbons and resins required >48 h to reach equilibrium, while the other materials required 3–30 min (240 min in the case of Chitosan/F–COF).

Several advanced materials were able to remove PFAS in challenging conditions (i.e. multi-PFAS adsorption in the presence of other organic constituents). Noticeably, FSQ-1 removed >85% of each of the 24 PFAS from a mixed solution within 15 min. Cys-COF nanospheres and ionic fluorogels could also remove >21 PFAS (including C4 PFAA GenX) at low concentrations within 15 and 30 min, respectively.

Aminated/amidated PEGDA, NU-1000, hollow Cys-COF nanospheres, P2-9+@IONPs, PANI, POT, and IF-20+ showed remarkable relative sorption of C4 PFAA (with respect to their longer chain counterparts) than other traditional and innovative materials.

With respect to maximum sorption capacity and from a material class-wise perspective, organic frameworks stand out, showing extremely high maximum mol/weight removal. This is attributed

not only to the regular structure of the organic frameworks but also (in the case of MOF) to the multiple interactions available for sorption, which generally increase the affinity towards PFAS [57]. In contrast, sorption fluctuations of short-chain PFAS were observed in the initial phase of adsorption kinetic experiments with materials heavily relying on electrostatic interactions like cationic QNC, likely due to the weak bonds formed between QNC and short-chain PFAA that caused noticeable desorption of the contaminants [13]. Despite this, nanocellulose- and lignocellulosic-based materials are also interesting alternatives given their high Q_m and short equilibrium time coupled with their biodegradability and wide availability. Some LDH also achieved high adsorption of PFAS and fast equilibrium kinetics, as the structure of LDHs also offers high tunability, high surface area, and a wide range of possible interactions.

Overall, many alternative adsorbents display great potential for PFAS removal under environmentally challenging conditions. Even if biomaterials such as functionalized cellulose represent a more economically and environmentally sustainable alternative than other materials, they must be further explored for both the removal of PFAS substitutes under simulated environmental conditions and reusability.

Although the discussion of the rate uptake kinetics is beyond the scope of this review, some authors have highlighted non-negligible flaws in the use of pseudo-first-order and pseudo-second-order kinetic models that favours the latter, such as the use of R^2 as the only or main criterion for the selection of the most appropriate model, an inadequate number of data points, or the indiscriminate use of the non-linear and linear form of the models [112,184].

4.3. Comparison between advanced and conventional materials

It is evident that traditional commercial materials and innovative ones comes with different pros and cons. The most valuable advantages of advanced materials are i) the tunability of pore size and morphology, as the closest they are to the adsorbate size, the stronger the adsorption [50], and ii) the extremely fast uptake kinetics in low-to-highly concentrated PFAS solutions (Fig. 2). On the other hand, the competitiveness of bio-based materials relies on the availability of raw materials and their low cost. A comprehensive analysis of the expenses associated with different (both bio-based and non-bio-based) adsorbents has been carried out recently [185]. The analysis considered various factors, among which raw material costs, operational costs of adsorption, cost trends, and cost of a gram of adsorbent relative to a gram of adsorbate removed. It emerged that the cost performance of numerous bio-adsorbents was relatively lower compared to synthetic or chemical adsorbents.

Compared to the reviewed materials, AC generally resulted less selective, which can be both an advantage and a disadvantage as they could remove differently charged PFAS simultaneously, as well as the plethora of other contaminants they are exposed to. Both AC and resins are well-known, full-scale tested materials and some of them showed overall good PFAS removal in the presence of OM, like the A860 resin by Purolite® [186]. The reusability of alternative materials also suffers from their higher selectivity. Taking β-CD polymers as an example, it has been highlighted that the degree of reusability/desorption of the same material can vary greatly between different micropollutants [160]. This is relevant when considering the wide range of pollutants in natural waters and wastewaters. As such, it would be advisable to consider the reviewed materials not as alternatives to IER and AC but as complementary sorbents to be used in a treatment train starting from the less selective (towards PFAS and especially short-chain ones) AC and then making use of more selective, highly efficient adsorbents [95], thus improving the efficacy and the adaptability of removal strategies [187]. In this view, materials showing a high relative removal of short-chain PFAS would be particularly attractive, as activated carbons are expected to efficiently remove long-chain PFAS, which will breakthrough later than the shorter homologues.

To effectively compare the reviewed materials against AC and IER, similar experimental conditions and (in the case of porous and/or powdered materials) similar surface area/granule size would be required. However, different experimental conditions have been used in the literature. PFAS concentrations in sorption tests vary widely (typically 2−3 orders of magnitude). Lower pollutant concentrations are associated with a decreased contact rate with the sorbent and with a lower concentration gradient between the bulk phase and the material. This, in turn, reduces adsorption capacity [59]. Moreover, PFAS like PFOS and PFOA can form micelles at mg/L and/or hemi-micelles at μg/L level [6]. This is known to affect their removal rate, but opposing results are reported in this regard [113]. Though it is widely described in the literature that such structures can block pore entrances and limit access to sorption sites, thus decreasing the adsorption capacity [114] or slowing down adsorption kinetics [6], some authors linked their formation to an increased adsorption of PFOA [188] Almost all adsorption tests were carried out at PFAS concentrations $\geq$1 μg/L.

Conducting tests representative of non-contaminated sites where PFAS occur at ng/L range is a necessary step toward a comprehensive assessment of the applicability of adsorption materials for lower concentration scenarios. However, it is acknowledged that achieving such testing conditions may pose challenges due to the analytical equipment requirements and complexity in sample preparation. Nevertheless, where similar conditions have been used, many of the proposed materials outperformed ACs and IER in terms of removal efficiency and were less sensible to the presence of NOM. The dosage of adsorbents also varies significantly, but even a comparison per unit of mass of different adsorbents would be only partially significant due to the different properties of the materials and availability of active sites. Moreover, while increasing the amount of adsorbent would generally result in greater removal of pollutants, this isn't always true: the newly-available active sites (occurring at higher dosages) may remain unsaturated, or might not be accessible due to factors like overlapping or aggregation of the material, as observed in studies by Militao et al. and Qin et al. [3,11].

PFAS tested are often limited to anionic PFAA. PFAS-polluted hotspots related to production areas or usage of AFFF are more likely to be contaminated by a wide range of PFAS. Though the inclusion of the substitutes of the legacy long-chain PFAS in adsorption studies has significantly increased in recent years, the removal of short-chain, novel, and emerging PFAS by both conventional and non-conventional sorbents is still overlooked. An ideal set of analytes should include PFBA, PFBS, PFOA, and PFOS as well as one-two PFECA/PFESA (which are well-known and subjected to regulations at the national to international level) and selected cationic, non-ionic, and zwitterionic PFAS detected in the environment, that should also be tested in mixed solutions. This would allow a more robust evaluation of adsorbents in terms of affinity and selectivity towards the most hydrophilic and short compounds.

4.4. Role of organic matter on PFAS adsorption

As seen, the co-occurrence of OM is mostly associated with the lower accessibility to pores and to the competition for adsorption sites. Depending on the type of coexisting organic pollutant and/or the concentration of OM, the adsorption performance of traditional vs alternative sorbents can change significantly [46]. HA is often

used as a surrogate of OM, with typically tested concentrations ranging from units to a few tens of mg/L, reflecting those usually found in natural waters [189,190]. However, dissolved organic matter can be highly heterogeneous [121] and encompasses a wide range of compounds including complex polymers and macromolecules, as well as (among others) trace organic substances and pollutants, such as carboxylic acids, pharmaceuticals, and personal care products, pesticides, etc. other than NOM [191]. This is particularly important if the tested material is supposed to be used in wastewater treatment plants, where these components are present at higher concentrations than in natural waters, like humic acid (occurring at around 50–100 mg/L) [192]. Some works carried out a broad evaluation of the influence of organic co-contaminants such as pharmaceuticals or non-fluorinated surfactants present in AFFF such as sodium dodecyl sulphate in addition to PFAS and mixed solutions [50,51,55] that better describe the selectivity of materials as opposed to the sole use of HA as a proxy for OM.

Many clay-based materials and COFs, besides PANI, DFB-CDP, TFN-CDP, and all-silica zeolites, were barely affected by the presence of OM at mg/L level. In comparison, the competition for adsorption sites and blockage of adsorbent pores of ACs is more pronounced (see SI part 1 for further information). Given the predominantly negative charge of ACs at environmental pH, their interaction of the typically used HA/FA (with negative zeta potential at circumneutral pH) arises from hydrophobic interactions, hence the competition with PFAS. The tolerance of IER to the presence of OM is generally higher than that of ACs as the adsorption mainly relies on electrostatic interactions.

In general, the interaction of the materials with the OM is a complex phaenomenon that has been linked to opposed results.

4.5. Recyclability, regenerability, and applicability

Many non-conventional materials could be reused for at least 3–10 regeneration cycles without significantly lowering the removal rate of analytes and with almost complete desorption of the adsorbed PFAS, with few exceptions like bifunctionalized PEGDA, PAF-45, and BT-TDC-COF (COF1) and BT-BDB-COF (COF2). Concerning substitutes, modified PEGDA, DMPAA-Q, and NU-1000 maintained the initial removal capacity of C4 PFAA and GenX over 5-8 adsorption/desorption cycles. Another ionic fluorogel (“IF-1”) consistently removed >75% of an 18 mg/L GenX solution over 5 adsorption-desorption cycles [163]. Indeed, the number of adsorption-desorption cycles performed varied considerably between publications evaluating the regeneration of adsorbents, and a comparison is not entirely possible. An appropriate number of cycles also depends on the mean of regeneration and on the amenability of the material to solvent washing, which is the most used regeneration method. For example, a slight morphological change on an MNP-fluorographene composite material was noted together with a partial separation of the attached magnetic NPs [45], although 2-MNPs@FG was able to remove >79% and >83% of PFOA and PFOS at the 12th desorption-adsorption cycle. Nevertheless, among the most remarkable materials in terms of reusability are cyclodextrin polymers, which can be regenerated over $\geq$5 adsorption/desorption cycles with negligible loss of performance for a plethora of micropollutants, including PFAS [157,161]. The removal of 24 and 22 PFAS in mixed solutions only slightly decreased in regeneration experiments over 3 and 4 cycles with the covalent organic frameworks FSQ-1 and Cys-COF, respectively.

A MeOH- or MeOH:H_2O-based solution added with NaCl represents the most used regeneration medium, as it weakens the hydrophobic and electrostatic interactions between the PFAS and the sorbent material [54,193]. Cl^- ions also replace anionic PFAS such as GenX on quaternary ammonium groups of adsorbents in MeOH solutions, as opposed to aqueous solutions [24]. Desorption tests have highlighted the partial immobilization of PFAS in the framework of some materials [194].

Other less-explored regeneration methods include the use of low-power ultrasound (900 kHz, 15.8 W) to efficiently desorb a mixture of PFAS to form a surface-functionalized GAC (polyDADMAC-GAC) without damaging the adsorbent structure. By reamending the adsorbent with polyDADMAC (that was partially removed due to sonication), the adsorption capacity for PFBA only decreased by 2–4% over four adsorption-desorption rounds [60]. Thermal desorption of PFOA (350 °C) was proven effective for beta-type zeolites, that were not damaged in the process, although management of the desorbed PFAS was not discussed further [51]. There are examples of thermoresponsive hydrogels that can desorb pollutants with hydrophobic moieties in response to the changing temperature that promotes hydration-dehydration of the gel structure, i.e. temporarily changing its overall hydrophobicity [167]. Other sustainable, biodegradable alternatives produced from low-cost and low-impact materials were designed as single-use materials [10,13]. Another proposed route to improve the cost-efficiency of AC regeneration has been the exploitation of an advanced oxidation process or hydrothermal alkaline treatment to desorb and degrade PFAS [195,196].

The full-scale in-situ and ex-situ application of adsorbent materials typically requires a packed column; hence, the smaller the adsorbent particle size, the higher the flow resistance. As for the hardly applicable powdered materials, solutions are required to immobilize the particles in support systems. For example, a composite sodium silicate-synthetic zeolite was proposed, although it did not outperform an unmodified natural zeolite because of the obstruction of adsorption sites [50]. Such a disadvantage has to be taken into account and other authors have proposed the use of larger-sized particles as scaffolds such as SiO_2 [23] o r encapsulating alginate beads [3,5]. These enclosing structures can also facilitate the simultaneous degradation of PFAS by encapsulated acclimated bacterial consortia with the adsorption on the structure itself and the biosorption in the microbes [197]. These larger structures would be much easier to implement in a packed column of a water treatment plant. Hydrogels have been used as carriers to immobilize magnetic and non-magnetic nanoparticles, which enhanced their adsorption capacity and facilitated their recovery (in the case of micronized gels with high surface area) from the water matrix [167].

Another important factor to assess the suitability of a material for water treatment is its cost. Some of the reported materials showed a competitive weight-based price in comparison to commercial ACs, which have been reported to vary between a few USD/Kg to 15–22 USD/Kg [198]. Lower costs (roughly 1.5–4 USD/Kg) were estimated for ACs derived from more sustainable/waste-derived sources like broiler litter or rice husks [199,200]. However, the cost of a material (including the long-used ACs) is hardly ever estimated, and, therefore, scarcely reported in the peer-reviewed literature. This further complicates an appropriate evaluation of the alternative adsorbents. This evaluation involves numerous variables, spanning from a country's inflation rate to raw material expenses, making it a challenging task. Nevertheless, the scientific community needs to undertake this challenge to boost the competitiveness of the new materials. Recently, some authors proposed the “adsorbent cost performance”, a generic metric representing the combined cost of production and use of a sorbent to remove 1 mol of a chemical based on its maximum uptake, per gram of the sorbent [185]. Such a metric could be applied to provide a preliminary cost analysis of a given material at the laboratory scale.

5. Concluding remarks and future perspectives

As time progresses, increasingly stringent enforceable and guideline concentration-based thresholds on well-known and widespread PFAS are being introduced [201], while the number of PFAS recorded in the environment is remarkably increasing. The diversity and the intrinsic modifiability of adsorbent materials can help address the growing array of substances belonging to this class, but research in this field needs to take into consideration the following aspects.

- It is unlikely that conventional adsorbents (especially ACs) will be easily replaced given their wide use, availability, and low cost. New materials should, therefore, be tailored to complement these materials. In this view, new adsorbent materials should be characterized by i) high PFAS selectivity ii) fast adsorption kinetics iii) high adsorption capacity at environmentally challenging conditions, and iv) environmental/economic sustainability. On the latter regard, the scientific community should make an effort in this direction for an easier transition towards the actual applicability of newly-proposed materials by broadly estimating their cost.
- Many materials functionalized with both fluorine-containing and amine-containing moieties showed fast kinetics, high adsorption efficiency, and selectivity towards PFAS.
- Among bio-based sorbents, nanocellulosic- and nanolignocellulosic-based materials showed good results. LDHs also represent widely available clayey materials with great potential for the adsorption of PFAS. Organic frameworks are advanced materials that showed the most impressive results, even in challenging experimental conditions.
- Innovative materials should be benchmarked against the widely applied ones in the same experimental conditions to assess their potential thoroughly. A few key organic competitors for adsorption should also be used to address selectivity.
- It is also mandatory to adopt a wider basic set of PFAS molecules to be tested including new-generation PFAS and short-chain PFAA. Moreover, there is a need for materials that are able to remove even non-ionic, zwitterionic and cationic PFAS.
- Adsorption tests should be carried out at both high and low (i.e., environmentally relevant) PFAS concentrations as well as in PFAS-polluted or PFAS-spiked environmental aqueous samples.

CRediT authorship contribution statement

Francesco Calore: Writing – review & editing, Writing – original draft, Methodology, Data curation, Conceptualization. **Elena Badetti:** Writing – review & editing, Writing – original draft, Supervision, Methodology, Data curation, Conceptualization. **Alessandro Bonetto:** Writing – review & editing, Writing – original draft, Data curation. **Anna Pozzobon:** Writing – original draft. **Antonio Marcomini:** Writing – review & editing, Validation, Supervision, Methodology, Conceptualization.

Declaration of competing interest

The authors declare that they have no known competing financial interests or personal relationships that could have appeared to influence the work reported in this paper.

Appendix A. Supplementary data

Supplementary data to this article can be found online at https://doi.org/10.1016/j.emcon.2024.100303.

References

[1] B.D. Turner, S.W. Sloan, G.R. Currell, Novel remediation of per- and polyfluoroalkyl substances (PFASs) from contaminated groundwater using Cannabis Sativa L. (hemp) protein powder, Chemosphere 229 (2019) 22–31, https://doi.org/10.1016/j.chemosphere.2019.04.139.

[2] E.T. Hernandez, B. Koo, L.E. Sofen, R. Amin, R.K. Togashi, A.I. Lall, D.J. Gisch, B.J. Kern, M.A. Rickard, M.B. Francis, Proteins as adsorbents for PFAS removal from water, Environ. Sci. Water Res. Technol. 8 (2022) 1188–1194, https://doi.org/10.1039/D1EW00501D.

[3] I.M. Militao, F. Roddick, R. Bergamasco, L. Fan, Rapid adsorption of PFAS: application of Moringa oleifera seed powder encapsulated in alginate beads, Environ. Technol. Innov. 28 (2022) 102761, https://doi.org/10.1016/J.ETI.2022.102761.

[4] S. Mantripragada, M. Dong, L. Zhang, Sustainable filter/adsorbent materials from cellulose-based electrospun nanofibrous membranes with soy protein coating for high-efficiency GenX fluorocarbon remediation from water, Cellulose 30 (2023) 7063–7078, https://doi.org/10.1007/s10570-023-05304-7.

[5] I.M. Militao, F. Roddick, L. Fan, L.C. Zepeda, R. Parthasarathy, R. Bergamasco, PFAS removal from water by adsorption with alginate-encapsulated plant albumin and rice straw-derived biochar, J. Water Process Eng. 53 (2023) 103616, https://doi.org/10.1016/J.JWPE.2023.103616.

[6] Q. Zhang, S. Deng, G. Yu, J. Huang, Removal of perfluorooctane sulfonate from aqueous solution by crosslinked chitosan beads: sorption kinetics and uptake mechanism, Bioresour. Technol. 102 (2011) 2265–2271, https://doi.org/10.1016/j.biortech.2010.10.040.

[7] S. Deng, Y.Q. Zheng, F.J. Xu, B. Wang, J. Huang, G. Yu, Highly efficient sorption of perfluorooctane sulfonate and perfluorooctanoate on a quaternized cotton prepared by atom transfer radical polymerization, Chem. Eng. J. 193–194 (2012) 154–160, https://doi.org/10.1016/j.cej.2012.04.005.

[8] S. Deng, L. Niu, Y. Bei, B. Wang, J. Huang, G. Yu, Adsorption of perfluorinated compounds on aminated rice husk prepared by atom transfer radical polymerization, Chemosphere 91 (2013) 124–130, https://doi.org/10.1016/j.chemosphere.2012.11.015.

[9] M. Ateia, M.F. Attia, A. Maroli, N. Tharayil, F. Alexis, D.C. Whitehead, T. Karanfil, Rapid removal of poly-and perfluorinated alkyl substances by poly(ethylenimine)-functionalized cellulose microcrystals at environmentally relevant conditions, Environ. Sci. Technol. Lett. 5 (2018) 764–769, https://doi.org/10.1021/acs.estlett.8b00556.

[10] J. Li, X. Li, Y. Da, J. Yu, B. Long, P. Zhang, C. Bakker, B.A. McCarl, J.S. Yuan, S.Y. Dai, Sustainable environmental remediation via biomimetic multifunctional lignocellulosic nano-framework, Nat. Commun. 13 (2022) 1–13, https://doi.org/10.1038/s41467-022-31881-5.

[11] F. Qin, W. Yao, Y. Liu, B. Zhu, Q. Yang, Y. Zheng, Polyethyleneimine functionalized cellulose-rich agroforestry residues for removing perfluorooctanoic acid: adsorption performance and mechanism, Cellulose (2023) 1–14, https://doi.org/10.1007/s10570-023-05090-2.

[12] B. Niu, M. Yu, C. Sun, L. Wang, Y. Niu, H. Huang, Y. Zheng, A comparative study for removal of perfluorooctanoic acid using three kinds of N-polymer functionalized calotropis gigantea fiber, J. Nat. Fibers 19 (2022) 2119–2128, https://doi.org/10.1080/15440478.2020.1798848.

[13] D. Li, C.S. Lee, Y. Zhang, R. Das, F. Akter, A.K. Venkatesan, B.S. Hsiao, Efficient removal of short-chain and long-chain PFAS by cationic nanocellulose, J. Mater. Chem. A 11 (2023) 9868–9883, https://doi.org/10.1039/D3TA01851B.

[14] J.T. Harris, G.D. De La Garza, A.M. Devlin, A.J. Mcneil, Rapid Removal of Poly- And Perfluoroalkyl Substances with Quaternized Wood Pulp, 2022, https://doi.org/10.1021/acsestwater.1c00396.

[15] S. Mantripragada, D. Deng, L. Zhang, Remediation of GenX from water by amidoxime surface-functionalized electrospun polyacrylonitrile nanofibrous adsorbent, Chemosphere 283 (2021) 131235, https://doi.org/10.1016/j.chemosphere.2021.131235.

[16] S. Mantripragada, D. Deng, L. Zhang, Algae-enhanced electrospun polyacrylonitrile nanofibrous membrane for high-performance short-chain PFAS remediation from water, Nanomaterials 13 (2023) 2646, https://doi.org/10.3390/NANO13192646.

[17] Y. Olshansky, A. Gomeniuc, J. Chorover, L. Abrell, J.A. Field, J. Hatton, J. He, R. Sierra-Alvarez, Tailored polyanilines are high-affinity adsorbents for per- and polyfluoroalkyl substances, ACS ES T Water 2 (2022) 1402–1410, https://doi.org/10.1021/acsestwater.2c00166.

[18] C. Xu, H. Chen, F. Jiang, Adsorption of perflourooctane sulfonate (PFOS) and perfluorooctanoate (PFOA) on polyaniline nanotubes, Colloids Surfaces A Physicochem. Eng. Asp. 479 (2015) 60–67, https://doi.org/10.1016/j.colsurfa.2015.03.045.

[19] J. He, A. Gomeniuc, Y. Olshansky, J. Hatton, L. Abrell, J.A. Field, J. Chorover, R. Sierra-Alvarez, Enhanced removal of per- and polyfluoroalkyl substances by crosslinked polyaniline polymers, Chem. Eng. J. 446 (2022) 137246, https://doi.org/10.1016/j.cej.2022.137246.

[20] W. Ji, L. Xiao, Y. Ling, C. Ching, M. Matsumoto, R.P. Bisbey, D.E. Helbling, W.R. Dichtel, Removal of GenX and perfluorinated alkyl substances from water by amine-functionalized covalent organic frameworks, J. Am. Chem. Soc. 140 (2018) 12677–12681, https://doi.org/10.1021/jacs.8b06958.

[21] C. He, Y. Yang, Y.J. Hou, T. Luan, J. Deng, Chitosan-coated fluoro-

functionalized covalent organic framework as adsorbent for efficient removal of per- and polyfluoroalkyl substances from water, Sep. Purif. Technol. 294 (2022) 121195, https://doi.org/10.1016/J.SEPPUR.2022.121195.
[22] J. Huang, Y. Shi, G. zhang Huang, S. Huang, J. Zheng, J. Xu, F. Zhu, G. Ouyang, Facile synthesis of a fluorinated-squaramide covalent organic framework for the highly efficient and broad-spectrum removal of per- and polyfluoroalkyl pollutants, Angew. Chem. Int. Ed. 61 (2022) e202206749, https://doi.org/10.1002/ANIE.202206749.
[23] J. Huang, Y. Shi, J. Xu, J. Zheng, F. Zhu, X. Liu, G. Ouyang, J. Huang, Y. Shi, J. Xu, J. Zheng, F. Zhu, G. Ouyang, X. Liu, Hollow covalent organic framework with "shell-confined" environment for the effective removal of anionic per- and polyfluoroalkyl substances, Adv. Funct. Mater. 32 (2022) 2203171, https://doi.org/10.1002/ADFM.202203171.
[24] W. Wang, Z. Zhou, H. Shao, S. Zhou, G. Yu, S. Deng, Cationic covalent organic framework for efficient removal of PFOA substitutes from aqueous solution, Chem. Eng. J. 412 (2021) 127509, https://doi.org/10.1016/J.CEJ.2020.127509.
[25] W. Wang, H. Shao, S. Zhou, D. Zhu, X. Jiang, G. Yu, S. Deng, Rapid removal of perfluoroalkanesulfonates from water by β-cyclodextrin covalent organic frameworks, ACS Appl. Mater. Interfaces 13 (2021) 48700–48708, https://doi.org/10.1021/acsami.1c14043.
[26] B. Wang, L.S. Lee, C. Wei, H. Fu, S. Zheng, Z. Xu, D. Zhu, Covalent triazine-based framework: a promising adsorbent for removal of perfluoroalkyl acids from aqueous solution, Environ. Pollut. 216 (2016) 884–892, https://doi.org/10.1016/J.ENVPOL.2016.06.062.
[27] W. Wang, S. Zhou, X. Jiang, G. Yu, S. Deng, Fluorinated quaternary ammonium covalent organic frameworks for selective and efficient removal of typical per-and polyfluoroalkyl substances, Chem. Eng. J. 474 (2023) 145629, https://doi.org/10.1016/j.cej.2023.145629.
[28] R. Li, S. Alomari, R. Stanton, M.C. Wasson, T. Islamoglu, O.K. Farha, T.M. Holsen, S. Mededovic Thagard, D.J. Trivedi, M. Wriedt, Efficient removal of per- and polyfluoroalkyl substances from water with zirconium-based metal–organic frameworks, Chem. Mater. 33 (2021) 3276–3285, https://doi.org/10.1021/acs.chemmater.1c00324.
[29] J. Pala, T. Le, M. Kasula, M. Rabbani Esfahani, Systematic investigation of PFOS adsorption from water by metal organic frameworks, activated carbon, metal organic Framework@Activated carbon, and functionalized metal organic frameworks, Sep. Purif. Technol. 309 (2023) 123025, https://doi.org/10.1016/J.SEPPUR.2022.123025.
[30] P.-H. Chang, C.-Y. Chen, R. Mukhopadhyay, W. Chen, Y.-M. Tzou, B. Sarkar, Novel MOF-808 metal-organic framework as highly efficient adsorbent of perfluorooctane sulfonate in water, J. Colloid Interface Sci. 623 (2022) 627–636, https://doi.org/10.1016/j.jcis.2022.05.050.
[31] P.-H. Chang, R. Mukhopadhyay, B. Zhong, Q.-Y. Yang, S. Zhou, Y.-M. Tzou, B. Sarkar, Synthesis and characterization of PCN-222 metal organic framework and its application for removing perfluorooctane sulfonate from water, J. Colloid Interface Sci. 636 (2023) 459–469, https://doi.org/10.1016/j.jcis.2023.01.032.
[32] Y. Hu, M. Guo, S. Zhang, W. Jiang, T. Xiu, S. Yang, M. Kang, Z. Dongye, Z. Li, L. Wang, Microwave synthesis of metal-organic frameworks absorbents (DUT-5-2) for the removal of PFOS and PFOA from aqueous solutions, Microporous Mesoporous Mater. 333 (2022) 111740, https://doi.org/10.1016/j.micromeso.2022.111740.
[33] Y. Li, Z. Yang, Y. Wang, Z. Bai, T. Zheng, X. Dai, S. Liu, D. Gui, W. Liu, M. Chen, L. Chen, J. Diwu, L. Zhu, R. Zhou, Z. Chai, T.E. Albrecht-Schmitt, S. Wang, A mesoporous cationic thorium-organic framework that rapidly traps anionic persistent organic pollutants, Nat. Commun. 8 (2017), https://doi.org/10.1038/s41467-017-01208-w.
[34] Q. Luo, C. Zhao, G. Liu, H. Ren, A porous aromatic framework constructed from benzene rings has a high adsorption capacity for perfluorooctane sulfonate, Sci. Rep. 6 (2016), https://doi.org/10.1038/srep20311.
[35] A. Yang, C. Ching, M. Easler, D.E. Helbling, W.R. Dichtel, Cyclodextrin polymers with nitrogen-containing tripodal crosslinkers for efficient PFAS adsorption, ACS Mater. Lett. 2 (2020) 1240–1245, https://doi.org/10.1021/acsmaterialslett.0c00240.
[36] L. Xiao, Y. Ling, A. Alsbaiee, C. Li, D.E. Helbling, W.R. Dichtel, β-Cyclodextrin polymer network sequesters perfluorooctanoic acid at environmentally relevant concentrations, J. Am. Chem. Soc. 139 (2017) 7689–7692, https://doi.org/10.1021/jacs.7b02381.
[37] M.J. Klemes, Y. Ling, C. Ching, C. Wu, L. Xiao, D.E. Helbling, W.R. Dichtel, Reduction of a tetrafluoroterephthalonitrile-β-cyclodextrin polymer to remove anionic micropollutants and perfluorinated alkyl substances from water, Angew. Chem. Int. Ed. 58 (2019) 12049–12053, https://doi.org/10.1002/anie.201905142.
[38] R. Wang, Z.-W. Lin, M.J. Klemes, M. Ateia, B. Trang, J. Wang, C. Ching, D.E. Helbling, W.R. Dichtel, A tunable porous β-cyclodextrin polymer platform to understand and improve anionic PFAS removal, ACS Cent. Sci. 2022 (2022) 663–669, https://doi.org/10.1021/acscentsci.2c00478.
[39] P.-J. Huang, M. Hwangbo, Z. Chen, Y. Liu, J. Kameoka, K.-H. Chu, Reusable functionalized hydrogel sorbents for removing long-and short-chain perfluoroalkyl acids (PFAAs) and GenX from aqueous solution, ACS Omega 3 (2018) 17447–17455, https://doi.org/10.1021/acsomega.8b02279.
[40] E. Kumarasamy, I.M. Manning, L.B. Collins, O. Coronell, F.A. Leibfarth, Ionic fluorogels for remediation of per-and polyfluorinated alkyl substances from water, ACS Cent. Sci. 6 (2020) 487–492, https://doi.org/10.1021/acscentsci.9b01224.
[41] M. Ateia, M. Arifuzzaman, S. Pellizzeri, M.F. Attia, N. Tharayil, J.N. Anker, T. Karanfil, Cationic polymer for selective removal of GenX and short-chain PFAS from surface waters and wastewaters at ng/L levels, Water Res. 163 (2019) 114874, https://doi.org/10.1016/j.watres.2019.114874.
[42] W.R. Wang, P.Y. Chen, J. Deng, Y. Chen, H.J. Liu, Carbon-dot hydrogels as superior carbonaceous adsorbents for removing perfluorooctane sulfonate from water, Chem. Eng. J. 435 (2022) 135021, https://doi.org/10.1016/J.CEJ.2022.135021.
[43] A. Saad, R. Mills, H. Wan, M.A. Mottaleb, L. Ormsbee, D. Bhattacharyya, Thermo-responsive adsorption-desorption of perfluoroorganics from water using PNIPAm hydrogels and pore functionalized membranes, J. Membr. Sci. 599 (2020) 117821, https://doi.org/10.1016/j.memsci.2020.117821.
[44] Q. Quan, H. Wen, S. Han, Z. Wang, Z. Shao, M. Chen, Fluorous-core nanoparticle-embedded hydrogel synthesized via tandem photo-controlled radical polymerization: facilitating the separation of perfluorinated alkyl substances from water, ACS Appl. Mater. Interfaces 12 (2020) 24319–24327, https://doi.org/10.1021/acsami.0c04646.
[45] W. Wang, Z. Xu, X. Zhang, A. Wimmer, E. Shi, Y. Qin, X. Zhao, B. Zhou, L. Li, Rapid and efficient removal of organic micropollutants from environmental water using a magnetic nanoparticles-attached fluorographene-based sorbent, Chem. Eng. J. 343 (2018) 61–68, https://doi.org/10.1016/j.cej.2018.02.101.
[46] Z. Du, S. Deng, S. Zhang, W. Wang, B. Wang, J. Huang, Y. Wang, G. Yu, B. Xing, Selective and fast adsorption of perfluorooctanesulfonate from wastewater by magnetic fluorinated vermiculite, Environ. Sci. Technol. 51 (2017) 8027–8035, https://doi.org/10.1021/acs.est.6b06540.
[47] Y. Zhou, Z. He, Y. Tao, Y. Xiao, T. Zhou, T. Jing, Y.Y.Y.Y. Zhou, S. Mei, Preparation of a functional silica membrane coated on Fe3O4 nanoparticle for rapid and selective removal of perfluorinated compounds from surface water sample, Chem. Eng. J. 303 (2016) 156–166, https://doi.org/10.1016/j.cej.2016.05.137.
[48] A.Z.M. Badruddoza, B. Bhattarai, R.P.S. Suri, Environmentally friendly β-Cyclodextrin–Ionic liquid polyurethane-modified magnetic sorbent for the removal of PFOA, PFOS, and Cr(VI) from water, ACS Sustain. Chem. Eng. 5 (2017) 9223–9232, https://doi.org/10.1021/acssuschemeng.7b02186.
[49] X. Tan, P. Dewapriya, P. Prasad, Y. Chang, X. Huang, Y. Wang, X. Gong, T.E. Hopkins, C. Fu, K.V. Thomas, H. Peng, A.K. Whittaker, C. Zhang, Efficient removal of perfluorinated chemicals from contaminated water sources using magnetic fluorinated polymer sorbents, Angew. Chem. Int. Ed. 61 (2022), https://doi.org/10.1002/ANIE.202213071.
[50] J.J. Licato, G.D. Foster, T.B. Huff, Zeolite composite materials for the simultaneous removal of pharmaceuticals, personal care products, and perfluorinated alkyl substances in water treatment, ACS ES T Water (2022), https://doi.org/10.1021/acsestwater.2c00024.
[51] M. Van den Bergh, A. Krajnc, S. Voorspoels, S.R. Tavares, S. Mullens, I. Beurroies, G. Maurin, G. Mali, D.E. De Vos, Highly selective removal of perfluorinated contaminants by adsorption on all-silica zeolite beta, Angew. Chem. Int. Ed. 59 (2020) 14086–14090, https://doi.org/10.1002/ANIE.202002953.
[52] M.S. Hossain, T. Dwyer Stuart, B. V Ramarao, C.C. Vanleuven, M. Wriedt, D. Kiemle, M. Satchwell, D. Kumar, Investigation into Cationic Surfactants and Polyelectrolyte-Coated β-Zeolites for Rapid and High-Capacity Adsorption of Short-And Long-Chain PFAS, 2023, https://doi.org/10.1021/acs.iecr.3c00468.
[53] A. Lauwers, J. Vercammen, D. De Vos, Adsorption of PFAS by all-silica zeolite β: insights into the effect of the water matrix, regeneration of the material, and continuous PFAS adsorption, ACS Appl. Mater. Interfaces 15 (2023) 52612–52621, https://doi.org/10.1021/ACSAMI.3C12321/SUPPL_FILE/AM3C12321_SI_001.PDF.
[54] X. Min, J. Huo, Q. Dong, S. Xu, Y. Wang, Enhanced sorption of perfluorooctanoic acid with organically functionalized layered double hydroxide, Chem. Eng. J. 446 (2022) 137019, https://doi.org/10.1016/J.CEJ.2022.137019.
[55] V. Alonso-de-Linaje, M.C. Mangayayam, D.J. Tobler, V. Rives, R. Espinosa, K.N. Dalby, Enhanced sorption of perfluorooctane sulfonate and perfluorooctanoate by hydrotalcites, Environ. Technol. Innov. 21 (2021) 101231, https://doi.org/10.1016/J.ETI.2020.101231.
[56] J. Huo, X. Min, Q. Dong, S. Xu, Y. Wang, Comparison of Zn–Al and Mg–Al layered double hydroxides for adsorption of perfluorooctanoic acid, Chemosphere 287 (2022) 132297, https://doi.org/10.1016/J.CHEMOSPHERE.2021.132297.
[57] X. Tan, Z. Jiang, W. Ding, M. Zhang, Y. Huang, Multiple interactions steered high affinity toward PFAS on ultrathin layered rare-earth hydroxide nanosheets: remediation performance and molecular-level insights, Water Res. 230 (2023) 119558, https://doi.org/10.1016/J.WATRES.2022.119558.
[58] P.H. Chang, Z. Li, W.T. Jiang, Calcination of hydrotalcite to enhance the removal of perfluorooctane sulfonate from water, Appl. Clay Sci. 190 (2020) 105563, https://doi.org/10.1016/J.CLAY.2020.105563.
[59] P.N. Omo-Okoro, C.J. Curtis, A. Miralles Marco, L. Melymuk, J.O. Okonkwo, Removal of per- and polyfluoroalkyl substances from aqueous media using synthesized silver nanocomposite-activated carbons, J. Environ. Sci. Eng. 19 (2021) 217–236, https://doi.org/10.1007/s40201-020-00597-3.
[60] P. Ramos, S. Singh Kalra, N.W. Johnson, C.M. Khor, A. Borthakur, B. Cranmer, G. Dooley, S.K. Mohanty, D. Jassby, J. Blotevogel, S. Mahendra, Enhanced removal of per- and polyfluoroalkyl substances in complex matrices by polyDADMAC-coated regenerable granular activated carbon, Environ. Pollut.

294 (2022) 118603, https://doi.org/10.1016/J.ENVPOL.2021.118603.
[61] J. Xu, Z. Liu, D. Zhao, N. Gao, X. Fu, Enhanced adsorption of perfluorooctanoic acid (PFOA) from water by granular activated carbon supported magnetite nanoparticles, Sci. Total Environ. 723 (2020) 137757, https://doi.org/10.1016/j.scitotenv.2020.137757.
[62] N. Saeidi, F.D. Kopinke, A. Georgi, What is specific in adsorption of perfluoroalkyl acids on carbon materials? Chemosphere 273 (2021) 128520 https://doi.org/10.1016/J.CHEMOSPHERE.2020.128520.
[63] J. Glüge, M. Scheringer, I.T. Cousins, J.C. DeWitt, G. Goldenman, D. Herzke, R. Lohmann, C.A. Ng, X. Trier, Z. Wang, An overview of the uses of per- and polyfluoroalkyl substances (PFAS), Environ. Sci. Process. Impacts. (2020) 2345–2373, https://doi.org/10.1039/d0em00291g.
[64] Z. Wang, A.M. Buser, I.T. Cousins, S. Demattio, W. Drost, O. Johansson, K. Ohno, G. Patlewicz, A.M. Richard, G.W. Walker, G.S. White, E. Leinala, A new OECD definition for per-and polyfluoroalkyl substances, Environ. Sci. Technol. 55 (2021) 15575–15578, https://doi.org/10.1021/acs.est.1c06896.
[65] I.T. Cousins, J.C. Dewitt, J. Glüge, G. Goldenman, D. Herzke, R. Lohmann, C.A. Ng, M. Scheringer, Z. Wang, The high persistence of PFAS is sufficient for their management as a chemical class, Environ. Sci. Process. Impacts. 22 (2020) 2307–2312, https://doi.org/10.1039/D0EM00355G.
[66] M.S. Johnson, R.C. Buck, I.T. Cousins, C.P. Weis, S.E. Fenton, Estimating environmental hazard and risks from exposure to per- and polyfluoroalkyl substances (PFASs): outcome of a SETAC focused topic meeting, Environ. Toxicol. Chem. 40 (2021) 543–549, https://doi.org/10.1002/etc.4784.
[67] C.F. Kwiatkowski, D.Q. Andrews, L.S. Birnbaum, T.A. Bruton, J.C. Dewitt, D.R.U. Knappe, M.V. Maffini, M.F. Miller, K.E. Pelch, A. Reade, A. Soehl, X. Trier, M. Venier, C.C. Wagner, Z. Wang, A. Blum, Scientific basis for managing PFAS as a chemical class, Environ. Sci. Technol. Lett. 7 (2020) 532–543, https://doi.org/10.1021/acs.estlett.0c00255.
[68] S.F. Nakayama, M. Yoshikane, Y. Onoda, Y. Nishihama, M. Iwai-Shimada, M. Takagi, Y. Kobayashi, T. Isobe, Worldwide trends in tracing poly- and perfluoroalkyl substances (PFAS) in the environment, TrAC, Trends Anal. Chem. 121 (2019), https://doi.org/10.1016/j.trac.2019.02.011.
[69] S. Zahm, J.P. Bonde, W.A. Chiu, J. Hoppin, J. Kanno, M. Abdallah, C.R. Blystone, M.M. Calkins, G.-H. Dong, D.C. Dorman, R. Fry, H. Guo, L.S. Haug, J.N. Hofmann, M. Iwasaki, M. Machala, F.R. Mancini, S.S. Maria-Engler, P. Møller, J.C. Ng, M. Pallardy, G.B. Post, S. Salihovic, J. Schlezinger, A. Soshilov, K. Steenland, I.-L. Steffensen, V. Tryndyak, A. White, S. Woskie, T. Fletcher, A. Ahmadi, N. Ahmadi, L. Benbrahim-Tallaa, W. Bijoux, S. Chittiboyina, A. de Conti, C. Facchin, F. Madia, H. Mattock, M. Merdas, E. Pasqual, E. Suonio, S. Viegas, L. Zupunski, R. Wedekind, M.K. Schubauer-Berigan, Carcinogenicity of perfluorooctanoic acid and perfluorooctanesulfonic acid, Lancet Oncol. (2023), https://doi.org/10.1016/S1470-2045(23)00622-8.
[70] S.E. Fenton, A. Ducatman, A. Boobis, J.C. DeWitt, C. Lau, C. Ng, J.S. Smith, S.M. Roberts, Per- and polyfluoroalkyl substance toxicity and human health review: current state of knowledge and strategies for informing future research, Environ. Toxicol. Chem. 40 (2021) 606–630, https://doi.org/10.1002/etc.4890.
[71] K. Mokra, Endocrine disruptor potential of short- and long-chain perfluoroalkyl substances (PFASs)-A synthesis of current knowledge with proposal of molecular mechanism, Int. J. Mol. Sci. 22 (2021) 2148, https://doi.org/10.3390/ijms22042148.
[72] G.T. Ankley, P. Cureton, R.A. Hoke, M. Houde, A. Kumar, J. Kurias, R. Lanno, C. McCarthy, J. Newsted, C.J. Salice, B.E. Sample, M.S. Sepúlveda, J. Steevens, S. Valsecchi, Assessing the ecological risks of per- and polyfluoroalkyl substances: current state-of-the science and a proposed path forward, Environ. Toxicol. Chem. 40 (2021) 564–605, https://doi.org/10.1002/ETC.4869.
[73] R.C. Buck, J. Franklin, U. Berger, J.M. Conder, I.T. Cousins, P. De Voogt, A.A. Jensen, K. Kannan, S.A. Mabury, S.P.J.J. van Leeuwen, Perfluoroalkyl and polyfluoroalkyl substances in the environment: terminology, classification, and origins, Integr, Environ. Assess. Manag. 7 (2011) 513–541, https://doi.org/10.1002/ieam.258.
[74] M. Ateia, A. Maroli, N. Tharayil, T. Karanfil, The overlooked short- and ultrashort-chain poly- and perfluorinated substances : a review, Chemosphere 220 (2019) 866–882, https://doi.org/10.1016/j.chemosphere.2018.12.186.
[75] K.A. Barzen-Hanson, S.C. Roberts, S. Choyke, K. Oetjen, A. McAlees, N. Riddell, R. McCrindle, P.L. Ferguson, C.P. Higgins, J.A. Field, Discovery of 40 classes of per- and polyfluoroalkyl substances in historical aqueous film-forming foams (AFFFs) and AFFF-impacted groundwater, Environ. Sci. Technol. 51 (2017) 2047–2057, https://doi.org/10.1021/acs.est.6b05843.
[76] F. Calore, P.P. Guolo, J. Wu, Q. Xu, J. Lu, A. Marcomini, Legacy and novel PFASs in wastewater, natural water, and drinking water: occurrence in Western Countries vs China, Emerg, Contam 9 (2023) 100228, https://doi.org/10.1016/j.emcon.2023.100228.
[77] J. Li, J. He, Z. Niu, Y. Zhang, Legacy per- and polyfluoroalkyl substances (PFASs) and alternatives (short-chain analogues, F-53B, GenX and FC-98) in residential soils of China: present implications of replacing legacy PFASs, Environ. Int. 135 (2020) 105419, https://doi.org/10.1016/j.envint.2019.105419.
[78] K. Satbhai, C. Vogs, J. Crago, Comparative toxicokinetics and toxicity of PFOA and its replacement GenX in the early stages of zebrafish, Chemosphere 308 (2022) 136131, https://doi.org/10.1016/j.chemosphere.2022.136131.
[79] S. Zhang, K. Chen, W. Li, Y. Chai, J. Zhu, B. Chu, N. Li, J. Yan, S. Zhang, Y. Yang, Varied thyroid disrupting effects of perfluorooctanoic acid (PFOA) and its novel alternatives hexafluoropropylene-oxide-dimer-acid (GenX) and ammonium 4,8-dioxa-3H-perfluorononanoate (ADONA) in vitro, Environ. Int. 156 (2021) 106745, https://doi.org/10.1016/J.ENVINT.2021.106745.
[80] S. Fustinoni, R. Mercadante, G. Lainati, S. Cafagna, D. Consonni, Kinetics of excretion of the perfluoroalkyl surfactant cC6O4 in humans, Toxics 11 (2023) 284, https://doi.org/10.3390/TOXICS11030284.
[81] H. Heidari, T. Abbas, Y.S. Ok, D.C.W. Tsang, A. Bhatnagar, E. Khan, GenX is not always a better fluorinated organic compound than PFOA: a critical review on aqueous phase treatability by adsorption and its associated cost, Water Res. 205 (2021) 117683, https://doi.org/10.1016/j.watres.2021.117683.
[82] S. Yadav, I. Ibrar, R.A. Al-Juboori, L. Singh, N. Ganbat, T. Kazwini, E. Karbassiyazdi, A.K. Samal, S. Subbiah, A. Altaee, Updated review on emerging technologies for PFAS contaminated water treatment, Chem. Eng. Res. Des. 182 (2022) 667–700, https://doi.org/10.1016/J.CHERD.2022.04.009.
[83] D.M. Wanninayake, Comparison of currently available PFAS remediation technologies in water: a review, J. Environ. Manag. 283 (2021) 111977, https://doi.org/10.1016/j.jenvman.2021.111977.
[84] I. Ross, J. McDonough, J. Miles, P. Storch, P. Thelakkat Kochunarayanan, E. Kalve, J. Hurst, S.S. Dasgupta, J. Burdick, A review of emerging technologies for remediation of PFASs, Remediation 28 (2018) 101–126, https://doi.org/10.1002/rem.21553.
[85] R. Mahinroosta, L. Senevirathna, A review of the emerging treatment technologies for PFAS contaminated soils, J. Environ. Manag. 255 (2020) 109896, https://doi.org/10.1016/j.jenvman.2019.109896.
[86] I.M. Militao, F.A. Roddick, R. Bergamasco, L. Fan, Removing PFAS from aquatic systems using natural and renewable material-based adsorbents: a review, J. Environ. Chem. Eng. 9 (2021) 105271, https://doi.org/10.1016/j.jece.2021.105271.
[87] T.D. Appleman, E.R. V Dickenson, C. Bellona, C.P. Higgins, Nanofiltration and granular activated carbon treatment of perfluoroalkyl acids, J. Hazard Mater. 260 (2013) 740–746, https://doi.org/10.1016/j.jhazmat.2013.06.033.
[88] T.D. Appleman, C.P. Higgins, O. Quiñones, B.J. Vanderford, C. Kolstad, J.C. Zeigler-Holady, E.R.V. Dickenson, O. Higgins, Christopher P. Quiñones, E.R.V. Dickenson, J.C. Zeigler-Holady, B.J. Vanderford, C. Kolstad, C.P. Higgins, O. Quiñones, B.J. Vanderford, C. Kolstad, J.C. Zeigler-Holady, E.R.V. Dickenson, Treatment of poly- and perfluoroalkyl substances in U.S. full-scale water treatment systems, Water Res. 51 (2014) 246–255, https://doi.org/10.1016/j.watres.2013.10.067.
[89] P. McCleaf, S. Englund, A. Östlund, K. Lindegren, K. Wiberg, L. Ahrens, Removal efficiency of multiple poly- and perfluoroalkyl substances (PFASs) in drinking water using granular activated carbon (GAC) and anion exchange (AE) column tests, Water Res. 120 (2017) 77–87, https://doi.org/10.1016/j.watres.2017.04.057.
[90] Y. Liu, T. Li, J. Bao, X. Hu, X. Zhao, L. Shao, C. Li, M. Lu, A review of treatment techniques for short-chain perfluoroalkyl substances, Appl. Sci. 12 (2022) (1941), https://doi.org/10.3390/APP12041941.
[91] M. Kah, D. Oliver, R. Kookana, Sequestration and potential release of PFAS from spent engineered sorbents, Sci. Total Environ. 765 (2021) 142770, https://doi.org/10.1016/j.scitotenv.2020.142770.
[92] D.Q. Zhang, W.L. Zhang, Y.N. Liang, Adsorption of perfluoroalkyl and polyfluoroalkyl substances (PFASs) from aqueous solution - a review, Sci. Total Environ. 694 (2019) 133606, https://doi.org/10.1016/j.scitotenv.2019.133606.
[93] M. Ateia, A. Alsbaiee, T. Karanfil, W. Ditchel, Efficient PFAS removal by amine-functionalized sorbents: critical review of the current literature, Environ. Sci. Technol. Lett. 6 (2019) 688–6985, https://doi.org/10.1021/acs.estlett.9b00659.
[94] R. Verduzco, M.S. Wong, Fighting PFAS with PFAS, RSC Adv. 6 (2020) 453–455, https://doi.org/10.1021/acscentsci.0c00164.
[95] R. Wang, C. Ching, W.R. Dichtel, D.E. Helbling, Evaluating the removal of per- and polyfluoroalkyl substances from contaminated groundwater with different adsorbents using a suspect screening approach, Environ. Sci. Technol. Lett. 7 (2020) 954–960, https://doi.org/10.1021/acs.estlett.0c00736.
[96] D.N. Kothawala, S.J. Köhler, A. Östlund, K. Wiberg, L. Ahrens, Influence of dissolved organic matter concentration and composition on the removal efficiency of perfluoroalkyl substances (PFASs) during drinking water treatment, Water Res. 121 (2017) 320–328, https://doi.org/10.1016/j.watres.2017.05.047.
[97] Z. Du, S. Deng, Y. Bei, Q. Huang, B. Wang, Adsorption behavior and mechanism of perfluorinated compounds on various adsorbents — a review, J. Hazard Mater. 274 (2014) 443–454, https://doi.org/10.1016/j.jhazmat.2014.04.038.
[98] C. Wu, M.J. Klemes, B. Trang, W.R. Dichtel, D.E. Helbling, Exploring the factors that influence the adsorption of anionic PFAS on conventional and emerging adsorbents in aquatic matrices, Water Res. 182 (2020), https://doi.org/10.1016/j.watres.2020.115950.
[99] A. Zaggia, L. Conte, L. Falletti, M. Fant, A. Chiorboli, L. Falletti, A. Zaggia, Use of strong anion exchange resins for the removal of perfluoroalkylated substances from contaminated drinking water in batch and continuous pilot plants, Water Res. 91 (2016) 137–146, https://doi.org/10.1016/j.watres.2015.12.039.
[100] G. Bertanza, G.U. Capoferri, M. Carmagnani, F. Icarelli, S. Sorlini, R. Pedrazzani, Long-term investigation on the removal of perfluoroalkyl substances in a full-scale drinking water treatment plant in the Veneto Region, Italy, Sci. Total Environ. 734 (2020) 139154, https://doi.org/10.1016/j.scitotenv.2020.139154.

[101] M.A. Uriakhil, T. Sidnell, A. De Castro Fernández, J. Lee, I. Ross, M. Bussemaker, Per- and poly-fluoroalkyl substance remediation from soil and sorbents: a review of adsorption behaviour and ultrasonic treatment, Chemosphere 282 (2021) 131025, https://doi.org/10.1016/j.chemosphere.2021.131025.
[102] B.C. Crone, T.F. Speth, D.G. Wahman, S.J. Smith, G. Abulikemu, E.J. Kleiner, J.G. Pressman, Occurrence of per- and polyfluoroalkyl substances (PFAS) in source water and their treatment in drinking water, Crit. Rev. Environ. Sci. Technol. (2019), https://doi.org/10.1080/10643389.2019.1614848.
[103] M.F. Rahman, S. Peldszus, W.B. Anderson, Behaviour and fate of perfluoroalkyl and polyfluoroalkyl substances (PFASs) in drinking water treatment: a review, Water Res. 50 (2014) 318–340, https://doi.org/10.1016/j.watres.2013.10.045.
[104] X.T. Bui, T.P.T. Vo, H.H. Ngo, W.S. Guo, T.T. Nguyen, Multicriteria assessment of advanced treatment technologies for micropollutants removal at large-scale applications, Sci. Total Environ. 563–564 (2016) 1050–1067, https://doi.org/10.1016/j.scitotenv.2016.04.191.
[105] F. Dixit, R. Dutta, B. Barbeau, P. Berube, M. Mohseni, PFAS removal by ion exchange resins: a review, Chemosphere 272 (2021) 129777, https://doi.org/10.1016/j.chemosphere.2021.129777.
[106] D.P. Siriwardena, R. James, K. Dasu, J. Thorn, R.D. Iery, F. Pala, D. Schumitz, S. Eastwood, N. Burkitt, Regeneration of per- and polyfluoroalkyl substance-laden granular activated carbon using a solvent based technology, J. Environ. Manag. 289 (2021) 112439, https://doi.org/10.1016/j.jenvman.2021.112439.
[107] W. Zhang, D. Zhang, Y. Liang, Nanotechnology in remediation of water contaminated by poly- and perfluoroalkyl substances: a review, Environ. Pollut. 247 (2019) 266–276, https://doi.org/10.1016/j.envpol.2019.01.045.
[108] R. Mukhopadhyay, B. Sarkar, K.N. Palansooriya, J.Y. Dar, N.S. Bolan, S.J. Parikh, C. Sonne, Y.S. Ok, Natural and engineered clays and clay minerals for the removal of poly- and perfluoroalkyl substances from water: state-of-the-art and future perspectives, Adv. Colloid Interface Sci. 297 (2021) 102537, https://doi.org/10.1016/J.CIS.2021.102537.
[109] M. Wang, A.A. Orr, J.M. Jakubowski, K.E. Bird, C.M. Casey, S.E. Hearon, P. Tamamis, T.D. Phillips, Enhanced adsorption of per- and polyfluoroalkyl substances (PFAS) by edible, nutrient-amended montmorillonite clays, Water Res. 188 (2021) 116534, https://doi.org/10.1016/j.watres.2020.116534.
[110] S. Kalam, S.A. Abu-Khamsin, M.S. Kamal, S. Patil, Surfactant adsorption isotherms: a review, ACS Omega 6 (2021) 32342–32348, https://doi.org/10.1021/acsomega.1c04661.
[111] M.A. Al-Ghouti, D.A. Da'ana, Guidelines for the use and interpretation of adsorption isotherm models: a review, J. Hazard Mater. 393 (2020) 122383, https://doi.org/10.1016/j.jhazmat.2020.122383.
[112] E.D. Revellame, D.L. Fortela, W. Sharp, R. Hernandez, M.E. Zappi, Adsorption kinetic modeling using pseudo-first order and pseudo-second order rate laws: a review, Clean. Eng. Technol. 1 (2020) 100032, https://doi.org/10.1016/j.clet.2020.100032.
[113] P.S. Pauletto, T.J. Bandosz, Activated carbon versus metal-organic frameworks: a review of their PFAS adsorption performance, J. Hazard Mater. 425 (2022) 127810, https://doi.org/10.1016/J.JHAZMAT.2021.127810.
[114] Q. Yu, R. Zhang, S. Deng, J. Huang, G. Yu, Sorption of perfluorooctane sulfonate and perfluorooctanoate on activated carbons and resin: kinetic and isotherm study, Water Res. 43 (2009) 1150–1158, https://doi.org/10.1016/j.watres.2008.12.001.
[115] M.C. Hansen, M.H. Børresen, M. Schlabach, G. Cornelissen, Sorption of perfluorinated compounds from contaminated water to activated carbon, J. Soils Sediments 10 (2010) 179–185, https://doi.org/10.1007/s11368-009-0172-z.
[116] H. Son, T. Kim, H.-S. Yoom, D. Zhao, B. An, The adsorption selectivity of short and long per- and polyfluoroalkyl substances (PFASs) from surface water using powder-activated carbon, Water 12 (2020), https://doi.org/10.3390/w12113287.
[117] B.K. Pramanik, S.K. Pramanik, F. Suja, A comparative study of coagulation, granular- and powdered-activated carbon for the removal of perfluorooctane sulfonate and perfluorooctanoate in drinking water treatment, Environ. Technol. 36 (2015) 2610–2617, https://doi.org/10.1080/09593330.2015.1040079.
[118] S. Deng, Y. Nie, Z. Du, Q. Huang, P. Meng, B. Wang, J. Huang, G. Yu, Enhanced adsorption of perfluorooctane sulfonate and perfluorooctanoate by bamboo-derived granular activated carbon, J. Hazard Mater. 282 (2015) 150–157, https://doi.org/10.1016/j.jhazmat.2014.03.045.
[119] M. Park, S. Wu, I.J. Lopez, J.Y. Chang, T. Karanfil, S.A. Snyder, Adsorption of perfluoroalkyl substances (PFAS) in groundwater by granular activated carbons: roles of hydrophobicity of PFAS and carbon characteristics, Water Res. 170 (2020) 115364, https://doi.org/10.1016/j.watres.2019.115364.
[120] R. Chen, X. Huang, G. Li, Y. Yu, B. Shi, Performance of in-service granular activated carbon for perfluoroalkyl substances removal under changing water quality conditions, Sci. Total Environ. 848 (2022) 157723, https://doi.org/10.1016/j.scitotenv.2022.157723.
[121] J. Yu, L. Lv, P. Lan, S. Zhang, B. Pan, W. Zhang, Effect of effluent organic matter on the adsorption of perfluorinated compounds onto activated carbon, J. Hazard Mater. 225–226 (2012) 99–106, https://doi.org/10.1016/j.jhazmat.2012.04.073.
[122] X. Lei, L. Yao, Q. Lian, X. Zhang, T. Wang, W. Holmes, G. Ding, D.D. Gang, M.E. Zappi, Enhanced adsorption of perfluorooctanoate (PFOA) onto low oxygen content ordered mesoporous carbon (OMC): adsorption behaviors and mechanisms, J. Hazard Mater. 421 (2022) 126810, https://doi.org/10.1016/j.jhazmat.2021.126810.
[123] N. Saeidi, F.D. Kopinke, A. Georgi, Understanding the effect of carbon surface chemistry on adsorption of perfluorinated alkyl substances, Chem. Eng. J. 381 (2020) 122689, https://doi.org/10.1016/J.CEJ.2019.122689.
[124] S.J. Chow, H.C. Croll, N. Ojeda, J. Klamerus, R. Capelle, J. Oppenheimer, J.G. Jacangelo, K.J. Schwab, C. Prasse, Comparative investigation of PFAS adsorption onto activated carbon and anion exchange resins during long-term operation of a pilot treatment plant, Water Res. 226 (2022) 119198, https://doi.org/10.1016/j.watres.2022.119198.
[125] C.C. Murray, R.E. Marshall, C.J. Liu, H. Vatankhah, C.L. Bellona, PFAS treatment with granular activated carbon and ion exchange resin: comparing chain length, empty bed contact time, and cost, J. Water Process Eng. 44 (2021) 102342, https://doi.org/10.1016/j.jwpe.2021.102342.
[126] A.C. Ellis, C.J. Liu, Y. Fang, T.H. Boyer, C.E. Schaefer, C.P. Higgins, T.J. Strathmann, Pilot study comparison of regenerable and emerging single-use anion exchange resins for treatment of groundwater contaminated by per- and polyfluoroalkyl substances (PFASs), Water Res. 223 (2022) 119019, https://doi.org/10.1016/j.watres.2022.119019.
[127] Y.-L. Liu, M. Sun, Ion exchange removal and resin regeneration to treat per- and polyfluoroalkyl ether acids and other emerging PFAS in drinking water, Water Res. 207 (2021) 117781, https://doi.org/10.1016/j.watres.2021.117781.
[128] Y. Gao, S. Deng, Z. Du, K. Liu, G. Yu, Adsorptive removal of emerging polyfluoroalky substances F-53B and PFOS by anion-exchange resin: a comparative study, J. Hazard Mater. 323 (2017) 550–557, https://doi.org/10.1016/j.jhazmat.2016.04.069.
[129] A. Maimaiti, S. Deng, P. Meng, W. Wang, B. Wang, J. Huang, Y. Wang, G. Yu, Competitive adsorption of perfluoroalkyl substances on anion exchange resins in simulated AFFF-impacted groundwater, Chem. Eng. J. 348 (2018) 494–502, https://doi.org/10.1016/j.cej.2018.05.006.
[130] R. Li, S. Alomari, T. Islamoglu, O.K. Farha, S. Fernando, S.M. Thagard, T.M. Holsen, M. Wriedt, Systematic study on the removal of per-and polyfluoroalkyl substances from contaminated groundwater using metal-organic frameworks, Environ. Sci. Technol. 55 (2021) 15162–15171, https://doi.org/10.1021/acs.est.1c03974.
[131] M. Sun, E. Arevalo, M. Strynar, A. Lindstrom, M. Richardson, B. Kearns, A. Pickett, C. Smith, D.R.U. Knappe, Legacy and emerging perfluoroalkyl substances are important drinking water contaminants in the cape fear river watershed of North Carolina, Environ. Sci. Technol. Lett. 3 (2016) 415–419, https://doi.org/10.1021/acs.estlett.6b00398.
[132] V. Franke, P. McCleaf, K. Lindegren, L. Ahrens, Efficient removal of per- and polyfluoroalkyl substances (PFASs) in drinking water treatment: nanofiltration combined with active carbon or anion exchange, Environ. Sci. Water Res. Technol. 5 (2019) 1836–1843, https://doi.org/10.1039/c9ew00286c.
[133] H. Sun, F.S. Cannon, X. He, Effective removal of perfluorooctanoate from groundwater using quaternary nitrogen-grafted granular activated carbon, J. Water Process Eng. 37 (2020) 101416, https://doi.org/10.1016/j.jwpe.2020.101416.
[134] C. Yuan, Y. Huang, F.S. Cannon, Z. Zhao, Adsorption mechanisms of PFOA onto activated carbon anchored with quaternary ammonium/epoxide-forming compounds: a combination of experiment and model studies, J. Environ. Sci. 98 (2020) 94–102, https://doi.org/10.1016/j.jes.2020.05.019.
[135] H. Guo, Y. Liu, W. Ma, L. Yan, K. Li, S. Lin, Surface molecular imprinting on carbon microspheres for fast and selective adsorption of perfluorooctane sulfonate, J. Hazard Mater. 348 (2018) 29–38, https://doi.org/10.1016/j.jhazmat.2018.01.018.
[136] V. Vinayagam, S. Murugan, R. Kumaresan, M. Narayanan, M. Sillanpää, D.V.N. Vo, O.S. Kushwaha, Protein nanofibrils as versatile and sustainable adsorbents for an effective removal of heavy metals from wastewater: a review, Chemosphere 301 (2022) 134635, https://doi.org/10.1016/J.CHEMOSPHERE.2022.134635.
[137] M. Peydayesh, R. Mezzenga, Protein nanofibrils for next generation sustainable water purification, Nat. Commun. 12 (2021) 1–17, https://doi.org/10.1038/s41467-021-23388-2.
[138] W. Yan, T. Qian, L. Zhang, L. Wang, Y. Zhou, Interaction of perfluorooctanoic acid with extracellular polymeric substances - role of protein, J. Hazard Mater. 401 (2021) 123381, https://doi.org/10.1016/j.jhazmat.2020.123381.
[139] J. Delva-Wiley, I. Jahan, R.H. Newman, L. Zhang, M. Dong, Computational analysis of the binding mechanism of GenX and HSA, ACS Omega 6 (2021) 29166–29170, https://doi.org/10.1021/acsomega.1c04592.
[140] N.L.D. Perera, J. Miksovska, K.E. O'Shea, Elucidation of specific binding sites and extraction of toxic Gen X from HSA employing cyclodextrin, J. Hazard Mater. 425 (2022) 127765, https://doi.org/10.1016/J.JHAZMAT.2021.127765.
[141] S.A. Malomo, R.E. Aluko, A comparative study of the structural and functional properties of isolated hemp seed (Cannabis sativa L.) albumin and globulin fractions, Food Hydrocolloids 43 (2015) 743–752, https://doi.org/10.1016/j.foodhyd.2014.08.001.
[142] J.H. Kim, J.H. Han, Y.C. Jung, Y.A. Kim, Mussel adhesive protein-coated titanium oxide nanoparticles for effective NO removal from versatile substrates, Chem. Eng. J. 378 (2019) 122164, https://doi.org/10.1016/J.CEJ.2019.122164.
[143] R. Dai, Y. Zhang, Z.Q. Shi, F. Yang, C.S. Zhao, A facile approach towards amino-coated ferroferric oxide nanoparticles for environmental pollutant removal, J. Colloid Interface Sci. 513 (2018) 647–657, https://doi.org/10.1016/J.JCIS.2017.11.070.

[144] W.-T. Chung, I.M.A. Mekhemer, M.G. Mohamed, A.M. Elewa, A.F.M. El-Mahdy, H.-H. Chou, S.-W. Kuo, K.C.-W. Wu, Recent advances in metal/covalent organic frameworks based materials: their synthesis, structure design and potential applications for hydrogen production, Coord. Chem. Rev. 483 (2023) 215066, https://doi.org/10.1016/j.ccr.2023.215066.
[145] S. Naghdi, M.M. Shahrestani, M. Zendehbad, H. Djahaniani, H. Kazemian, D. Eder, Recent advances in application of metal-organic frameworks (MOFs) as adsorbent and catalyst in removal of persistent organic pollutants (POPs), J. Hazard Mater. 442 (2023) 130127, https://doi.org/10.1016/j.jhazmat.2022.130127.
[146] E. Karbassiyazdi, M. Kasula, S. Modak, J. Pala, M. Kalantari, A. Altaee, M.R. Esfahani, A. Razmjou, A juxtaposed review on adsorptive removal of PFAS by metal-organic frameworks (MOFs) with carbon-based materials, ion exchange resins, and polymer adsorbents, Chemosphere 311 (2023) 136933, https://doi.org/10.1016/j.chemosphere.2022.136933.
[147] F. Dixit, B. Barbeau, S.G. Mostafavi, M. Mohseni, PFOA and PFOS removal by ion exchange for water reuse and drinking applications: role of organic matter characteristics, Environ. Sci. Water Res. Technol. 5 (2019) 1782–1795, https://doi.org/10.1039/C9EW00409B.
[148] S. Rojas, P. Horcajada, Metal-organic frameworks for the removal of emerging organic contaminants in water, Chem. Rev. 120 (2020) 8378–8415, https://doi.org/10.1021/acs.chemrev.9b00797.
[149] L.H. Mohd Azmi, D.R. Williams, B.P. Ladewig, Polymer-assisted modification of metal-organic framework MIL-96 (Al): influence of HPAM concentration on particle size, crystal morphology and removal of harmful environmental pollutant PFOA, Chemosphere 262 (2021) 128072, https://doi.org/10.1016/j.chemosphere.2020.128072.
[150] C. Zhao, Y. Xu, F. Xiao, J. Ma, Y. Zou, W. Tang, Perfluorooctane sulfonate removal by metal-organic frameworks (MOFs): insights into the effect and mechanism of metal nodes and organic ligands, Chem. Eng. J. 406 (2021) 126852, https://doi.org/10.1016/j.cej.2020.126852.
[151] D. Barpaga, J. Zheng, K.S. Han, J.A. Soltis, V. Shutthanandan, S. Basuray, B.P. McGrail, S. Chatterjee, R.K. Motkuri, Probing the sorption of perfluorooctanesulfonate using mesoporous metal-organic frameworks from aqueous solutions, Inorg. Chem. 58 (2019) 8339–8346, https://doi.org/10.1021/acs.inorgchem.9b00380.
[152] C.A. Clark, K.N. Heck, C.D. Powell, M.S. Wong, Highly defective UiO-66 materials for the adsorptive removal of perfluorooctanesulfonate, ACS Sustain. Chem. Eng. 7 (2019) 6619–6628, https://doi.org/10.1021/acssuschemeng.8b05572.
[153] K. Liu, S. Zhang, X. Hu, K. Zhang, A. Roy, G. Yu, Understanding the adsorption of PFOA on MIL-101(Cr)-Based anionic-exchange metal-organic frameworks: comparing DFT calculations with aqueous sorption experiments, Environ. Sci. Technol. 49 (2015) 8657–8665, https://doi.org/10.1021/acs.est.5b00802.
[154] T. Selman Erkal, N. Shamsuddin, S. Kirmizialtin, A. Ozgur Yazaydin, Computational investigation of Structure–Function relationship in fluorine-functionalized MOFs for PFOA capture from water, J. Phys. Chem. C 127 (2023) 3216, https://doi.org/10.1021/acs.jpcc.2c07737.
[155] J. Liu, P.K. Thallapally, B.P. Mc Grail, D.R. Brown, J. Liu, Progress in adsorption-based CO2 capture by metal–organic frameworks, Chem. Soc. Rev. 41 (2012) 2308–2322, https://doi.org/10.1039/C1CS15221A.
[156] A. Alsbaiee, B.J. Smith, L. Xiao, Y. Ling, D.E. Helbling, W.R. Dichtel, Rapid removal of organic micropollutants from water by a porous β-cyclodextrin polymer, Nature 529 (2015) 190–194, https://doi.org/10.1038/nature16185.
[157] Y. Ling, M.J. Klemes, L. Xiao, A. Alsbaiee, W.R. Dichtel, D.E. Helbling, Benchmarking micropollutant removal by activated carbon and porous β-cyclodextrin polymers under environmentally relevant scenarios, Environ. Sci. Technol. 51 (2017) 7590–7598. https://pubs.acs.org/doi/full/10.1021/acs.est.7b00906.
[158] S.T.M.L.D. Senevirathna, S. Tanaka, S. Fujii, C. Kunacheva, H. Harada, B.H.A.K.T. Ariyadasa, B.R. Shivakoti, Adsorption of perfluorooctane sulfonate (n-PFOS) onto non ion-exchange polymers and granular activated carbon: batch and column test, Desalination 260 (2010) 29–33, https://doi.org/10.1016/j.desal.2010.05.005.
[159] D.P. Siriwardena, M. Crimi, T.M. Holsen, C. Bellona, C. Divine, E. Dickenson, Influence of groundwater conditions and co-contaminants on sorption of perfluoroalkyl compounds on granular activated carbon, Remed. J. 29 (2019) 5–15, https://doi.org/10.1002/rem.21603.
[160] E.D. Ozelcaglayan, W.J. Parker, β-Cyclodextrin functionalized adsorbents for removal of organic micropollutants from water, Chemosphere 320 (2023) 137964, https://doi.org/10.1016/J.CHEMOSPHERE.2023.137964.
[161] A. Alsbaiee, B.J. Smith, L. Xiao, Y. Ling, D.E. Helbling, W.R. Dichtel, Rapid removal of organic micropollutants from water by a porous β-cyclodextrin polymer, Nature 529 (2015) 190–194, https://doi.org/10.1038/nature16185.
[162] E.M. Ahmed, Hydrogel: preparation, characterization, and applications: a review, J. Adv. Res. 6 (2015) 105–121, https://doi.org/10.1016/j.jare.2013.07.006.
[163] I.M. Manning, N. Guan Pin Chew, H.P. Macdonald, K.E. Miller, M.J. Strynar, O. Coronell, F.A. Leibfarth, Hydrolytically stable ionic fluorogels for high-performance remediation of per- and polyfluoroalkyl substances (PFAS) from natural water, Angew. Chem. Int. Ed. (2022), https://doi.org/10.1002/anie.202208150.
[164] E.M. Frazar, A. Smith, T. Dziubla, J.Z. Hilt, Thermoresponsive cationic polymers: PFAS binding performance under variable pH, temperature and comonomer composition, Gels 8 (2022) 668, https://doi.org/10.3390/GELS8100668/S1.
[165] W. Wang, A. Maimaiti, H. Shi, R. Wu, R. Wang, Z. Li, D. Qi, G. Yu, S. Deng, Adsorption behavior and mechanism of emerging perfluoro-2-propoxypropanoic acid (GenX) on activated carbons and resins, Chem. Eng. J. 364 (2019) 132–138, https://doi.org/10.1016/j.cej.2019.01.153.
[166] A. Choudhary, D. Bedrov, Interaction of short-chain PFAS with polycationic gels: how much fluorination is necessary for efficient adsorption? ACS Macro Lett. 11 (2022) 1123–1128, https://doi.org/10.1021/acsmacrolett.2c00383.
[167] Y. Seida, H. Tokuyama, Hydrogel adsorbents for the removal of hazardous pollutants- requirements and available functions as adsorbent, Gels 8 (2022) 220, https://doi.org/10.3390/GELS8040220.
[168] Q. Zhao, X. Zhao, J. Cao, Advanced nanomaterials for degrading persistent organic pollutants, Adv. Nanomater. Pollut. Sens. Environ. Catal. (2019) 249–305, https://doi.org/10.1016/B978-0-12-814796-2.00007-1.
[169] W.K. Dodds, J.P. Guinnip, A.E. Schechner, P.J. Pfaff, B.S. Emma, Fate and toxicity of engineered nanomaterials in the environment: a meta-analysis, Sci. Total Environ. 796 (2021) 148843, https://doi.org/10.1016/J.SCITOTENV.2021.148843.
[170] G. Patel, C. Patra, S.P. Srinivas, M. Kumawat, P.N. Navya, H.K. Daima, Methods to evaluate the toxicity of engineered nanomaterials for biomedical applications: a review, Environ. Chem. Lett. 196 (19) (2021) 4253–4274, https://doi.org/10.1007/S10311-021-01280-1, 2021.
[171] A.S. Adeleye, J.R. Conway, K. Garner, Y. Huang, Y. Su, A.A. Keller, Engineered nanomaterials for water treatment and remediation: costs, benefits, and applicability, Chem. Eng. J. 286 (2016) 640–662, https://doi.org/10.1016/j.cej.2015.10.105.
[172] M. Mancinelli, C. Stevanin, M. Ardit, T. Chenet, L. Pasti, A. Martucci, PFAS as emerging pollutants in the environment: a challenge with FAU type and silver-FAU exchanged zeolites for their removal from water, J. Environ. Chem. Eng. 10 (2022) 108026, https://doi.org/10.1016/J.JECE.2022.108026.
[173] H. Zhang, I. bin Samsudin, S. Jaenicke, G.K. Chuah, Zeolites in catalysis: sustainable synthesis and its impact on properties and applications, Catal. Sci. Technol. 12 (2022) 6024–6039, https://doi.org/10.1039/D2CY01325H.
[174] L. Qian, F.D. Kopinke, A. Georgi, Photodegradation of perfluorooctanesulfonic acid on Fe-zeolites in water, Environ. Sci. Technol. 55 (2021) 614–622, https://doi.org/10.1021/ACS.EST.0C04558/ASSET/IMAGES/MEDIUM/ES0C04558_M020.GIF.
[175] L. Qian, F.D. Kopinke, T. Scherzer, J. Griebel, A. Georgi, Enhanced degradation of perfluorooctanoic acid by heat-activated persulfate in the presence of zeolites, Chem. Eng. J. 429 (2022) 132500, https://doi.org/10.1016/J.CEJ.2021.132500.
[176] J.L.X. Hong, T. Maneerung, S.N. Koh, S. Kawi, C.H. Wang, Conversion of coal fly ash into zeolite materials: synthesis and characterizations, process design, and its cost-benefit analysis, Ind. Eng. Chem. Res. 56 (2017) 11565–11574, https://doi.org/10.1021/ACS.IECR.7B02885/ASSET/IMAGES/LARGE/IE-2017-02885Q_0008. JPEG.
[177] C. Ziejewska, A. Grela, M. Łach, J. Marczyk, N. Hordyńska, M. Szechyńska-Hebda, M. Hebda, Eco-friendly zeolites for innovative purification of water from cationic dye and heavy metal ions, J. Clean. Prod. 406 (2023) 136947, https://doi.org/10.1016/J.JCLEPRO.2023.136947.
[178] S. Gao, H. Peng, B. Song, J. Zhang, W. Wu, J. Vaughan, P. Zardo, J. Vogrin, S. Tulloch, Z. Zhu, Synthesis of zeolites from low-cost feeds and its sustainable environmental applications, J. Environ. Chem. Eng. 11 (2023) 108995, https://doi.org/10.1016/J.JECE.2022.108995.
[179] A. Shahzad, J. Ali, M. Wajid Ullah, G.G. Aregay, J. Ifthikar, S. Manan, G. Yang, Z. Chen, Z. Chen, Interlayered modified hydroxides for removal of graphene oxide from water: mechanism and secondary applications, Sep. Purif. Technol. 284 (2022) 120305, https://doi.org/10.1016/j.seppur.2021.120305.
[180] S. Daniel, S. Thomas, Layered double hydroxides: fundamentals to applications, Layer. Double Hydroxide Polym, Nanocomposites (2020) 1–76, https://doi.org/10.1016/B978-0-08-101903-0.00001-5.
[181] X. Zhu, M. Lyu, T. Ge, J. Wu, C. Chen, F. Yang, D. O'Hare, R. Wang, Modified layered double hydroxides for efficient and reversible carbon dioxide capture from air, Cell Reports Phys. Sci. 2 (2021) 100484, https://doi.org/10.1016/J.XCRP.2021.100484.
[182] B. Yan, J. Liu, Molecular framework for designing Fluoroclay with enhanced affinity for per- and polyfluoroalkyl substances, Water Res. X. 19 (2023) 100175, https://doi.org/10.1016/j.wroa.2023.100175.
[183] P.S. Pauletto, M. Florent, T.J. Bandosz, Insight into the mechanism of perfluorooctanesulfonic acid adsorption on highly porous media: sizes of hydrophobic pores and the extent of multilayer formation, Carbon N. Y. 191 (2022) 535–545, https://doi.org/10.1016/J.CARBON.2022.02.006.
[184] J.P. Simonin, On the comparison of pseudo-first order and pseudo-second order rate laws in the modeling of adsorption kinetics, Chem. Eng. J. 300 (2016) 254–263, https://doi.org/10.1016/j.cej.2016.04.079.
[185] J.O. Ighalo, F.O. Omoarukhe, V.E. Ojukwu, K.O. Iwuozor, C.A. Igwegbe, Cost of adsorbent preparation and usage in wastewater treatment: a review, Clean. Chem. Eng. 3 (2022) 100042, https://doi.org/10.1016/j.clce.2022.100042.
[186] F. Dixit, B. Barbeau, S.G. Mostafavi, M. Mohseni, PFAS and DOM removal using an organic scavenger and PFAS-specific resin: trade-off between regeneration and faster kinetics, Sci. Total Environ. 754 (2021) 142107, https://doi.org/10.1016/j.scitotenv.2020.142107.
[187] D. Lu, S. Sha, J. Luo, Z. Huang, X. Zhang Jackie, Treatment train approaches for the remediation of per- and polyfluoroalkyl substances (PFAS): a critical review, J. Hazard Mater. 386 (2020) 121963, https://doi.org/10.1016/

j.jhazmat.2019.121963.
[188] Y. Wang, J. Niu, Y. Li, T. Zheng, Y. Xu, Y. Liu, Performance and mechanisms for removal of perfluorooctanoate (PFOA) from aqueous solution by activated carbon fiber, RSC Adv. 5 (2015) 86927–86933, https://doi.org/10.1039/C5RA15853B.
[189] F. Liu, D. Wang, Dissolved organic carbon concentration and biodegradability across the global rivers: a meta-analysis, Sci. Total Environ. (2021) 151828, https://doi.org/10.1016/j.scitotenv.2021.151828.
[190] S. Yu, J. Liu, Y. Yin, M. Shen, Interactions between engineered nanoparticles and dissolved organic matter: a review on mechanisms and environmental effects, J. Environ. Sci. 63 (2018) 198–217, https://doi.org/10.1016/j.jes.2017.06.021.
[191] I. Michael-Kordatou, C. Michael, X. Duan, X. He, D.D. Dionysiou, M.A. Mills, D. Fatta-Kassinos, Dissolved effluent organic matter: characteristics and potential implications in wastewater treatment and reuse applications, Water Res. 77 (2015) 213–248, https://doi.org/10.1016/j.watres.2015.03.011.
[192] T. Alomar, H. Qiblawey, F. Almomani, R.I. Al-Raoush, D.S. Han, N.M. Ahmad, Recent advances on humic acid removal from wastewater using adsorption process, J. Water Process Eng. 53 (2023) 103679, https://doi.org/10.1016/j.jwpe.2023.103679.
[193] T.H. Boyer, Y. Fang, A. Ellis, R. Dietz, Y.J. Choi, C.E. Schaefer, C.P. Higgins, T.J. Strathmann, Anion exchange resin removal of per- and polyfluoroalkyl substances (PFAS) from impacted water: a critical review, Water Res. 200 (2021) 117244, https://doi.org/10.1016/J.WATRES.2021.117244.
[194] Y. Li, Z. Yang, Y. Wang, Z. Bai, T. Zheng, X. Dai, S. Liu, D. Gui, W. Liu, M. Chen, L. Chen, J. Diwu, L. Zhu, R. Zhou, Z. Chai, T.E. Albrecht-Schmitt, S. Wang, A mesoporous cationic thorium-organic framework that rapidly traps anionic persistent organic pollutants, Nat. Commun. 8 (2017), https://doi.org/10.1038/s41467-017-01208-w.
[195] O. Soker, S. Hao, B.G. Trewyn, C.P. Higgins, T.J. Strathmann, Application of hydrothermal alkaline treatment to spent granular activated carbon: destruction of adsorbed PFASs and adsorbent regeneration, Environ. Sci. Technol. Lett. 10 (2023) 425–430, https://doi.org/10.1021/acs.estlett.3c00161.
[196] M. Crimi, T. Holsen, C. Bellona, C. Divine, E. Dickenson, In situ treatment train for remediation of perfluoroalkyl contaminated groundwater: in situ chemical oxidation of sorbed contaminants (ISCO-SC) - final report. https://clu-in.org/download/techfocus/horizontal-wells/ER-2423_Final_Report.pdf, 2017. March 26, 2023).
[197] S. Sorn, H. Hara-Yamamura, S. Vet, M. Xiao, E.M.V. Hoek, R. Honda, Biological treatment of perfluorooctanesulfonic acid (PFOS) using microbial capsules of a polysulfone membrane, Chemosphere 329 (2023), https://doi.org/10.1016/J.CHEMOSPHERE.2023.138585.
[198] E. Menya, P.W. Olupot, H. Storz, M. Lubwama, Y. Kiros, Production and performance of activated carbon from rice husks for removal of natural organic matter from water: a review, Chem. Eng. Res. Des. 129 (2018) 271–296, https://doi.org/10.1016/J.CHERD.2017.11.008.
[199] I.M. Lima, A. McAloon, A.A. Boateng, Activated carbon from broiler litter: process description and cost of production, Biomass Bioenergy 32 (2008) 568–572, https://doi.org/10.1016/J.BIOMBIOE.2007.11.008.
[200] X. Song, Y. Zhang, C. Chang, Novel method for preparing activated carbons with high specific surface area from rice husk, Ind. Eng. Chem. Res. 51 (2012) 15075–15081, https://doi.org/10.1021/IE3012853/ASSET/IMAGES/LARGE/IE-2012-012853_0008. JPEG.
[201] G.B. Post, Recent US state and federal drinking water guidelines for per- and polyfluoroalkyl substances, Environ. Toxicol. Chem. 40 (2021) 550–563, https://doi.org/10.1002/ETC.4863.